MACROPHAGES: AN OVERLOOKED LATENT VIRAL RESERVOIR IN SIV INFECTION

By
Claudia Regina Avalos

A dissertation submitted to Johns Hopkins University in conformity with the requirements for the degree of Doctor of Philosophy

Baltimore, Maryland

July 2016

Abstract

HIV infection remains a worldwide epidemic without prospects of a cure. While antiretroviral therapy (ART) successfully decreases plasma viral load and prevents new cells from becoming infected, long-lived latently infected cells remain in blood and tissues. $CD4^+$ T cells have been extensively studied and characterized as a major latent reservoir; however less is known about macrophages, another cell infected by HIV. A better understanding of all the latent reservoirs is needed in order to devise strategies for eradication.

HIV infects both $CD4^+$ T cells and cells from the myeloid lineage such as blood monocytes and tissue macrophages early during infection. While most $CD4^+$ T cells become activated and die during the infection, some become memory cells and are able to persist in the body from months to years. Recent findings suggest that macrophages behave in a similar manner and have been shown to proliferate *in situ* contributing to new cells. Furthermore, tissue macrophages are found throughout the body in organs such as lungs, spleen, and brain among others. Infection of macrophages in these tissues has not been characterized nor the frequency of these cells compared to infected resting $CD4^+$ T cells. Therefore we developed methods, which quantitated and compared both major cellular reservoirs ($CD4^+$ T cells and macrophages). $CD4^+$ T cells from the blood and spleen were assayed using the quantitative viral outgrowth assay (QVOA) while monocytes in the blood and macrophages in the bronchoalveolar lavage fluid, lungs, spleen and brain of SIV-infected pigtailed macaques were assayed using a similar assay, the macrophage quantitative viral outgrowth assay (MΦ-QVOA).

The era of ART led to a decline in the frequency of HIV associated pathologies such as HIV-associated neurocognitive disorders (HAND). However, mild to moderate forms of HAND are still observed in viral controlled patients on successful ART. Markers of inflammation in the CSF are often reported in ART-treated patients showing signs of neurological impairment; therefore, low levels of macrophage activation and viral production in the brain are presumed to contribute to HAND. A debate still exists as to whether macrophages fit the definition of a latent reservoir. Replication-competent virus has not been recovered from latently infected macrophages in SIV or HIV-infected individuals on long-term suppression. Therefore, we used our MΦ-QVOA assay to quantitate the frequency of infection of macrophages in brain of SIV-infected ART-treated macaques. Despite long-term ART treatment of SIV-infected macaques, brain macrophages were shown to contain replication competent virus demonstrating for the first time latently infected microglia. In addition, markers of macrophage activation and neuronal damage were detected in the CSF of the ART suppressed macaques, suggesting in part that latently infected macrophages contribute to CNS inflammation. *In situ* hybridization from two brain regions confirmed the presence of rare SIV RNA positive cells but underestimated the size of the reservoir, as did tissue RNA and DNA measurements. The virus obtained in the MΦ-QVOA cultures caused productive infection in peripheral blood mononuclear cells *de novo*, thus demonstrating that the macrophage reservoir contained functional viral genomes and could spread from the brain to the periphery upon ART interruption. Finally, monocytes in the blood and macrophages in the bronchoalveolar lavage fluid, lungs, and spleen were assayed using the MΦ-QVOA and compared to the frequency of latently infected resting $CD4^+$ T cells

in the blood and spleen of SIV-infected ART-treated pigtailed macaques. Our findings confirmed that macrophages are latently infected in these peripheral tissues and the size of the reservoir was equivalent to the resting $CD4^+$ T cell reservoir.

The data presented here demonstrated that macrophages are yet another obstacle to HIV eradication, and suggest that macrophages contribute to the ongoing viral replication in tissues, thus playing a pivotal role in long-term tissue inflammation.

Thesis Advisor: Janice Clements, Ph.D.

Thesis Reader: Alan Scott, Ph.D.

Acknowledgements

Earning a doctoral degree is something that I never thought possible. The last six years have been full of ups and downs and I don't think that I could have done it without my support system. I would like to thank God for giving me the strength to make it through the process, and I have a lot of people to be grateful to: my mentors, my friends, my family, and everyone who supported me throughout my career as a scientist.

First I would like to thank my advisor Dr. Janice Clements. Janice took me on during my second year as a graduate student and helped me develop my thesis project. She has guided me, challenged me, and allowed me to develop as a scientist with every passing year. Despite her many obligations as the Vice Dean of Faculty for the School of Medicine, Janice always made time to meet with her students and discuss any challenges or celebrate exciting results. Her enthusiasm for the field of HIV research and immunology is contagious, and her curiosity for science motivated me to keep going, even when I didn't know what to do next. Janice has always been supportive of my passions outside of research and encouraged me to pursue a path in medicine. Her dedication to the lab, her patience, enthusiasm, hard work, positive attitude, and passion for science makes me aspire to be more like her in the future. I am blessed to have met her and honored to have learned from her not only how to be a better scientist, but also a better leader and a strong woman in science.

I would also like to thank Dr. Lucio Gama for his support and guidance during my Ph.D. training. Lucio was the first person I met in the Retrovirus Laboratory in addition to Janice, and he took me under his wing from day one. I have greatly benefited from his advice and support. I owe all of my technical training to him and I wouldn't have been

able to succeed without his direction. Lucio always tackled challenges with a positive energy and his love of science combined with his drive for knowledge was an inspiration for everyone in lab. I am delighted to have met him and honored to have worked with him over the years.

Working in a collaborative environment such as the Retrovirus Laboratory provided me with infinite assistance without which I could not have finished my projects. I would like to thank the faculty members: Dr. Joseph Mankowski, Dr. Christine Zink, Dr. Kelly Pate, Dr. Kenneth Witwer, Dr. David Graham and Dr. Sarah Beck. In addition, I am grateful to the outstanding team of lab managers, technician and graduate students: Brandon Bullock, Suzanne Queen, Ming Li, Erin Shirk, Elizabeth Engle, Sarah Price, Ellen Forsyth, Rachel Weinberg, Kevin Najarro, Julia Drewes, Kelly Meulendyke, Dillon Muth, and Josh Croteau. I am especially thankful to Ming Li for her tremendous amount of help with more than 200 qRT-PCR experiments. In addition to Ming's hard work, her kindness and positive demeanor always brightened my days. Finally, I must acknowledge past and current members of the Clements' laboratory who provided me with incredible support: Julia Pin (Russell), Jeanne Sisk, Dionna Williams, Lauren Askew and Celina Abreu. I am eternally grateful to Celina for helping me finish up my experiments when I needed it the most and for taking over the grueling effort of the MΦ-QVOAs. Julia, Jeanne, Dionna, and Celina provided me valuable feedback and having them in the lab made me look forward to coming to work every day.

I am also grateful for the assistance of the administrative team of the Retrovirus Laboratory: Woodland Pomeroy, Cathy Rada, Sharon Molander, Wendy Elza, and Emma

Ey. In special, I am indebted to Woodland for always being available and helping me setup every thesis committee meeting and every event with such perfection.

I would like to thank my thesis committee members, Dr. Alan Scott, Dr. Andrea Cox and Dr. David Mosser for taking the time to guide me throughout my Ph.D. and beyond. Dr. Andrea Cox helped me navigate through the steps necessary for applying to medical school and allowed me to shadow her in the infectious disease clinic at Hopkins. In addition she introduced me to Dr. Michael Chattergoon to whom I am very grateful and who played a significant role in helping me become a first year medical student. He allowed me to shadow him at the infectious disease clinic and at the viral hepatitis clinic, and always shared with me the latest information on viral diseases, clinical trials and new treatments. Dr. Chattergoon advised me about medical school, research and life situations. He was instrumental in helping me decide to apply to medical school.

I am also grateful to Dr. David Mosser who not only committed to driving about 1 hour from the University of Maryland College Park campus every time we had a thesis committee meeting, but also shared his infinite knowledge of macrophage polarization agents and activation states. Last but not least, I am indebted to Dr. Alan Scott for agreeing to review my thesis dissertation in five days, for being my thesis committee chair, and for becoming my mentor even before I joined the Retrovirus Laboratory.

Even though I only spent a year and a half with him, I must also give special thanks to Dr. Landon King and his research group, Dr. Neil Aggarwal, Dr. Franco D'Alessio, Dr. Brian Garibaldi, Dr. Jason Mock, Dr. Venkataramana Sidhaye, Yoshiki Eto, and Eric Chau. Landon was very supportive and caring. Not a day went by that he didn't ask how I was and how my family was. Everyone in the King lab was also very

collaborative and I will never forget our multiple lab outings to Chipotle and Five Guys. They introduced me to the world of macrophages and my desire to become a physician-scientist was born in that lab. I am very grateful for the time I spent with them and I remember them dearly.

I am eternally grateful to the Cellular and Molecular Medicine Graduate program, in special Leslie Lichter, Colleen Graham, Bob Casero and Rajini Rao. Leslie and Colleen became my Baltimore Moms; Rajini and Bob believed in me and gave me the opportunity to pursue my Ph.D. I also thank Rajini for being an extraordinary woman in science role model.

Equally important in my life are my mentors from Florida State University, without whom I would have never pursued a doctoral degree. I would like to thank Dr. Susan Blessing, Dr. Nick Cogan, Dr. Tim Cross and Dr. Gregory Dudley. Dr. Blessing accepted me into the Women in Math Science and Engineering Program and has been my mentor since my first semester in college. She motivated me to apply to Johns Hopkins for a graduate degree and has encouraged me throughout my Ph.D. Dr. Cogan, Dr. Cross and Dr. Dudley took me on as an undergraduate research assistant and taught me everything I knew about science. I am grateful for my experiences at Florida State.

Perhaps the most influential people in my life, I am very thankful and blessed to have such an amazing family and I know that I wouldn't be where I am without them. My mom, Regina Avalos, and my dad, Carlos Avalos, have always been by my side and offered me words of encouragement. They always put their children first and thanks to their efforts we moved from El Salvador to the United States in 2004. They never passed

a chance to tell all their friends about their children with pride, a pride so strong that made us want to excel at every task at hand. My dad used to say that I was his eyes, and his unconditional belief in me drove me to achieve new heights. To my mom, who not only is my best friend but also my role model, I appreciate all your advice, your confidence in me, your love, and your support. I am also grateful for the love and support of my younger siblings Carlos Avalos Jr. and Gaby Avalos. Even though they made my life difficult at times, they helped me become a better role model for them. I also appreciate my grandparents, cousins, uncles and aunts, who have been in my life motivating and rejoicing with me.

I was fortunate to have met my soul mate in graduate school, Vesselin Penchev. Vessi not only served as my example as a CMM grad student, he was also my rock. He supported me, and listened to my many many many laboratory-troubleshooting problems. He stayed countless nights with me in lab, keeping me company, helping me, and giving me advice when I didn't know how to do something at 10 pm in lab. Vessi became my companion, my best friend and soon thereafter my husband. He was by my side during the good and the bad parts of my Ph.D. He helped me pick myself back up when my father passed away in 2013 and motivated me to keep going when I would tell him that I was ready to quit while I was ahead. He was always understanding of the rigor of lab work and never stopped taking care of me. I am looking forward to see what the future holds for us as medical students at the University of Maryland.

With Vessi, I gained a father, Ruslan Penchev, a mother, Anelia Pencheva, a brother-in-law, Radostin Penchev and a sister-in-law, Luisa Pencheva. I am thankful for their love and support, their words of encouragement and their company.

I would also like to acknowledge my friends near and far that listened to me and inspired me. My friends from childhood Leticia Sanchez, Danelia Zambrana, Marcela Olivares and Beatriz Orellana who not only supported me when I moved to the United States in 2004 but also kept in touch with me despite the distance. They are my sisters, and also my bridesmaids. Every occasion I went back to El Salvador, they treated as if I had never left and embraced me as family. I'd like to thank my friends in Baltimore, Diana Castiblanco and Jennifer Silverman who were always there for me even if it was just for a girls' night out. And I appreciate Ross McMillan and Ted Ewachiew, Vessi's lab mates who also became my Baltimore friends.

Finally, I am grateful to the Baltimore Karate Club who helped me grow into a stronger woman, taught me to face my fears, and inspired me to seek perfection of character, to be faithful, endeavor, and respect others. In special, I would like to thank Sensei Igor Miletic, Sensei Ed Davis, Rob Laschever, Florence Caputo, and Kenneth Stewart.

TABLE OF CONTENTS

LIST OF TABLES

LIST OF FIGURES

CHAPTER II.

CHAPTER III.

LIST OF FIGURES

CHAPTER IV.

I. Introduction

History of HIV Infection

The first cases of an acquired immune deficiency disorder were described in 1981 when previously healthy individuals started showing signs of *Pneumocystis carinii* (now known to be *P. jiroveci*) pneumonia and Kaposi sarcoma, which were accompanied by depletion of $CD4^+$ lymphocytes (1-4). Soon thereafter, a virus was isolated and linked to be the disease called the acquired immune deficiency disorder or AIDS (5). However, it wasn't until 1985 that the term Human Immunodeficiency Virus (HIV) was used (6). Genetic evaluation of the virus estimates that humans became infected with strains of HIV in 1920 (7), during a crossover event of Simian Immunodeficiency Virus (SIV) most likely caused by hunting of non-human primates in Africa (8, 9). Early findings showed that HIV is a member of the lentivirus family and therefore infects both macrophages and $CD4^+$ T cells (10-12) and shares the characteristic long incubation of the virus prior to clinical manifestations and terminal disease (13).

Approximately 37 million individuals are currently living with HIV worldwide according to the World Health Organization (WHO) statistics from 2014. HIV continues to be a major public health issue with more than 70% of HIV infections located in sub-Saharan Africa. Since first being described as a new disease, HIV has taken the lives of 34 million people, and the WHO estimates that 2 million people become infected every year. Antiretroviral therapies (ART) have been successful in controlling viremia in HIV-infected patients and help prevent the progression to AIDS; however, there is no vaccine that prevents infection or a cure for the infected individuals so ART must be taken life-long (14). Further research is needed to advance the understanding of HIV persistence despite ART and to better identify viable strategies for an HIV cure (15).

Current Strategies for Eradication

HIV persistence despite ART is thought to be the product of long-lived latently infected cells, *de novo* infection, and failure of the immune system to detect and eliminate the latent reservoir. The best-characterized latent reservoir is resting $CD4^+$ T cells in HIV-infected patient on successful ART regimens (16, 17). Macrophages do not currently fit the definition of a latent reservoir (18); therefore current strategies towards HIV eradication have been developed to target only $CD4^+$ T cells.

The challenge to complete clearance of HIV is the ability of the virus to integrate its viral DNA into the genome of infected cells. ART prevents new infection of susceptible cells but treatment neither eliminates infected cells nor removes the viral genome from the cellular genome. Unless all infected cells that harbor replication competent virus are cleared, infection restarts when ART is interrupted. The only case of an HIV cure to date is a single HIV-infected man who received a bone marrow transplant from a donor who had a homozygous CCR5 delta32 deletion (19, 20). Without a functional CCR5 chemokine receptor, HIV does not efficiently infect human cells. After discontinuation of ART and full reconstitution of blood and tissues with donor-derived cells, the patient showed no sign of HIV infection. This case renewed interest in devising an HIV cure by activating latently infected cells such that the immune system would recognize the infected cells and eliminate the reservoir, a strategy termed "Shock-and-kill" (21, 22).

Several methods have been tried to activate and eliminate latently infected resting $CD4^+$ T cell (23, 24). These include activating T cells with cytokines (25), histone

deacetylase inhibitors (26), phorbol esters that stimulate protein kinase C activity (27, 28) and RNA guided excision of integrated HIV (29). While some of these methods proved promising in decreasing the number of latently infected resting $CD4^+$ T cells in *in vitro* assays, none resulted in a decrease on the $CD4^+$ T cell reservoir in human clinical trials (22, 30, 31). Further, none of the approaches used to target the $CD4^+$ T cell reservoir are known to target other potential cellular reservoirs (macrophages).

Macrophage Heterogeneity

Macrophages are the first line of defense against pathogens and become differentially activated in response to the tissue environment in which they reside. Macrophages have been characterized *in vitro* as classically activated (M1), or alternatively activated (M2a, M2b and M2c) (32, 33). Classical activation of macrophages was initially attributed to a Th1 type of response to the secreted molecules of $CD4^+$ Th1 cells. M1 macrophages, which are induced by IFNγ, TNFα, and LPS, display a pro-inflammatory phenotype, enhanced microbicidal activity and secretion of pro-inflammatory cytokines (34). Following the same rationale, alternatively activated macrophages were attributed to a Th2 type of response and were eventually expanded to include all other types of macrophages. M2a macrophages, which are induced by IL4 and IL13, play an important role in wound healing, allergy, response to parasites, and tissue remodeling (35). M2b macrophages are induced by immune complexes and the activation of Fcγ receptors in the presence of TLR signals such as LPS or IL1β through the TLR4 receptor and IL1R respectively (36). Finally, M2c macrophages, which are induced by IL10, TGFβ, and glucocorticoids, have also been termed de-activated or regulatory

macrophages due to their production of anti-inflammatory cytokines (34, 36). Macrophages phenotypes have been studied mainly *in vitro* and not in tissues *in situ*. The role of macrophage polarization in viral infection has begun to be studied *in vitro* but the role of macrophage polarization *in vivo* and is role in viral infections and in the case of HIV viral latency in largely unknown.

Macrophages in HIV infection

Antiretroviral drugs are able to diminish viral load below the limit of detection, but latent reservoirs persist in resting $CD4^+$ T cells and macrophages in tissues (37). Unlike infected $CD4^+$ T cells, tissue macrophages do not undergo cell death as a result of infection and can harbor latent viral DNA for long periods of time (38, 39). Moreover, HIV/SIV infected macrophages are not efficiently killed by $CD8^+$ T cells like infected $CD4^+$ T cells (40, 41). Finally, ART often displays differential antiviral activity in macrophages compared to $CD4^+$ T cells (38). While the $CD4^+$ latent reservoirs in HIV and SIV have been well-characterized, little is known about the establishment and extent of latent reservoirs in tissue macrophage populations and in particular, in the highly diverse populations of tissue-resident macrophages.

Recent fate mapping analyses show that tissue-resident macrophages, such as alveolar macrophages, splenic red pulp macrophages, and microglia, are derived from embryonic yolk sac progenitor cells that self-renew with little to no contribution from circulating monocytes during homeostasis contrary to previous beliefs (42-47). Our lab also recently demonstrated that the spleen is comprised of a mixture of three populations of macrophages, based on the expression of CD68, CD163 and Mac387 markers, which

become differentially infected in pigtailed macaques. In this study, fetal derived $CD163^{+}CD68^{+}$ macrophages became preferentially depleted with SIV infection and the changes in these cell types remained throughout the course of infection (48). Moreover, macrophage CD163 expression was upregulated, which has been previously shown to promote higher HIV infection in these cells (49). Thus, HIV/ SIV infection not only affects the polarization of tissue macrophages but also changes the macrophage populations that comprise the tissue. It is unclear whether macrophage ontogeny drives differential latent states or how the different macrophage populations respond to polarization agents or activating stimuli. Further research is needed in the area of macrophage infection and subsequent latency, despite the lack of specific mechanisms of HIV/SIV infection and latency it is clear that macrophages differ substantially from $CD4^{+}$ T cells.

Quantitative viral outgrowth assay (QVOA)

Our laboratory developed and characterized a consistent, accelerated SIV macaque model for HIV AIDS and neurologic disease (21). In this model, infection of macrophages occurs in lymph nodes, spleen, heart, lungs, peripheral nervous systems, and brain (50-54). Non-human primate models provide a tool to study systemic SIV infection and offer a window into SIV infection of tissue macrophages compared to $CD4^{+}$ T cells. The frequency of HIV or SIV infection of macrophages in tissues has been previously examined (55, 56). However, in most of these studies infection was measured by viral DNA in cells isolated from tissues; this approach overestimates the frequency of productively infected cells due to the large presence of defective proviruses in infected

cells *in vivo* (57, 58). A more rigorous approach to quantify cells that harbor replication competent virus is the quantitative viral outgrowth assay (QVOA). The QVOA was developed to quantitate the number of HIV-infected resting $CD4^+$ T cells that produce infectious virus (59-61). This assay has been used to quantify the number of resting $CD4^+$ lymphocytes *in vivo* in HIV infected individuals on antiretroviral therapy (ART) that harbor replication-competent viral genomes and serves as the gold standard for studying viral latency in lymphocytes (57, 59).

Using the same concept, we developed a macrophage quantitative viral outgrowth assay (MΦ-QVOA) to measure the size of the macrophage cellular reservoir in comparison to the resting $CD4^+$ T cell reservoir. This work provides the first evidence that macrophages contain replication-competent virus that leads to latent infection in SIV-infected ART-treated pigtailed macaques.

REFERENCES

1. **Gottlieb MS, Schroff R, Schanker HM, Weisman JD, Fan PT, Wolf RA, Saxon A.** 1981. Pneumocystis carinii pneumonia and mucosal candidiasis in previously healthy homosexual men: evidence of a new acquired cellular immunodeficiency. N Engl J Med **305:**1425-1431.
2. **Masur H, Michelis MA, Greene JB, Onorato I, Stouwe RA, Holzman RS, Wormser G, Brettman L, Lange M, Murray HW, Cunningham-Rundles S.** 1981. An outbreak of community-acquired Pneumocystis carinii pneumonia: initial manifestation of cellular immune dysfunction. N Engl J Med **305:**1431-1438.
3. **Centers for Disease C.** 1981. Follow-up on Kaposi's sarcoma and Pneumocystis pneumonia. MMWR Morb Mortal Wkly Rep **30:**409-410.
4. **Centers for Disease C.** 1981. Kaposi's sarcoma and Pneumocystis pneumonia among homosexual men--New York City and California. MMWR Morb Mortal Wkly Rep **30:**305-308.
5. **Barre-Sinoussi F, Chermann JC, Rey F, Nugeyre MT, Chamaret S, Gruest J, Dauguet C, Axler-Blin C, Vezinet-Brun F, Rouzioux C, Rozenbaum W, Montagnier L.** 1983. Isolation of a T-lymphotropic retrovirus from a patient at risk for acquired immune deficiency syndrome (AIDS). Science **220:**868-871.
6. **Case K.** 1986. Nomenclature: human immunodeficiency virus. Ann Intern Med **105:**133.
7. **Korber B, Muldoon M, Theiler J, Gao F, Gupta R, Lapedes A, Hahn BH, Wolinsky S, Bhattacharya T.** 2000. Timing the ancestor of the HIV-1 pandemic strains. Science **288:**1789-1796.
8. **Sharp PM, Hahn BH.** 2010. The evolution of HIV-1 and the origin of AIDS. Philosophical transactions of the Royal Society of London Series B, Biological sciences **365:**2487-2494.
9. **Wolfe ND, Switzer WM, Carr JK, Bhullar VB, Shanmugam V, Tamoufe U, Prosser AT, Torimiro JN, Wright A, Mpoudi-Ngole E, McCutchan FE, Birx DL, Folks TM, Burke DS, Heneine W.** 2004. Naturally acquired simian retrovirus infections in central African hunters. Lancet **363:**932-937.
10. **Lifson JD, Feinberg MB, Reyes GR, Rabin L, Banapour B, Chakrabarti S, Moss B, Wong-Staal F, Steimer KS, Engleman EG.** 1986. Induction of CD4-dependent cell fusion by the HTLV-III/LAV envelope glycoprotein. Nature **323:**725-728.
11. **Gartner S, Markovits P, Markovitz DM, Kaplan MH, Gallo RC, Popovic M.** 1986. The role of mononuclear phagocytes in HTLV-III/LAV infection. Science (New York, NY) **233:**215-219.
12. **Ho DD, Rota TR, Hirsch MS.** 1986. Infection of monocyte/macrophages by human T lymphotropic virus type III. J Clin Invest **77:**1712-1715.
13. **Gonda MA, Wong-Staal F, Gallo RC, Clements JE, Narayan O, Gilden RV.** 1985. Sequence homology and morphologic similarity of HTLV-III and visna virus, a pathogenic lentivirus. Science **227:**173-177.
14. **Volberding PA, Deeks SG.** 2010. Antiretroviral therapy and management of HIV infection. Lancet (London, England) **376:**49-62.

15. **International ASSWGoHIVC, Deeks SG, Autran B, Berkhout B, Benkirane M, Cairns S, Chomont N, Chun TW, Churchill M, Di Mascio M, Katlama C, Lafeuillade A, Landay A, Lederman M, Lewin SR, Maldarelli F, Margolis D, Markowitz M, Martinez-Picado J, Mullins JI, Mellors J, Moreno S, O'Doherty U, Palmer S, Penicaud MC, Peterlin M, Poli G, Routy JP, Rouzioux C, Silvestri G, Stevenson M, Telenti A, Van Lint C, Verdin E, Woolfrey A, Zaia J, Barre-Sinoussi F.** 2012. Towards an HIV cure: a global scientific strategy. Nat Rev Immunol **12:**607-614.
16. **Finzi D, Blankson J, Siliciano JD, Margolick JB, Chadwick K, Pierson T, Smith K, Lisziewicz J, Lori F, Flexner C, Quinn TC, Chaisson RE, Rosenberg E, Walker B, Gange S, Gallant J, Siliciano RF.** 1999. Latent infection of CD4+ T cells provides a mechanism for lifelong persistence of HIV-1, even in patients on effective combination therapy. Nat Med **5:**512-517.
17. **Finzi D, Hermankova M, Pierson T, Carruth LM, Buck C, Chaisson RE, Quinn TC, Chadwick K, Margolick J, Brookmeyer R, Gallant J, Markowitz M, Ho DD, Richman DD, Siliciano RF.** 1997. Identification of a reservoir for HIV-1 in patients on highly active antiretroviral therapy. Science **278:**1295-1300.
18. **Eisele E, Siliciano RF.** 2012. Redefining the viral reservoirs that prevent HIV-1 eradication. Immunity **37:**377-388.
19. **Hutter G, Nowak D, Mossner M, Ganepola S, Mussig A, Allers K, Schneider T, Hofmann J, Kucherer C, Blau O, Blau IW, Hofmann WK, Thiel E.** 2009. Long-term control of HIV by CCR5 Delta32/Delta32 stem-cell transplantation. N Engl J Med **360:**692-698.
20. **Allers K, Hutter G, Hofmann J, Loddenkemper C, Rieger K, Thiel E, Schneider T.** 2011. Evidence for the cure of HIV infection by CCR5Delta32/Delta32 stem cell transplantation. Blood **117:**2791-2799.
21. **Deeks SG.** 2012. HIV: Shock and kill. Nature **487:**439-440.
22. **Spivak AM, Planelles V.** 2016. HIV-1 Eradication: Early Trials (and Tribulations). Trends Mol Med **22:**10-27.
23. **Richman DD, Margolis DM, Delaney M, Greene WC, Hazuda D, Pomerantz RJ.** 2009. The challenge of finding a cure for HIV infection. Science **323:**1304-1307.
24. **Lewin S, Evans V, Elliott J, Spire B, Chomont N.** 2011. Finding a cure for HIV: will it ever be achievable? Journal of the International AIDS Society **14:**4.
25. **Chun T-W, Engel D, Mizell SB, Ehler LA, Fauci AS.** 1998. Induction of HIV-1 Replication in Latently Infected CD4+ T Cells Using a Combination of Cytokines. The Journal of Experimental Medicine **188:**83-91.
26. **Archin NM, Espeseth A, Parker D, Cheema M, Hazuda D, Margolis DM.** 2009. Expression of Latent HIV Induced by the Potent HDAC Inhibitor Suberoylanilide Hydroxamic Acid. AIDS Research and Human Retroviruses **25:**207-212.
27. **Kulkosky J.** 2001. Prostratin: activation of latent HIV-1 expression suggests a potential inductive adjuvant therapy for HAART. Blood **98:**3006-3015.
28. **Jiang G, Mendes EA, Kaiser P, Sankaran-Walters S, Tang Y, Weber MG, Melcher GP, Thompson GR, Tanuri A, Pianowski LF, Wong JK, Dandekar**

S. 2014. Reactivation of HIV latency by a newly modified Ingenol derivative via protein kinase Cδ-NF-κB signaling. AIDS (London, England) **28:**1555-1566.
29. **Kaminski R, Chen Y, Fischer T, Tedaldi E, Napoli A, Zhang Y, Karn J, Hu W, Khalili K.** 2016. Elimination of HIV-1 Genomes from Human T-lymphoid Cells by CRISPR/Cas9 Gene Editing. Scientific reports **6:**22555.
30. **Sagot-Lerolle N, Lamine A, Chaix ML, Boufassa F, Aboulker JP, Costagliola D, Goujard C, Pallier C, Delfraissy JF, Lambotte O, study AE.** 2008. Prolonged valproic acid treatment does not reduce the size of latent HIV reservoir. AIDS **22:**1125-1129.
31. **Lewin SR, Evans VA, Elliott JH, Spire B, Chomont N.** 2011. Finding a cure for HIV: will it ever be achievable? J Int AIDS Soc **14:**4.
32. **Cassetta L, Cassol E, Poli G.** 2011. Macrophage polarization in health and disease. TheScientificWorldJournal **11:**2391-2402.
33. **Cassol E, Cassetta L, Alfano M, Poli G.** 2010. Macrophage polarization and HIV-1 infection. Journal of leukocyte biology **87:**599-608.
34. **Gordon S, Taylor P.** 2005. Monocyte and macrophage heterogeneity. Nature reviews Immunology **5:**953-964.
35. **Gordon S, Martinez F.** 2010. Alternative activation of macrophages: mechanism and functions. Immunity **32:**593-604.
36. **Martinez F, Sica A, Mantovani A, Locati M.** 2008. Macrophage activation and polarization. Frontiers in bioscience : a journal and virtual library **13:**453-461.
37. **Smith MZ, Wightman F, Lewin SR.** 2012. HIV reservoirs and strategies for eradication. Curr HIV/AIDS Rep **9:**5-15.
38. **Gavegnano C, Schinazi R.** 2009. Antiretroviral therapy in macrophages: implication for HIV eradication. Antiviral chemistry & chemotherapy **20:**63-78.
39. **Aquaro S, Caliò R, Balzarini J, Bellocchi M, Garaci E, Perno C.** 2002. Macrophages and HIV infection: therapeutical approaches toward this strategic virus reservoir. Antiviral research **55:**209-225.
40. **Walker-Sperling VE, Buckheit RW, 3rd, Blankson JN.** 2014. Comparative analysis of the capacity of elite suppressor CD4+ and CD8+ T cells to inhibit HIV-1 replication in monocyte-derived macrophages. J Virol **88:**9789-9798.
41. **Vojnov L, Martins MA, Bean AT, Veloso de Santana MG, Sacha JB, Wilson NA, Bonaldo MC, Galler R, Stevenson M, Watkins DI.** 2012. The majority of freshly sorted simian immunodeficiency virus (SIV)-specific CD8(+) T cells cannot suppress viral replication in SIV-infected macrophages. J Virol **86:**4682-4687.
42. **Davies LC, Jenkins SJ, Allen JE, Taylor PR.** 2013. Tissue-resident macrophages. Nat Immunol **14:**986-995.
43. **Ginhoux F, Jung S.** 2014. Monocytes and macrophages: developmental pathways and tissue homeostasis. Nat Rev Immunol **14:**392-404.
44. **Prinz M, Priller J.** 2014. Microglia and brain macrophages in the molecular age: from origin to neuropsychiatric disease. Nat Rev Neurosci **15:**300-312.
45. **Gomez Perdiguero E, Klapproth K, Schulz C, Busch K, Azzoni E, Crozet L, Garner H, Trouillet C, de Bruijn MF, Geissmann F, Rodewald HR.** 2015. Tissue-resident macrophages originate from yolk-sac-derived erythro-myeloid progenitors. Nature **518:**547-551.

46. **Yona S, Kim KW, Wolf Y, Mildner A, Varol D, Breker M, Strauss-Ayali D, Viukov S, Guilliams M, Misharin A, Hume DA, Perlman H, Malissen B, Zelzer E, Jung S.** 2013. Fate mapping reveals origins and dynamics of monocytes and tissue macrophages under homeostasis. Immunity **38:**79-91.
47. **Hashimoto D, Chow A, Noizat C, Teo P, Beasley MB, Leboeuf M, Becker CD, See P, Price J, Lucas D, Greter M, Mortha A, Boyer SW, Forsberg EC, Tanaka M, van Rooijen N, Garcia-Sastre A, Stanley ER, Ginhoux F, Frenette PS, Merad M.** 2013. Tissue-resident macrophages self-maintain locally throughout adult life with minimal contribution from circulating monocytes. Immunity **38:**792-804.
48. **Williams DW, Engle EL, Shirk EN, Queen SE, Gama L, Mankowski JL, Zink MC, Clements JE.** 2016. Splenic Damage during SIV Infection: Role of T-Cell Depletion and Macrophage Polarization and Infection. Am J Pathol doi:10.1016/j.ajpath.2016.03.019.
49. **Tuluc F, Meshki J, Spitsin S.** 2014. HIV infection of macrophages is enhanced in the presence of increased expression of CD163 induced by substance P. Journal of leukocyte … doi:10.1189/jlb.4AB0813-434RR.
50. **Haase AT.** 1986. Pathogenesis of lentivirus infections. Nature **322:**130-136.
51. **Kelly KM, Tarwater PM, Karper JM, Bedja D, Queen SE, Tunin RS, Adams RJ, Kass DA, Mankowski JL.** 2012. Diastolic dysfunction is associated with myocardial viral load in simian immunodeficiency virus-infected macaques. AIDS **26:**815-823.
52. **Laast VA, Shim B, Johanek LM, Dorsey JL, Hauer PE, Tarwater PM, Adams RJ, Pardo CA, McArthur JC, Ringkamp M, Mankowski JL.** 2011. Macrophage-mediated dorsal root ganglion damage precedes altered nerve conduction in SIV-infected macaques. Am J Pathol **179:**2337-2345.
53. **Babas T, Vieler E, Hauer DA, Adams RJ, Tarwater PM, Fox K, Clements JE, Zink MC.** 2001. Pathogenesis of SIV pneumonia: selective replication of viral genotypes in the lung. Virology **287:**371-381.
54. **Zink MC, Clements JE.** 2002. A novel simian immunodeficiency virus model that provides insight into mechanisms of human immunodeficiency virus central nervous system disease. J Neurovirol **8 Suppl 2:**42-48.
55. **McIlroy D, Autran B, Cheynier R, Clauvel JP, Oksenhendler E, Debre P, Hosmalin A.** 1996. Low infection frequency of macrophages in the spleens of HIV+ patients. Res Virol **147:**115-121.
56. **Cribbs SK, Lennox J, Caliendo AM, Brown LA, Guidot DM.** 2015. Healthy HIV-1-infected individuals on highly active antiretroviral therapy harbor HIV-1 in their alveolar macrophages. AIDS Res Hum Retroviruses **31:**64-70.
57. **Eriksson S, Graf EH, Dahl V, Strain MC, Yukl SA, Lysenko ES, Bosch RJ, Lai J, Chioma S, Emad F, Abdel-Mohsen M, Hoh R, Hecht F, Hunt P, Somsouk M, Wong J, Johnston R, Siliciano RF, Richman DD, O'Doherty U, Palmer S, Deeks SG, Siliciano JD.** 2013. Comparative analysis of measures of viral reservoirs in HIV-1 eradication studies. PLoS Pathog **9:**e1003174.
58. **Ho YC, Shan L, Hosmane NN, Wang J, Laskey SB, Rosenbloom DI, Lai J, Blankson JN, Siliciano JD, Siliciano RF.** 2013. Replication-competent

noninduced proviruses in the latent reservoir increase barrier to HIV-1 cure. Cell **155:**540-551.

59. **Siliciano JD, Siliciano RF.** 2005. Enhanced culture assay for detection and quantitation of latently infected, resting CD4+ T-cells carrying replication-competent virus in HIV-1-infected individuals. Methods Mol Biol **304:**3-15.
60. **Rosenbloom DIS, Elliott O, Hill AL, Henrich TJ.** 2015. Designing and interpreting limiting dilution assays: general principles and applications to the latent reservoir for HIV-1. bioRxiv.
61. **Laird GM, Eisele EE, Rabi SA, Lai J, Chioma S, Blankson JN, Siliciano JD, Siliciano RF.** 2013. Rapid quantification of the latent reservoir for HIV-1 using a viral outgrowth assay. PLoS Pathog **9:**e1003398.

II. Quantitation of Productively Infected Monocytes and Macrophages of SIV-Infected Macaques

The following section of the dissertation has been published previously and the text is quoted verbatim from the following:

Quantitation of Productively Infected Monocytes and Macrophages of SIV-Infected Macaques. Claudia R. Avalos, Sarah L. Price, Ellen R. Forsyth, Julia N. Pin, Erin N. Shirk, Brandon T. Bullock, Suzanne E. Queen, Ming Li, Dane Gellerup, Shelby L. O'Connor, M. Christine Zink, Joseph L. Mankowski, Lucio Gama, Janice E. Clements. J. Virol. 2016. 90(12), pp. 5643-5656.
PMCID: PMC4886778.

The scientific and technical contributions of the other authors to this work can be found in the acknowledgments section at the end of Chapter II.

Quantitation of Productively Infected Monocytes and Macrophages of SIV-Infected Macaques

Claudia R. Avalos[1], Sarah L. Price[1], Ellen R. Forsyth[1], Julia N. Pin[1], Erin N. Shirk[1], Brandon T. Bullock[1], Suzanne E. Queen[1], Ming Li[1], Dane Gellerup[4], Shelby L. O'Connor[4], M. Christine Zink[1,2], Joseph L. Mankowski[1,2,3], Lucio Gama[1], Janice E. Clements[1,2,3,#]

[1]Department of Molecular and Comparative Pathobiology, Johns Hopkins University School of Medicine, Baltimore, Maryland, United States of America.

[2]Department of Pathology, Johns Hopkins University School of Medicine, Baltimore, Maryland, United States of America.

[3]Department of Neurology, Johns Hopkins University School of Medicine, Baltimore, Maryland, United States of America.

[4]Department of Pathology and Laboratory Medicine, University of Wisconsin School of Medicine, United States of America.

Running Title: Quantitation of SIV-infected myeloid cells.

Word Counts: Abstract (228), Importance (150), Text (5,462)

[#]Corresponding author, E-mail: jclements@jhmi.edu (JEC)

ABSTRACT

Despite the success of combined antiretroviral therapy (ART), HIV remains a life-long infection because of latent viral reservoirs in infected patients. The contribution of $CD4^+$ T cells to infection and disease progression has been extensively studied. However, during early HIV infection macrophages in the brain and other tissues are infected and contribute to tissue specific diseases, such as encephalitis and dementia in brain and pneumonia in lung. The extent of infection of monocytes and macrophages has not been rigorously assessed with assays comparable to those used to study infection of $CD4^+$ T cells and to evaluate the number of $CD4^+$ T cells that harbor infectious viral genomes. To assess the contribution of productively infected monocytes and macrophages to HIV and SIV infected cells *in vivo*, we developed a quantitative virus outgrowth assay (QVOA) based on similar assays used to quantitate $CD4^+$ T cell latent reservoirs in ART suppressed HIV- and SIV-infected individuals. $CD11b^+$ selected myeloid cells were serially diluted and co-cultured with susceptible cells to amplify virus. TCRβ RNA was measured as a control to assess the potential contribution of $CD4^+$ T cells in the assay. Virus production in the supernatant was quantitated by qRT-PCR. Productively infected myeloid cells were detected in blood, bronchoalveolar lavage, lungs, spleen, and brain, demonstrating that these cells persist throughout SIV infection and have the potential to contribute to the viral reservoir during ART.

IMPORTANCE

Infection of $CD4^+$ T cells and their role as latent reservoirs has been rigorously assessed; however, the frequency of productively infected monocytes and macrophages *in vivo* has not been similarly studied. Myeloid cells, unlike lymphocytes, are resistant to the cytopathic effects of HIV. Moreover, tissue-resident macrophages have the ability to self-renew and persist in the body for months to years. Thus, tissue macrophages, once infected, have the characteristics of a potentially stable viral reservoir. A better understanding of the number of productively infected macrophages is crucial to further evaluate the role of infected myeloid cells as a potential viral reservoir. Here we compare the frequency of productively infected $CD4^+$ T cells and macrophages in a SIV-macaque model. We developed a critical assay that will allow us to quantitate myeloid cells containing viral genomes that lead to productive infection in SIV-infected macaques and assess the role of macrophages as potential reservoirs.

INTRODUCTION

Lentiviruses infect myeloid lineage cells in tissues and these cells are responsible for the multi-organ disease characteristic of this family of retroviruses (1-3). HIV was the first primate lentivirus identified that infects $CD4^+$ T cells as well as myeloid cells in blood and tissues of infected individuals (4-6). HIV infects myeloid cells in lymph nodes, spleen, heart, lungs, peripheral nervous system, and the central nervous system (CNS) (7-11). HIV encodes genes that specifically interact and/or interfere with restriction factors present in myeloid cells, providing evolutionary evidence that HIV replication in myeloid cells is important for virus replication and pathogenesis *in vivo* (12).

Myeloid cells were thought to be terminally differentiated cells with a limited lifespan. However, recent studies have demonstrated that resident tissue macrophages are capable of self-renewal and that monocytes from blood differentiate into distinct macrophage phenotypes after entering tissues (13, 14). Moreover, tissue-resident macrophages, such as alveolar macrophages, splenic red pulp macrophages, and microglia, are derived from embryonic yolk sac progenitor cells that self-renew with little to no contribution from circulating monocytes during homeostasis (15-18). Furthermore, HIV- and SIV-infected macrophages are not efficiently killed by $CD8^+$ T cells as are infected $CD4^+$ T cells (19, 20). Thus, resident tissue macrophages remain in tissues long-term, are relatively resistant to the cytopathic effects of HIV infection compared to $CD4^+$ T cells, and may serve as stable viral reservoirs.

SIV macaque models have been used to study the pathogenesis of SIV *in vivo*, as models of HIV infection in humans. Like HIV, SIV infects both $CD4^+$ T cells and macrophages in blood, tissues, and brain (21-25). Our laboratory developed and

characterized a consistent, accelerated SIV macaque model resulting in AIDS and CNS disease (in ~80% of macaques) in three months compared to the longer course of disease pathogenesis and frequency of CNS disease in other SIV models (21). Another model to study CNS infection used depletion of $CD8^+$ T cells in SIV-infected macaques resulting in increased accumulation of infected macrophages in the CNS and heightened severity of neurological disease, suggesting that infection of macrophages plays a key role in CNS disease (26).

The frequency of HIV or SIV infection of macrophages in tissues has been examined previously in a number of studies (27, 28). Infection is quantified by measuring viral DNA in cells isolated from tissues; however, this approach overestimates the number of productively infected $CD4^+$ T cells due to the presence of a large proportion of defective proviruses *in vivo* (29, 30). A more rigorous approach to quantify cells that harbor replication competent virus is the quantitative viral outgrowth assay (QVOA), which quantitates the number of HIV-infected resting $CD4^+$ T cells that produce infectious virus (31-33). This assay has been used to quantify the number of resting $CD4^+$ lymphocytes *in vivo* in HIV infected individuals on antiretroviral therapy (ART) that harbor replication competent viral genomes and serves as one of the major assays for studying viral latency in that cell type (29, 31).

Using a QVOA that our laboratory developed for SIV-infected non-human primate $CD4^+$ T cells, we previously demonstrated that the number of infected resting $CD4^+$ T cells in SIV-suppressed macaque blood and tissues was equivalent to the number of infected resting $CD4^+$ T cells in HIV-infected humans on ART (31-35). In this study, we developed a novel macrophage quantitative viral outgrowth assay (МΦ-QVOA) to

assess the frequency of productively SIV-infected monocytes (in blood) and macrophages (in tissues) using a well-characterized SIV macaque model (36-38). To determine the potential contribution of $CD4^+$ T cells to the quantitation of macrophages, we also assessed the number of $CD3^+$ T cells in each assay by measuring TCRβ RNA.

Using the myeloid MΦ-QVOA, we show that during chronic SIV infection productively infected monocytes or macrophages are present in blood, bronchoalveolar lavage (BAL), lungs, spleen, and brain. This assay can also be used to quantify HIV and SIV productively infected myeloid cells that may contribute to viral persistence and latency in ART-treated humans and macaques.

MATERIALS AND METHODS

Animal Studies

Fourteen juvenile pigtailed macaques (*Macaca nemestrina*) were inoculated intravenously with the SIV/DeltaB670 swarm and the macrophage-tropic clone SIV/17E-Fr as previously described (36, 38, 39). One macaque Pm11 was treated 12 days post-inoculation (d.p.i.) with 12.5 mg fluconazole and 5mg paroxetine once/day orally and euthanized at ~80 d.p.i. as previously described (40). Three macaques Pm12, Pm13, and Pm14 were treated 28 days prior to virus inoculation with 2mg/kg minocycline twice/day orally and were euthanized during asymptomatic infection (~35 d.p.i.). These macaques were added to the study to investigate macrophage infection at different time after infections. These treatments did not affect either plasma viral load or disease progression (40). Eleven macaques were euthanized during late-stage infection (50-87 days post-inoculation (d.p.i.)), and three macaques were euthanized during chronic infection (34-36 d.p.i.; **Error! Reference source not found.**). Blood and cerebrospinal fluid (CSF) samples were collected longitudinally post-infection. When macaques were euthanized, they were perfused with sterile saline to remove blood and circulating virus as described elsewhere (35). Viral loads in plasma and CSF, $CD4^+$ T cell counts in blood, and viral RNA levels in tissues were determined for all macaques in the study (**Error! Reference source not found.**). To assess the extent of CNS inflammation and pathology, brain tissue was evaluated as previously described and scored ranging from none to severe (38). These studies were performed in accordance with federal guidelines and institutional policies.

Isolation of Myeloid Cells and Lymphocytes from Blood and Tissues

Peripheral blood mononuclear cells (PBMCs) were isolated by density gradient centrifugation on a 1.077g/mL Percoll/Hanks gradient (GE Healthcare, Pittsburgh PA) according to manufacturer's protocol. Bronchoalveolar lavage (BAL) was obtained by passing 250 mL of sterile saline (Life Technologies, Grand Island NY) via bronchoscope. BAL cells were isolated by passing lavage samples through a 183 μm pore size sterile mesh. Spleen and lung cells were mechanically removed from tissues using an 18-gauge needle and passed through a 100 μm cell strainer. Brain parenchymal macrophages and microglia were isolated as previously described (41).

Blood, BAL, lung, and spleen macrophages were cultured in RPMI 1640 media (Life Technologies) supplemented with 20% heat-inactivated human AB serum (Gemini Bio Products, West Sacramento CA), 100 U/mL penicillin-streptomycin (Life Technologies), 20 μg/mL gentamycin (Life Technologies), 2mM L-glutamine (Life Technologies), 2 mM sodium pyruvate (Sigma), 10 mM HEPES buffer (Life Technologies), and 50 ng/mL recombinant human Macrophage Colony Stimulating Factor (M-CSF) (R&D, Minneapolis MN). Brain macrophages were cultured in DMEM (Life Technologies) supplemented with 5% heat-inactivated bovine serum FBS (Atlanta Biologicals), 5% IS Giant Cell Tumor Conditioned Media (Irvine Scientific, Santa Ana CA), 100 U/mL penicillin- streptomycin (Life Technologies), 70 μg/mL gentamycin (Life Technologies), 2 mM L-glutamine (Life Technologies), 3 mM sodium pyruvate (Sigma), and 10 mM HEPES buffer (Life Technologies).

$CD4^+$ T cells were cultured in RPMI supplemented with 10% heat-inactivated bovine serum (Atlanta Biologicals), 100 U/mL penicillin-streptomycin (Life

Technologies), 1% T cell growth factor (31), and 100 U/mL IL-2 (Novartis, NY, NY). Samples were analyzed fresh, or frozen viably and rapidly thawed in corresponding media prior cell isolation.

Macrophage Quantitative Viral Outgrowth Assay (MΦ-QVOA)

Monocytes and tissue macrophages strongly express the integrin CD11b (42), a common myeloid marker (43-46). Myeloid cells were purified based on expression of CD11b with a non-human primate CD11b antibody-conjugated Microbead kit (Miltenyi Biotec, Auburn CA) according to the manufacturer's protocol. The purified macrophages were cultured in triplicate in a ten-fold limiting dilution in the presence of 10 μM zidovudine (Sigma) and 25 nM darunavir (Janssen, Titusville NJ) for 3 days for cell attachment or 7 days for differentiation of peripheral blood monocytes. Poly-L-lysine coated plates (Sigma) were used and plates were spun down at 2,000 rpm (872xg) for 10 minutes to increase cell adherence. Cells were washed twice with HBSS (Life Technologies) to remove non-adherent $CD3^+$ lymphocytes. Media containing 10 ng/mL recombinant human Tumor Necrosis Factor alpha (TNFα) (ProSpec, East Brunswick NJ) and 1x10^5 CEMx174 cells/well were added to each well. CEMx174 cells served to expand the virus released from infected cells as previously described (47). Media were replenished with TNFα after 4 days in co-culture; supernatants and cell lysates were collected following 12 days of co-culture with CEMx174 cells. The presence of replication-competent virus was determined by isolating RNA from supernatant and measuring SIV RNA by qRT-PCR. The frequency of cells harboring replication-competent virus was determined by limiting dilution assay statistics (32) and expressed as

infectious units per million (IUPM). Two sets of negative control wells with CEMx174 cells only were added to the cultures. In addition, to determine the number of $CD3^+$ T cells that were in the assay, duplicate control wells of $CD11b^+$ macrophages without CEMx174 cells were used to measure TCRβ RNA as described below.

Generation of RNA Standards for TCRβ RNA Assay

RNA isolated from macaque $CD3^+$ T cells was reverse transcribed into cDNA using the SuperScript II enzyme kit (Life Technologies) with 4.1mM $MgCl_2$, 0.5 mM dNTP, 1mM DTT, 150 ng random hexamers, 1x first strand buffer, and 1 unit of RNase OUT in a 20 uL reaction. The sample was incubated at 25°C for 15 min, 42°C for 40 min, 85°C for 10 min, and 25°C for 10 min. Resulting cDNA was amplified by PCR using the PCR SuperMix High Fidelity kit (Life Technologies) with the TCRβ primers as follows: Fwd- 5'-GAG GAC CTG AAA AAG GTG TTC-3', and Rev- 5'-CAT AGA GGA TGG TGG CAG ACA-3', designed for the constant region of TCRβ chain of macaques as previously described (48). The mix was incubated for 30 seconds at 94°C followed by 35 cycles of 94°C for 15 seconds, 50°C for 15 seconds, and 68°C for 30 seconds, then incubated at 72°C for 10 min. The resulting TCRβ PCR product was cloned into a pCR2.1 TOPO vector, sequenced, and confirmed. For *in vitro* RNA transcription, the plasmid was digested with BamHI, and TCRβ RNA was then generated with the Mega Script T7 kit (Life Technologies) and used as control transcript for the standard curve.

Quantitation of TCRβ RNA

TCRβ RNA was quantitated by qRT-PCR using QuantiTect Kit (Qiagen), the above described primers, and the following probe 5'-/56-FAM/ACT TCC GCT/ZEN/ GCC AAG TCC AGT TCT AT/3IABkFQ/-3' based on sequence analyses of macaque TCRβ RNA. Cycling conditions were as follows: 50°C for 30 min, 95°C for 15 min, 45 cycles of 94°C for 15 sec, 55°C for 15 sec, and 60°C for 30 sec. *18s* ribosomal RNA was multiplexed with the TCRβ RNA to control for cell counts. To determine the average number of TCRβ copies per $CD3^+$ T cell, PBMCs from seven uninfected macaques were labeled with PE-conjugated anti-CD3 clone SP34 (BD Bioscience, San Jose CA) and magnetically separated using an EasySep™ PE Positive Selection Kit (Stemcell Technologies, Vancouver BC, Canada). Purity of the cells was confirmed by flow cytometry (Figure 2A). A minimum of 4 aliquots of a million $CD3^+$ T cells from each macaque were used to isolate RNA that was analyzed by qRT-PCR for TCRβ RNA and the number of copies of TCRβ RNA per macaque $CD3^+$ T cell was calculated (Figure 2B).

Flow Cytometry

All $CD11b^+$ myeloid cells were labeled with PE conjugated anti-CD3 clone SP34 (BD Bioscience) and FITC conjugated anti-CD11b clone Bear1 (Beckman Coulter, Brea CA) to assess selection efficiency. Purified $CD4^+$ T cells were stained with antibodies for HLA-DR clone L243 (Biolegend), CD3 clone SP34-2 (BD Bioscience), CD4 clone OKT4 (Biolegend), CD8 clone RPA-T8 (Biolegend), and TCRγδ clone B1.1 (eBioscience). Cells were stained for 20 minutes at room temperature in 100 μL PBS 2% FBS and fixed for 10 min with Fix/Lyse buffer (Becton Dickinson, Franklin Lakes, NJ).

After fixation, samples were analyzed in a BD LSRFortessa Flow Cytometer using DIVA software (Becton Dickinson, Franklin Lakes NJ). The gating of $CD3^+$ T cells was easily visualized as small $CD3^+$ non auto-fluorescent cells. All data were analyzed using FlowJo software. $CD4^+$ T cell and monocyte cell counts were analyzed as previously described (38).

Fluorescence Microscopy

Co-cultured live monocyte-derived macrophages were treated at 37°C for 4 hours with 10 μM pHrodo Green *Escherichia coli* bioparticles (Life Technologies), which can be phagocytosed only by functional macrophages and are non-fluorescent at neutral pH, fluorescing in the acidic pH of phagosomes (49). Cells were then stained at room temperature for 20 minutes with two drops/mL NucBlue Live nuclear marker (Life Technologies), a Hoechst 33342 nuclear marker that emits fluorescence when bound to DNA (50). Images were taken on a Nikon Eclipse TE200 Fluorescence Microscope and merged using Adobe Photoshop CS4 (Adobe, San Jose CA).

T Cell Viral Outgrowth Assay

Total $CD4^+$ T cells were enriched with a non-human primate microbead isolation kit (Miltenyi Biotec), which depleted cells expressing CD8, CD11b, CD16, CD20, CD56, and CD66abce. Infected $CD4^+$ T cells were quantified by using a previously described five-fold limiting dilution assay (34, 35, 47). Cells were co-cultured with CEMx174 for two weeks. Culture supernatant was analyzed for SIV RNA by qRT-PCR. The

frequencies of infected cells were determined by limiting dilution assay statistics (32) and were expressed in terms of infectious units per million (IUPM).

RNA Isolation from Cells and Tissues

RNA from cell cultures was isolated with RNeasy Plus Mini Kit (Qiagen, Valencia CA) according to manufacturer's protocol with modifications. An on-column DNase digestion was performed using the RNase-free DNase kit (Qiagen) with the addition of four units of TURBO DNase (Life Technologies) to the enzyme mix. 200 μL of fluid (from CSF, plasma, and culture supernatants) was isolated using the QIAamp MinElute Virus Spin Kit (Qiagen) according to manufacturer's protocol with modifications. An on-column DNase digestion was performed using the RNase-free DNase kit (Qiagen), with the addition of three units of RQ1 DNase (Promega, Madison WI) to the enzyme mix.

Frozen tissues were isolated with RNase STAT-60 (Tel Test Inc., Friendswood TX) and homogenized with the FastPrep®-24 instrument (MP Biomedicals, Santa Ana CA) in lysing matrix D tubes (MP Biomedicals). The sample was separated with chloroform and the aqueous phase was treated with isopropanol to precipitate RNA. The RNA was purified with the RNeasy Mini Kit (Qiagen), with an on-column DNase digestion using the RNase-free DNase kit (Qiagen), and the addition of three units of RQ1 DNase (Promega) to the enzyme mix.

Quantitation of SIV RNA

SIV RNA was measured by qRT-PCR using the QuantiTect Virus Kit (Qiagen) and primers in the SIV *gag* region as previously described (34, 51, 52). Three reactions were performed for each sample. To control for DNA contamination, one reaction was analyzed without reverse transcriptase. Samples were analyzed using the Rotogene thermocycler (Qiagen).

PBMC infection

PBMCs from uninfected pigtailed macaques were isolated by Percoll density gradient and plated in 48 well plates in RPMI media supplemented with 2 μg/mL recombinant human IL-2 (Life Technologies) and 2 μg/mL PHA-M (Life Technologies) overnight. PBMCs were spinoculated for 2 hours with 100 μL supernatants of triplicate independent wells from macaques Pm6 and Pm4 (blood, spleen, microglia and lung) MΦ-QVOAs. PBMCs were infected for 5 hours at 37°C, the supernatant was removed, and excess virus washed five times with sterile saline. Media were replaced and supplemented with 2 μg/mL IL-2 (Life Technologies). Supernatants were collected at days 5, 10, and 13 post-inoculation.

SIV *env* sequence analyses

Supernatant RNA was reverse transcribed into cDNA using the SuperScript III reverse transcriptase enzyme kit (Life Technologies) according to manufacturer's protocol. Resulting cDNA was amplified using the Platinum PCR SuperMix High Fidelity kit (Life Technologies), according to manufacturer's protocol, with two rounds of nested PCR against SIV *env* primers. The primer sequences were as follows: 1st round

(Fwd: 5'-ARG AAT GCG ACA ATT CCC CT-3'; Rev: 5'-TCC ATC ATY CTT GTG CAT GAA G-3') and 2nd round (Fwd: 5'- CAG TCA CAG AAC AGG CAA TAG A-3'; Rev: 5'-TAA GCA AAG CAT AAC CTG GMG GT-3'). Both rounds were amplified with the same cycling conditions: 94°C for 1 minute then 40 cycles of 94°C for 30 seconds, 55°C for 30 seconds, 72°C for 1 minute. Resulting product was ~560 base pairs. The PCR product was purified using the DNA clean & concentrator-5 kit (Zymo Research) according to manufacturer's protocol and sequenced on an Illumina MiSeq. Sequences were analyzed using Geneious version 8.0 (Biomatters, Auckland, New Zealand).

Statistics

Infected cell frequencies in limiting dilution assays were calculated using the IUPMStats v1.0 infection frequency calculator (http://silicianolab.johnshopkins.edu) (32). Correlations were computed using a two-tailed nonparametric Spearman rank correlation analysis. Statistics were performed using Prism Software (GraphPad Software, La Jolla CA).

RESULTS

Development of the macrophage viral outgrowth assay (MΦ-QVOA).

The viral outgrowth assay used to measure productively infected HIV and SIV infected resting $CD4^+$ T cells uses highly purified resting $CD4^+$ T cells that are serially diluted and activated with IL-2 (31, 33). To amplify infectious virus produced by $CD4^+$ T cells, susceptible human cell lines are added to each well (MT4 or CEMx174 cells) and virus in the cell supernatants is quantified by qRT-PCR or ELISA (33-35, 47). The frequency of productively infected cells is calculated based on the number of virus or viral RNA positive in each of the serial dilutions (32, 33).

Our macrophage quantitative viral outgrowth assay (MΦ-QVOA) was based on same experimental approach as the $CD4^+$ T cell QVOA. Monocytes and tissue macrophages strongly express the integrin CD11b (42) and could be separated from other cell types by sorting with CD11b Miltenyi magnetic beads (43-46). The $CD11b^+$ cells were serially diluted and antiretroviral drugs were added to the culture to prevent virus spread from non-adherent $CD4^+$ T cells. Unlike T cells, macrophages do not divide exponentially when activated in culture and require adherence to culture plates when grown *in vitro* (53). After monocytes or macrophages adhered to the culture plate, residual non-adherent T cells were removed from each well (Figure 1C).

The purity of myeloid cells selected with CD11b beads was assessed by flow cytometry by examining cells that expressed CD3 and CD11b. $CD11b^+$ myeloid cells from blood, BAL, lungs, spleen, and brain from fourteen SIV-infected macaques were analyzed. Flow cytometry analyses of PBMCs isolated from blood after $CD11b^+$ selection showed that there were <1% $CD3^+$ cells in the selected cells (Figure 1A). The

percentage of $CD11b^+$ cells selected from tissues ranged from 94% - 99.1% (Figure 1B). $CD11b^+$ cells adhered to the culture plates and any residual $CD3^+$ lymphocytes that remained in the culture supernatant did not proliferate (Figure 2C).

To evaluate the presence of contaminating $CD4^+$ T cells in the macrophage cultures, $CD11b^+$ macrophage control wells without CEMx174 cells were analyzed at 12 days post-seeding, lysed, and TCRβ RNA was quantitated by qRT-PCR. TCRβ RNA is present in macaque $CD3^+$ T cells with an average of 3.8 ± 0.8 copies per cell, as it was determined by qRT-PCR (Figure 2B).

The number of $CD3^+$ T cells quantified prior to $CD11b^+$ selection, after $CD11b^+$ selection, and at the end of the MΦ-QVOAs in the control wells without CEMx174 cells was calculated (Figure 2C). On average, less than 0.9% $CD3^+$ T cells remained in the monocyte-derived macrophages, 0.3% and 1.5% in the BAL and lung macrophages, respectively, 2.5% in the splenic macrophages, and 0.06% in the brain MΦ-QVOAs at the end of the assay. Based on the frequency of infection of $CD4^+$ T cells quantitated by the standard QVOA in Table 3 and the $CD4^+$ T cell percentages by flow cytometry in the blood and spleen, we calculated that there was on average less than one infected $CD4^+$ T cell in any of the MΦ-QVOA assays (Table 2). Therefore, the small number of $CD4^+$ T cells that remained in the wells was not sufficient to contribute to virus quantitated in the MΦ-QVOAs.

To ensure that SIV virus gene expression was active in all the infected macrophages, TNFα, a potent activator of macrophages and the U1 monocytic cell line (54, 55), was added to all wells along with CEMx174 cells to expand replication-

competent viruses. CEMx174 is a T/B cell hybrid line used widely to propagate all strains of SIV, including those used to infect the macaques in this study (47, 56).

Cell supernatants and lysates were isolated separately after 12 days of co-cultivation (Figure 3A). Viral RNA was isolated from cell supernatants from triplicate wells and quantitated individually by qRT-PCR. Wells were considered positive for SIV when RNA levels were higher than 50 copies per 200 μL of supernatant, which is the threshold of detection for qRT-PCR. The frequency of infectious virus per million (IUPM) was calculated using limiting dilution statistical analyses (32).

To determine the viability of the macrophages co-cultured with CEMx174 cells, phagocytosis, a function of viable macrophages, was measured by assessing the number of cells that engulfed pHrodo green *E. coli* bioparticles (Figure 3B). Both CEMx174 cells and macrophages were stained with NucBlue live nuclear stain. The number of cells stained with both markers in each dilution of macrophages reflected the number of viable $CD11b^+$ macrophages plated in the well. Despite the numerous CEMx174 in the co-culture system and the prolonged cell activation, the number of double-labeled macrophages reflected the number originally plated. Furthermore, wells from 10^6 $CD11b^+$ macrophages plated with CEMx174 cells (second column) and without (last column) showed equivalent number of double-labeled cells. This suggests that the macrophages remained viable throughout the MΦ-QVOA experiment despite the co-culture conditions. Finally, Figure 3B demonstrated that macrophages, unlike lymphocytes, did not expand in culture; therefore the MΦ-QVOA assay is only a minimum estimate of the size of the reservoir.

Quantitation of productively infected myeloid cells and CD4$^+$ T in blood and tissues.

The SIV MΦ-QVOA assay was used to quantitate the number of productively infected monocytes in blood and macrophages in BAL, lungs, spleen, and brain of SIV-infected macaques (Figure 4). The quantitation of infected macrophages is an estimate of infection based on the assumption that the cells isolated are representative of the population in each tissue. The frequency of productively infected macrophages in each tissue varied among the macaques, with the highest number in spleen (median 424 IUPM), a secondary lymphoid tissue that contains both CD4$^+$ T cells and tissue resident macrophages. The high frequency of productively infected macrophages was found in macaques with late stage disease (>84 d.p.i) as well as chronic disease (34-36 d.p.i) suggesting that there is a steady state level of infected macrophages in spleen or that there is replenishment of infected macrophages throughout infection due to macrophage turnover. In lung, the number of productively infected interstitial macrophages were also very similar between the animals with late stage and chronic infection and the mean is ~2.5 fold higher than the infected alveolar macrophages. However, when the interstitial and alveolar macrophages were compared within the same macaques, the levels correlated significantly (r=1, p<0.05) (Figure 5). The interstitial macrophages are derived from blood monocytes, and interestingly, monocyte-derived macrophages from blood had 31.5 IUPM, equivalent to levels in interstitial macrophages (32.2 IUPM) (Figure 4).

The majority of the CD11b$^+$ cells isolated from brain represent microglia; however, perivascular macrophages, which are monocyte-derived-macrophages from blood, also express CD11b. Brain microglia/macrophages had the widest range of productively infected cells among all the tissues and between macaques. While spleen

contained the highest number of infected cells, the brain of animals with mild to severe CNS disease contained the next highest level of infected cells (median 231 IUPM). The two macaques with the most productively infected cells (Pm3 and Pm4 with 24,000 IUPM) had severe encephalitis and high levels of viral RNA in brain. The macaques without CNS disease had undetectable numbers of infected microglia/macrophages (Table 3) and little or no detectable viral RNA in the brain (Pm9 through Pm12) (Table 1). The number of productively infected microglia/macrophages trended toward a correlation with SIV RNA in the two regions of the brain with the highest levels of viral RNA, basal ganglia (r=0.71) and parietal cortex (r=0.64) (Figure 5).

Productively infected $CD4^+$ T cells in the blood had a median of 206 IUPM, almost 10 fold higher than the number of infected monocytes in blood (34, 35). However, there was no correlation between plasma viral load and the frequency of infected macrophages or lymphocytes in a particular tissue or blood. The QVOAs provided a comparison of the minimum estimate of productive infection in the two major SIV target cells. Further, it suggested that macrophages are a significant source of virus from tissues during chronic infection.

Infectivity and sequence analyses of virus from MΦ-QVOA

To confirm that virus produced in the MΦ-QVOAs was replication competent, supernatants that contained virus from the MΦ-QVOA from blood monocyte-derived macrophages, lung, spleen, and brain of SIV-infected macaques Pm4 and Pm6 were used to infect PBMCs isolated from uninfected macaques. After infection, supernatants from the newly infected PBMCs were analyzed at multiple time points for SIV RNA by qRT-

PCR. Viral spread was observed in all wells (Figure 6B), indicating that all original MΦ-QVOA supernatants contained replication competent virus. Interestingly, wells with <50 copies per 200 μL of supernatant in the spleen (red symbols) efficiently infected the PBMCs suggesting that the virus in the MΦ-QVOAs was infectious even when there was low levels of SIV RNA found in the supernatants. This provides evidence that this novel viral outgrowth assay functioned like the $CD4^+$ T cell QVOA.

Sequence analysis of the V1 region of SIV *env* was performed with virus isolated from the QVOA wells done in both $CD4^+$ T cells and macrophages from the spleens of SIV-infected macaques Pm4, Pm5 and Pm6. The predominant virus found in the MΦ-QVOA and the $CD4^+$ T cell QVOA was very similar within the spleens of the same macaque (Figure 7A and 7C). Furthermore, the virus produced from $CD4^+$ T cells and macrophages of three animals also had very similar sequences (Figure 7B). To exclude the possibility of virus selection from co-culture with CEMx174 cells, virus isolated from control $CD11b^+$ macrophage wells without CEMx174 cells was also analyzed. Only one macrophage control well had a sequence different than the predominant sequence in the other MΦ-QVOA wells. This suggests that co-culture with CEMx174 cells did not significantly affect the viruses that replicated and were detected in the MΦ-QVOA. Further, the similarity of the infectious virus isolated from $CD4^+$ T cells and macrophages in spleen during chronic infection suggest that SIV viruses in spleen at this period are dual-tropic infecting both $CD4^+$ T cells and macrophages.

DISCUSSION

HIV and SIV infection in tissues and *in vitro* has been widely studied. However, the number of macrophages in tissues and monocytes in blood that harbor replication competent virus has not been quantitated. In this study, we developed an assay to measure the number of blood monocytes and tissue macrophages that contain replication competent virus. This assay is based on our previous macaque $CD4^+$ T cell QVOA. The assay required an understanding that macrophages require culture conditions for adherence and that they do not undergo exponential expansion, as do $CD4^+$ T cells. The *in vitro* culture of primary tissue macrophages also required different conditions for each tissue that we studied, unlike isolation of $CD4^+$ T cells from blood and tissues. In order to select macrophages from tissues, expression of the CD11b antigen was used since it is uniformly expressed on monocytes and macrophages. In addition, to exclude the contribution of $CD4^+$ T cells to this assay we developed an assay for the detection and quantitation of TCRβ RNA.

Using this MΦ-QVOA, we quantitated the number of macrophages that contained replication-competent virus in blood, BAL, lung, spleen and brain of SIV-infected macaques. We demonstrated that macrophages isolated from the blood and from several tissues of SIV-infected macaques harbored replication-competent virus. We also showed that the blood-derived and tissue macrophages used in the MΦ-QVOA had normal phagocytic function and remained viable throughout the assay despite prolonged culture and activation with TNFα. Further, virus produced by the cells in the MΦ-QVOA was capable of *de novo* infection of macaque PBMCs. Finally, we characterized the virus isolated from the MΦ-QVOA by analyzing *env* sequences and virus infectivity in

PBMCs. *Env* sequences from viruses isolated from $CD4^+$ T cell and macrophage QVOAs were not substantially different. All isolated viruses replicated efficiently in PBMC suggesting no selection in macrophages for altered virus tropism.

The number of productively infected macrophages in a given tissue was surprisingly similar from macaque to macaque, whereas the number of productively infected macrophages varied widely in different tissues from the same SIV-infected macaque. The near 10-fold difference in productively infected monocytes compared to $CD4^+$ T cells in blood suggests that monocytes are either less susceptible to SIV infection, have a higher turnover, or harbor more viral genomes that are not replication competent. The highest number of infected macrophages (424 IUPM) was measured in spleen demonstrating that splenic macrophages are highly susceptible to SIV infection and harbor high levels of productive genomes. This suggests a role for tissue microenvironments in mediating virus infection of macrophages (57, 58). Populations of macrophages that reside in each tissue may be differentially susceptible to SIV/HIV infection based on the cytokine profiles of the organs (59-61).

It has been recently demonstrated that tissues contain two phenotypically different macrophage populations that are derived either from resident, i.e. fetal-derived macrophages or monocyte-derived macrophages that enter tissues from the bloodstream (62, 63). There are many indications that both types of macrophages harbor persistent virus after ART suppression. HIV patients that have completely controlled plasma viral load yet have detectable virus in the CSF, some with accompanying CNS symptoms (64, 65). HIV and SIV infection in brain is predominantly in resident microglia and perivascular macrophages (66-68). In addition, lung inflammation is ongoing in some

patients suppressed on ART, in part, due to infected tissue macrophages (69, 70). ART suppression of virus replication at all stages of disease likely leads to the persistence of infected myeloid cells in tissues. The MΦ-QVOA assay that we have developed can be used for human monocytes and macrophages and the TCRβ RNA qRT-PCR assay can detect transcripts from both human and macaque $CD3^+$ T cells. The MΦ-QVOA assay will be important in measuring the number of myeloid cells in tissues of ART-suppressed macaques and HIV-infected individuals on ART.

We have previously reported a significant correlation between CNS pathology and elevated CSF viral load, but not plasma viral load (38); this has also been reported in HIV-infected individuals with CNS encephalitis prior to ART (71). Quantitation of productively infected macrophages in the brain using the MΦ-QVOA strongly supports the hypothesis that $CD11b^+$ microglia/macrophages in the brain are the major contributors to CNS infection since the number of infected macrophages in both basal ganglia and parietal cortex brain showed a trend towards a correlation with viral RNA levels, but not plasma viral load. It is important to note that even in a model with high prevalence of CNS pathology similar to human disease, not all of the macaques in this study developed severe CNS disease. However, those that did develop mild-severe CNS disease had the highest frequency of infected macrophages in the brain. This study suggests that the frequency of infection of macrophages in the brain is directly correlated with and leads to CNS pathology.

In this study, both blood and tissue from untreated SIV-infected macaques were analyzed because the numbers of productively SIV-infected myeloid cells and $CD4^+$ T cells in tissues during infection have not previously been measured. Our results establish

that productively infected tissue macrophages can be quantitated, that the virus produced is infectious, and that there is no TCRβ RNA detectable in the infected macrophages. A recent report concluded that tissue macrophages in SIV-infected macaques contained SIV DNA from phagocytosis of $CD4^+$ T cells and that tissue macrophages were not a major source of virus *in vivo* (72). In sharp contrast, we developed novel optimized methods for isolation and evaluation of tissue macrophages, to demonstrate clearly that SIV-infected tissue macrophages produce abundant replication competent virus. Of note, these novel assays provide a minimum estimate of productively infected $CD4^+$ T cells and myeloid cells in SIV-infected tissues *in vivo*. It is possible that phagocytized $CD4^+$ T cells infects macrophages *in vivo* as it has been demonstrated *in vitro* (73), although a recent study using mouse models has indicated that macrophages can sustain replication *in vivo* independently of T cells (74). Using our techniques, it will now be possible to quantify the number of latently infected $CD4^+$ T cells and persistently infected myeloid cells that harbor replication competent virus in SIV-infected macaques suppressed by ART to advance our understanding of HIV latency.

FUNDING INFORMATION

This study was supported by NCRR and the Office of Research Infra- structure Programs (ORIP) of the NIH (grant P40 OD013117) and NIH grants P01 MH070306, NS077869, NS076357, U19-0AI076113, and R56 AI118753. The funders had no role in the study design, data collection and interpretation, or the decision to submit the work for publication.

ACKNOWLEDGEMENTS

We thank Jeanne Sisk for assistance and the Johns Hopkins School of Medicine Retrovirus Laboratory for technical assistance and guidance. We declare no conflict of interest.

Author contributions:

C.R.A., J.E.C. and L.G. conceived the study. C.R.A. designed and implemented the MΦ-QVOA, and prepared the manuscript. S.L.P. performed the $CD4^+$ QVOA and PBMC spinoculation; C.R.A. analyzed the data. J.N.R. and C.R.A. designed and implemented the TCRβ RNA assay; E.R.F. prepared the TCRβ RNA standards for qRT-PCR. C.R.A. and E.N.S. performed the flow cytometry analyses. E.N.S., B.T.B. and S.E.Q. isolated tissue cells and prepared animal characteristics data. C.R.A. and M.L. performed qRT-PCR. D.G. and S.L.O. performed sequencing analyses. C.R.A., M.C.Z., J.L.M., L.G. and J.E.C. edited the manuscript.

REFERENCES

1. **Gendelman HE, Narayan O, Molineaux S, Clements JE, Ghotbi Z.** 1985. Slow, persistent replication of lentiviruses: role of tissue macrophages and macrophage precursors in bone marrow. Proc Natl Acad Sci U S A **82:**7086-7090.
2. **Cheevers WP, McGuire TC.** 1985. Equine infectious anemia virus: immunopathogenesis and persistence. Reviews of infectious diseases **7:**83-88.
3. **Ho DD, Rota TR, Hirsch MS.** 1986. Infection of monocyte/macrophages by human T lymphotropic virus type III. J Clin Invest **77:**1712-1715.
4. **Lifson JD, Feinberg MB, Reyes GR, Rabin L, Banapour B, Chakrabarti S, Moss B, Wong-Staal F, Steimer KS, Engleman EG.** 1986. Induction of CD4-dependent cell fusion by the HTLV-III/LAV envelope glycoprotein. Nature **323:**725-728.
5. **Gallo RC.** 1991. Human retroviruses: a decade of discovery and link with human disease. J Infect Dis **164:**235-243.
6. **Chiu IM, Yaniv A, Dahlberg JE, Gazit A, Skuntz SF, Tronick SR, Aaronson SA.** 1985. Nucleotide sequence evidence for relationship of AIDS retrovirus to lentiviruses. Nature **317:**366-368.
7. **Haase AT.** 1986. Pathogenesis of lentivirus infections. Nature **322:**130-136.
8. **Kelly KM, Tarwater PM, Karper JM, Bedja D, Queen SE, Tunin RS, Adams RJ, Kass DA, Mankowski JL.** 2012. Diastolic dysfunction is associated with myocardial viral load in simian immunodeficiency virus-infected macaques. AIDS **26:**815-823.
9. **Laast VA, Shim B, Johanek LM, Dorsey JL, Hauer PE, Tarwater PM, Adams RJ, Pardo CA, McArthur JC, Ringkamp M, Mankowski JL.** 2011. Macrophage-mediated dorsal root ganglion damage precedes altered nerve conduction in SIV-infected macaques. Am J Pathol **179:**2337-2345.
10. **Babas T, Vieler E, Hauer DA, Adams RJ, Tarwater PM, Fox K, Clements JE, Zink MC.** 2001. Pathogenesis of SIV pneumonia: selective replication of viral genotypes in the lung. Virology **287:**371-381.
11. **Zink MC, Clements JE.** 2002. A novel simian immunodeficiency virus model that provides insight into mechanisms of human immunodeficiency virus central nervous system disease. J Neurovirol **8 Suppl 2:**42-48.
12. **Stevenson M.** 2015. Role of myeloid cells in HIV-1-host interplay. J Neurovirol **21:**242-248.
13. **Yona S, Kim KW, Wolf Y, Mildner A, Varol D, Breker M, Strauss-Ayali D, Viukov S, Guilliams M, Misharin A, Hume DA, Perlman H, Malissen B, Zelzer E, Jung S.** 2013. Fate mapping reveals origins and dynamics of monocytes and tissue macrophages under homeostasis. Immunity **38:**79-91.
14. **Hashimoto D, Chow A, Noizat C, Teo P, Beasley MB, Leboeuf M, Becker CD, See P, Price J, Lucas D, Greter M, Mortha A, Boyer SW, Forsberg EC, Tanaka M, van Rooijen N, Garcia-Sastre A, Stanley ER, Ginhoux F, Frenette PS, Merad M.** 2013. Tissue-resident macrophages self-maintain locally throughout adult life with minimal contribution from circulating monocytes. Immunity **38:**792-804.

15. **Davies LC, Jenkins SJ, Allen JE, Taylor PR.** 2013. Tissue-resident macrophages. Nat Immunol **14:**986-995.
16. **Ginhoux F, Jung S.** 2014. Monocytes and macrophages: developmental pathways and tissue homeostasis. Nat Rev Immunol **14:**392-404.
17. **Prinz M, Priller J.** 2014. Microglia and brain macrophages in the molecular age: from origin to neuropsychiatric disease. Nat Rev Neurosci **15:**300-312.
18. **Gomez Perdiguero E, Klapproth K, Schulz C, Busch K, Azzoni E, Crozet L, Garner H, Trouillet C, de Bruijn MF, Geissmann F, Rodewald HR.** 2015. Tissue-resident macrophages originate from yolk-sac-derived erythro-myeloid progenitors. Nature **518:**547-551.
19. **Walker-Sperling VE, Buckheit RW, 3rd, Blankson JN.** 2014. Comparative analysis of the capacity of elite suppressor CD4+ and CD8+ T cells to inhibit HIV-1 replication in monocyte-derived macrophages. J Virol **88:**9789-9798.
20. **Vojnov L, Martins MA, Bean AT, Veloso de Santana MG, Sacha JB, Wilson NA, Bonaldo MC, Galler R, Stevenson M, Watkins DI.** 2012. The majority of freshly sorted simian immunodeficiency virus (SIV)-specific CD8(+) T cells cannot suppress viral replication in SIV-infected macrophages. J Virol **86:**4682-4687.
21. **Clements JE, Mankowski JL, Gama L, Zink MC.** 2008. The accelerated simian immunodeficiency virus macaque model of human immunodeficiency virus-associated neurological disease: from mechanism to treatment. J Neurovirol **14:**309-317.
22. **Ribeiro Dos Santos P, Rancez M, Pretet JL, Michel-Salzat A, Messent V, Bogdanova A, Couedel-Courteille A, Souil E, Cheynier R, Butor C.** 2011. Rapid dissemination of SIV follows multisite entry after rectal inoculation. PLoS One **6:**e19493.
23. **Yen PJ, Mefford ME, Hoxie JA, Williams KC, Desrosiers RC, Gabuzda D.** 2014. Identification and characterization of a macrophage-tropic SIV envelope glycoprotein variant in blood from early infection in SIVmac251-infected macaques. Virology **458-459:**53-68.
24. **Francella N, Gwyn SE, Yi Y, Li B, Xiao P, Elliott ST, Ortiz AM, Hoxie JA, Paiardini M, Silvestri G, Derdeyn CA, Collman RG.** 2013. CD4+ T cells support production of simian immunodeficiency virus Env antibodies that enforce CD4-dependent entry and shape tropism in vivo. J Virol **87:**9719-9732.
25. **Williams KC, Burdo TH.** 2009. HIV and SIV infection: the role of cellular restriction and immune responses in viral replication and pathogenesis. APMIS **117:**400-412.
26. **Williams K, Westmoreland S, Greco J, Ratai E, Lentz M, Kim WK, Fuller RA, Kim JP, Autissier P, Sehgal PK, Schinazi RF, Bischofberger N, Piatak M, Lifson JD, Masliah E, Gonzalez RG.** 2005. Magnetic resonance spectroscopy reveals that activated monocytes contribute to neuronal injury in SIV neuroAIDS. J Clin Invest **115:**2534-2545.
27. **McIlroy D, Autran B, Cheynier R, Clauvel JP, Oksenhendler E, Debre P, Hosmalin A.** 1996. Low infection frequency of macrophages in the spleens of HIV+ patients. Res Virol **147:**115-121.

28. **Cribbs SK, Lennox J, Caliendo AM, Brown LA, Guidot DM.** 2015. Healthy HIV-1-infected individuals on highly active antiretroviral therapy harbor HIV-1 in their alveolar macrophages. AIDS Res Hum Retroviruses **31:**64-70.
29. **Eriksson S, Graf EH, Dahl V, Strain MC, Yukl SA, Lysenko ES, Bosch RJ, Lai J, Chioma S, Emad F, Abdel-Mohsen M, Hoh R, Hecht F, Hunt P, Somsouk M, Wong J, Johnston R, Siliciano RF, Richman DD, O'Doherty U, Palmer S, Deeks SG, Siliciano JD.** 2013. Comparative analysis of measures of viral reservoirs in HIV-1 eradication studies. PLoS Pathog **9:**e1003174.
30. **Ho YC, Shan L, Hosmane NN, Wang J, Laskey SB, Rosenbloom DI, Lai J, Blankson JN, Siliciano JD, Siliciano RF.** 2013. Replication-competent noninduced proviruses in the latent reservoir increase barrier to HIV-1 cure. Cell **155:**540-551.
31. **Siliciano JD, Siliciano RF.** 2005. Enhanced culture assay for detection and quantitation of latently infected, resting CD4+ T-cells carrying replication-competent virus in HIV-1-infected individuals. Methods Mol Biol **304:**3-15.
32. **Rosenbloom DIS, Elliott O, Hill AL, Henrich TJ.** 2015. Designing and interpreting limiting dilution assays: general principles and applications to the latent reservoir for HIV-1. bioRxiv.
33. **Laird GM, Eisele EE, Rabi SA, Lai J, Chioma S, Blankson JN, Siliciano JD, Siliciano RF.** 2013. Rapid quantification of the latent reservoir for HIV-1 using a viral outgrowth assay. PLoS Pathog **9:**e1003398.
34. **Shen A, Zink MC, Mankowski JL, Chadwick K, Margolick JB, Carruth LM, Li M, Clements JE, Siliciano RF.** 2003. Resting CD4+ T Lymphocytes but Not Thymocytes Provide a Latent Viral Reservoir in a Simian Immunodeficiency Virus-Macaca nemestrina Model of Human Immunodeficiency Virus Type 1-Infected Patients on Highly Active Antiretroviral Therapy. Journal of Virology **77:**4938-4949.
35. **Dinoso JB, Rabi SA, Blankson JN, Gama L, Mankowski JL, Siliciano RF, Zink MC, Clements JE.** 2009. A simian immunodeficiency virus-infected macaque model to study viral reservoirs that persist during highly active antiretroviral therapy. J Virol **83:**9247-9257.
36. **Mankowski JL, Flaherty MT, Spelman JP, Hauer DA, Didier PJ, Amedee AM, Murphey-Corb M, Kirstein LM, Munoz A, Clements JE, Zink MC.** 1997. Pathogenesis of simian immunodeficiency virus encephalitis: viral determinants of neurovirulence. J Virol **71:**6055-6060.
37. **Zink MC, Spelman JP, Robinson RB, Clements JE.** 1998. SIV infection of macaques - modeling the progression to AIDS dementia. Journal of Neurovirology **4:**249-259.
38. **Zink MC, Suryanarayana K, Mankowski JL, Shen A, Piatak M, Jr., Spelman JP, Carter DL, Adams RJ, Lifson JD, Clements JE.** 1999. High viral load in the cerebrospinal fluid and brain correlates with severity of simian immunodeficiency virus encephalitis. J Virol **73:**10480-10488.
39. **Babas T, Dewitt JB, Mankowski JL, Tarwater PM, Clements JE, Zink MC.** 2006. Progressive selection for neurovirulent genotypes in the brain of SIV-infected macaques. AIDS **20:**197-205.

40. **Meulendyke KA, Queen SE, Engle EL, Shirk EN, Liu J, Steiner JP, Nath A, Tarwater PM, Graham DR, Mankowski JL, Zink MC.** 2014. Combination fluconazole/paroxetine treatment is neuroprotective despite ongoing neuroinflammation and viral replication in an SIV model of HIV neurological disease. J Neurovirol **20:**591-602.
41. **Babas T, Munoz D, Mankowski JL, Tarwater PM, Clements JE, Zink MC.** 2003. Role of microglial cells in selective replication of simian immunodeficiency virus genotypes in the brain. J Virol **77:**208-216.
42. **Arnaout MA.** 1990. Structure and function of the leukocyte adhesion molecules CD11/CD18. Blood **75:**1037-1050.
43. **Harms AS, Tansey MG.** 2013. Isolation of murine postnatal brain microglia for phenotypic characterization using magnetic cell separation technology. Methods Mol Biol **1041:**33-39.
44. **Marek R, Caruso M, Rostami A, Grinspan JB, Das Sarma J.** 2008. Magnetic cell sorting: a fast and effective method of concurrent isolation of high purity viable astrocytes and microglia from neonatal mouse brain tissue. J Neurosci Methods **175:**108-118.
45. **Dupuis M, Denis-Mize K, Woo C, Goldbeck C, Selby MJ, Chen MC, Otten GR, Ulmer JB, Donnelly JJ, Ott G, McDonald DM.** 2000. Distribution of DNA vaccines determines their immunogenicity after intramuscular injection in mice. Journal of Immunology **165:**2850-2858.
46. **Roca H, Varsos ZS, Sud S, Craig MJ, Ying C, Pienta KJ.** 2009. CCL2 and interleukin-6 promote survival of human CD11b+ peripheral blood mononuclear cells and induce M2-type macrophage polarization. J Biol Chem **284:**34342-34354.
47. **Shen A, Yang HC, Zhou Y, Chase AJ, Boyer JD, Zhang H, Margolick JB, Zink MC, Clements JE, Siliciano RF.** 2007. Novel pathway for induction of latent virus from resting CD4(+) T cells in the simian immunodeficiency virus/macaque model of human immunodeficiency virus type 1 latency. J Virol **81:**1660-1670.
48. **Smith MZ, Asher TE, Venturi V, Davenport MP, Douek DC, Price DA, Kent SJ.** 2008. Limited maintenance of vaccine-induced simian immunodeficiency virus-specific CD8 T-cell receptor clonotypes after virus challenge. J Virol **82:**7357-7368.
49. **Miksa M, Komura H, Wu R, Shah KG, Wang P.** 2009. A novel method to determine the engulfment of apoptotic cells by macrophages using pHrodo succinimidyl ester. J Immunol Methods **342:**71-77.
50. **Kilgore JA, Dolman NJ, Davidson MW.** 2013. A review of reagents for fluorescence microscopy of cellular compartments and structures, Part II: reagents for non-vesicular organelles. Curr Protoc Cytom **66:**Unit 12 31.
51. **Gama L, Shirk EN, Russell JN, Carvalho KI, Li M, Queen SE, Kalil J, Zink MC, Clements JE, Kallas EG.** 2012. Expansion of a subset of CD14highCD16negCCR2low/neg monocytes functionally similar to myeloid-derived suppressor cells during SIV and HIV infection. J Leukoc Biol **91:**803-816.

52. **Meulendyke KA, Pletnikov MV, Engle EL, Tarwater PM, Graham DR, Zink MC.** 2012. Early minocycline treatment prevents a decrease in striatal dopamine in an SIV model of HIV-associated neurological disease. J Neuroimmune Pharmacol **7:**454-464.
53. **Martinez FO, Gordon S, Locati M, Mantovani A.** 2006. Transcriptional profiling of the human monocyte-to-macrophage differentiation and polarization: new molecules and patterns of gene expression. J Immunol **177:**7303-7311.
54. **Fernandez G, Zaikos TD, Khan SZ, Jacobi AM, Behlke MA, Zeichner SL.** 2013. Targeting IkappaB proteins for HIV latency activation: the role of individual IkappaB and NF-kappaB proteins. J Virol **87:**3966-3978.
55. **Gallastegui E, Marshall B, Vidal D, Sanchez-Duffhues G, Collado JA, Alvarez-Fernandez C, Luque N, Terme JM, Gatell JM, Sanchez-Palomino S, Munoz E, Mestres J, Verdin E, Jordan A.** 2012. Combination of biological screening in a cellular model of viral latency and virtual screening identifies novel compounds that reactivate HIV-1. J Virol **86:**3795-3808.
56. **Stefano KA, Collman R, Kolson D, Hoxie J, Nathanson N, Gonzalezscarano F.** 1993. Replication of a Macrophage-Tropic Strain of Human-Immunodeficiency-Virus Type-1 (Hiv-1) in a Hybrid Cell-Line, Cemx174, Suggests That Cellular Accessory Molecules Are Required for Hiv-1 Entry. Journal of Virology **67:**6707-6715.
57. **Cassetta L, Cassol E, Poli G.** 2011. Macrophage polarization in health and disease. TheScientificWorldJournal **11:**2391-2402.
58. **Okabe Y, Medzhitov R.** 2014. Tissue-specific signals control reversible program of localization and functional polarization of macrophages. Cell **157:**832-844.
59. **Mantovani A, Sica A, Sozzani S, Allavena P, Vecchi A, Locati M.** 2004. The chemokine system in diverse forms of macrophage activation and polarization. Trends in immunology **25:**677-686.
60. **Mulder R, Banete A, Basta S.** 2014. Spleen-derived macrophages are readily polarized into classically activated (M1) or alternatively activated (M2) states. Immunobiology **219:**737-745.
61. **Cassol E, Cassetta L, Alfano M, Poli G.** 2010. Macrophage polarization and HIV-1 infection. Journal of leukocyte biology **87:**599-608.
62. **Cai Y, Sugimoto C, Liu DX, Midkiff CC, Alvarez X, Lackner AA, Kim WK, Didier ES, Kuroda MJ.** 2015. Increased monocyte turnover is associated with interstitial macrophage accumulation and pulmonary tissue damage in SIV-infected rhesus macaques. J Leukoc Biol **97:**1147-1153.
63. **Ortiz AM, DiNapoli SR, Brenchley JM.** 2015. Macrophages Are Phenotypically and Functionally Diverse across Tissues in Simian Immunodeficiency Virus-Infected and Uninfected Asian Macaques. J Virol **89:**5883-5894.
64. **Garvey LJ, Everitt A, Winston A, Mackie NE, Benzie A.** 2009. Detectable cerebrospinal fluid HIV RNA with associated neurological deficits, despite suppression of HIV replication in the plasma compartment. AIDS **23:**1443-1444.
65. **Eden A, Fuchs D, Hagberg L, Nilsson S, Spudich S, Svennerholm B, Price RW, Gisslen M.** 2010. HIV-1 viral escape in cerebrospinal fluid of subjects on suppressive antiretroviral treatment. J Infect Dis **202:**1819-1825.

66. **Williams KC, Corey S, Westmoreland SV, Pauley D, Knight H, deBakker C, Alvarez X, Lackner AA.** 2001. Perivascular macrophages are the primary cell type productively infected by simian immunodeficiency virus in the brains of macaques: implications for the neuropathogenesis of AIDS. J Exp Med **193:**905-915.
67. **Kim W-K, Alvarez X, Fisher J, Bronfin B, Westmoreland S, McLaurin J, Williams K.** 2006. CD163 identifies perivascular macrophages in normal and viral encephalitic brains and potential precursors to perivascular macrophages in blood. The American journal of pathology **168:**822-834.
68. **Cosenza MA, Zhao M-L, Si Q, Lee SC.** 2006. Human Brain Parenchymal Microglia Express CD14 and CD45 and are Productively Infected by HIV-1 in HIV-1 Encephalitis. Brain Pathology **12:**442-455.
69. **Agostini C, Sancetta R, Cerutti A, Semenzato G.** 1995. Alveolar macrophages as a cell source of cytokine hyperproduction in HIV-related interstitial lung disease. Journal of leukocyte biology **58:**495-500.
70. **Crothers K, Thompson BW, Burkhardt K, Morris A, Flores SC, Diaz PT, Chaisson RE, Kirk GD, Rom WN, Huang L, Lung HIVS.** 2011. HIV-associated lung infections and complications in the era of combination antiretroviral therapy. Proc Am Thorac Soc **8:**275-281.
71. **McArthur JC, McClernon DR, Cronin MF, Nance-Sproson TE, Saah AJ, St Clair M, Lanier ER.** 1997. Relationship between human immunodeficiency virus-associated dementia and viral load in cerebrospinal fluid and brain. Ann Neurol **42:**689-698.
72. **Calantone N, Wu F, Klase Z, Deleage C, Perkins M, Matsuda K, Thompson EA, Ortiz AM, Vinton CL, Ourmanov I, Lore K, Douek DC, Estes JD, Hirsch VM, Brenchley JM.** 2014. Tissue myeloid cells in SIV-infected primates acquire viral DNA through phagocytosis of infected T cells. Immunity **41:**493-502.
73. **Baxter AE, Russell RA, Duncan CJ, Moore MD, Willberg CB, Pablos JL, Finzi A, Kaufmann DE, Ochsenbauer C, Kappes JC, Groot F, Sattentau QJ.** 2014. Macrophage infection via selective capture of HIV-1-infected CD4+ T cells. Cell Host Microbe **16:**711-721.
74. **Honeycutt JB, Wahl A, Baker C, Spagnuolo RA, Foster J, Zakharova O, Wietgrefe S, Caro-Vegas C, Madden V, Sharpe G, Haase AT, Eron JJ, Garcia JV.** 2016. Macrophages sustain HIV replication in vivo independently of T cells. J Clin Invest doi:10.1172/JCI84456.

Animal ID	**Duration of Infection** (days)	**CNS Score**	**CD4⁺ T cell counts** (cells/μL blood)	**Monocyte Counts** (cells/μL blood)	**Plasma Viral Load** (SIV copies /mL)	**CSF Viral Load** (SIV copies /mL)	**Parietal Cortex** (SIV copies/ tissue μg RNA)	**Basal Ganglia** (SIV copies/ tissue μg RNA)	**Lung** (SIV copies/ tissue μg RNA)	**Spleen** (SIV copies/ tissue μg RNA)
Pm 1	62	Severe	166	1,271	6.50E+07	9.85E+06	5.65E+06	4.10E+06	74,024	2.59E+06
Pm 2	60	Severe	57	45	8.83E+07	2.43E+07	1.30E+06	1.11E+06	99,416	675,000
Pm 3	50	Severe	113	1,022	4.24E+07	4.98E+06	826,254	1.55E+06	503,785	1.22E+06
Pm 4	84	Severe	52	4,333	1.49E+09	1.14E+07	4.63E+06	1.92E+06	1,543	1.61E+07
Pm 5	86	Mild	222	493	1.18E+07	1.84E+07	1.48E+06	807,774	247	1.19E+07
Pm 6	85	None	396	525	3.65E+08	166,022	699	10,632	1,197	8.45E+06
Pm 7	83	None	418	767	1.05E+07	117,088	22	14,995	332	8.68E+06
Pm 8	79	None	56	416	2.20E+06	129,536	ND	ND	129	5.51E+06
Pm 9	87	None	464	874	1.25E+06	112,867	ND	ND	152	4.40E+06
Pm 10	84	None	693	1,071	300,229	12,105	ND	ND	1,797	204,000
Pm 11[a]	84	None	119	612	651,191	142,755	196	ND	282	268,000
Pm 12[b]	34	None	681	481	4.55E+08	20,761	ND	ND	741	866,000
Pm 13[b]	35	None	390	350	1.72E+08	8.41E+07	3,365	96,705	421	1.62E+06
Pm 14[b]	36	None	758	588	8.37E+07	1.33E+06	1,364	586	253	377,000

[a] Treated with fluconazole and paroxetine at day 12 post inoculation.

[b] Pre-treated with minocycline 28 days prior infection.

Treatments did not affect virus replication or progression of disease.

Abbreviations:

ND: under the limit of detection

Pm: Pigtail macaque

Table 1. Detailed characterization of the SIV-infected macaques in the study.

	Animal ID	CD4+ T cell IUPM	% CD3+ T cells in MΦ-QVOA by TCRβ	%CD4+ T cells of CD3+ cells	% CD4+ T cells in MΦ-QVOA by TCRβ	Infected CD4+ T cells in MΦ-QVOA	CD11b+ macrophage IUPM
Blood	Pm 4	8.08	0.17	48	0.08	0.0	369.97
	Pm 5	40.52	1.27	44	0.56	0.2	139. 38
	Pm 6	205.84	2.01	32	0.64	1.3	23,116.35
	Pm 7	71.06	0	34	0	0	2.07
	Pm 8	1,121.51	0	34	0	0	<0.1
	Pm 9	81.70	2.20	31	0.69	0.6	45.96
	Pm 12	420	0	64	0	0	8.48
	Pm 13	205.84	1.58	32	0.50	1.0	16.97
	Pm 14	1121.51	0.31	54	0.17	1.9	4.62
Spleen	Pm 4	40.52	0.36	17	0.06	0.0	423.93
	Pm 5	9.14	6.23	23	1.41	0.1	854.58
	Pm 6	40.52	5.74	6	0.32	0.1	93,280.33
	Pm 9	205.84	2.02	9	0.18	0.4	23.12

Red: below limit of detection.

Table 2. Calculation of infected CD4+ T cells in MΦ-QVOA assays in Blood and Spleen.

Animal ID	CNS Score	Blood MΦ-QVOA	BAL MΦ-QVOA	Lung MΦ-QVOA	Spleen MΦ-QVOA	Brain MΦ-QVOA	Blood $CD4^+$ QVOA	Spleen $CD4^+$ QVOA
Pm 1	Severe					231.16		
Pm 2	Severe					93.28		
Pm 3	Severe					23,978.95		
Pm 4	Severe	369.97	1,481.48	1,838.35	423.93	23,116.35	8.08	40.52
Pm 5	Mild	139. 38	57.79	46.23	854.58	427.29	40.52	9.14
Pm 6	None	23,116.35	18.38	46.07	93,280.33	42.39	205.84	40.52
Pm 7	None	2.07					71.06	81.70
Pm 8	None	<0.1					1,121.51	205.84
Pm 9	None	45.96	1.81	<1.0	23.12	<0.42	81.70	205.84
Pm 10	None					<2.31		
Pm 11	None					<1.05		
Pm 12	None	8.48	<1.0	11.56	57.79	<0.2	420	
Pm 13	None	16.97	8.48	18.38	462.33	231.16	205.84	
Pm 14	None	4.62	4.62	9.19	313.67	42.42	1121.51	

Red: below limit of detection.

Table 3. QVOA and Infectious Units per million cells (IUPM) in Blood and Tissues.

Figure 1. Analysis of CD11b+ monocytes and macrophages.

$CD11b^+$ selected cells were stained with antibodies for CD11b and CD3 to identify myeloid cells and lymphocytes. (A) Representative flow cytometry dot plots of (left) the cell population after non-human primate bead isolation and (right) the highly purified population of $CD11b^+$ monocytes. (B) The frequency of $CD11b^+$ (open bars) and $CD3^+$ cells (closed bars) was determined by flow cytometry in the indicated compartment. (C) Non-adherent cells from MΦ-QVOA were removed and analyzed by flow cytometry. Flow cytometry dot plots are shown for a representative animal. Cells were analyzed by FSC and SSC (left), and for macrophage and T cell markers (right). Data presented as mean with standard deviation.

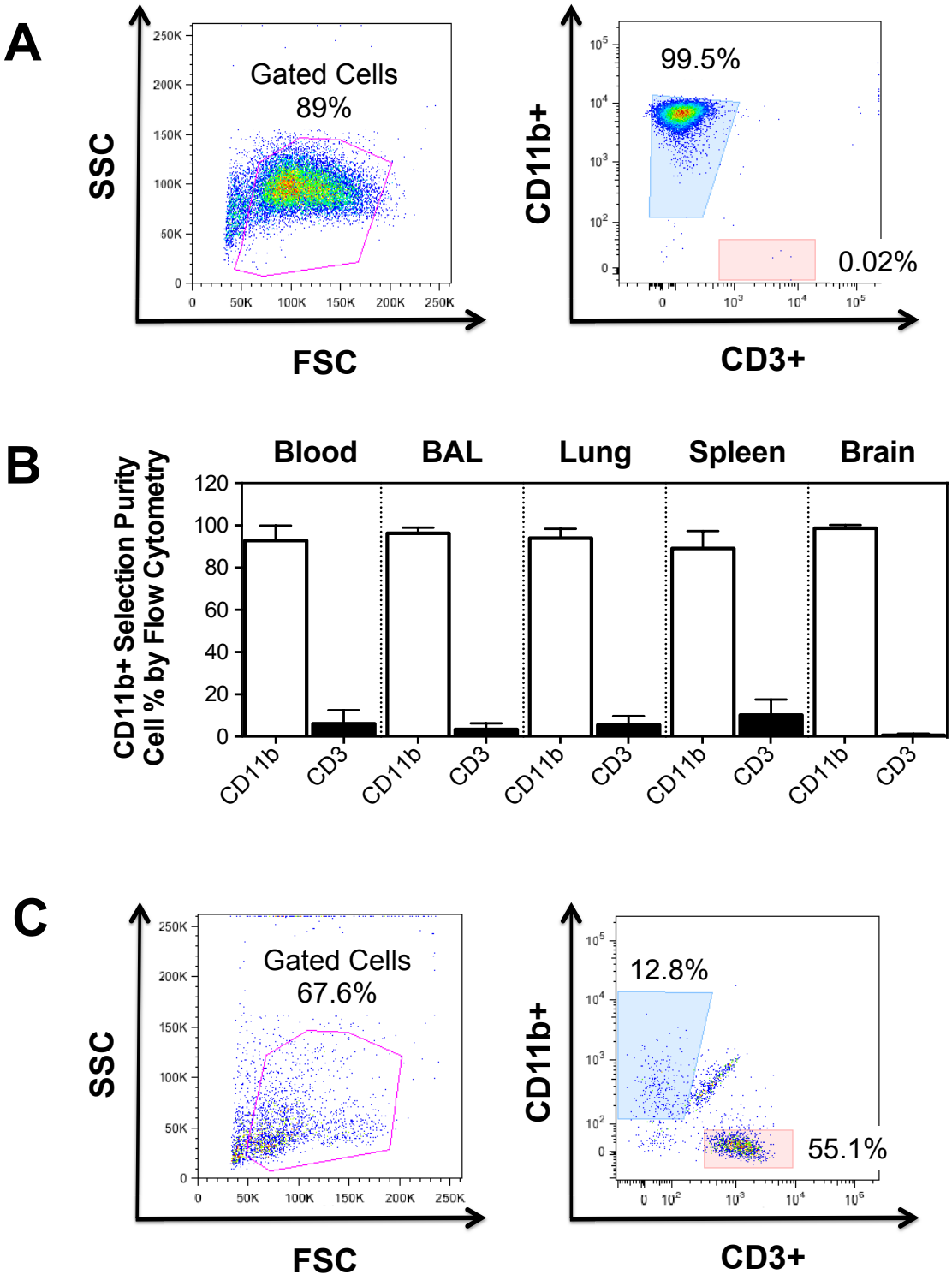
A
Gated Cells
89%
SSC
FSC
99.5%
0.02%
CD11b+
CD3+
B
Blood
BAL
Lung
Spleen
Brain
CD11b+ Selection Purity
Cell % by Flow Cytometry
CD11b
CD3
C
Gated Cells
67.6%
SSC
FSC
12.8%
55.1%
CD11b+
CD3+

Figure 2. Establishment of the TCRβ RNA assay.

$CD3^+$ Lymphocytes from PBMCs of seven uninfected macaques were purified using an anti-CD3 antibody positive selection kit. $CD3^+$ cells were analyzed by flow cytometry. (A) Representative SSC/FSC dot plots (left) and CD11b/CD3 (right) are shown. (B) The average number of TCRβ RNA copies per $CD3^+$ T cell was determined by qRT-PCR. (C) TCRβ RNA in MΦ-QVOA cell lysates from indicated compartments was measured by qRT-PCR and the average number of $CD3^+$ T cells per 10^5 cells was calculated prior to selection (open bars), following CD11b isolation (hatched bars), and in $CD11b^+$ macrophage control wells (closed bars) from MΦ-QVOA. Data represented as mean with standard deviation.

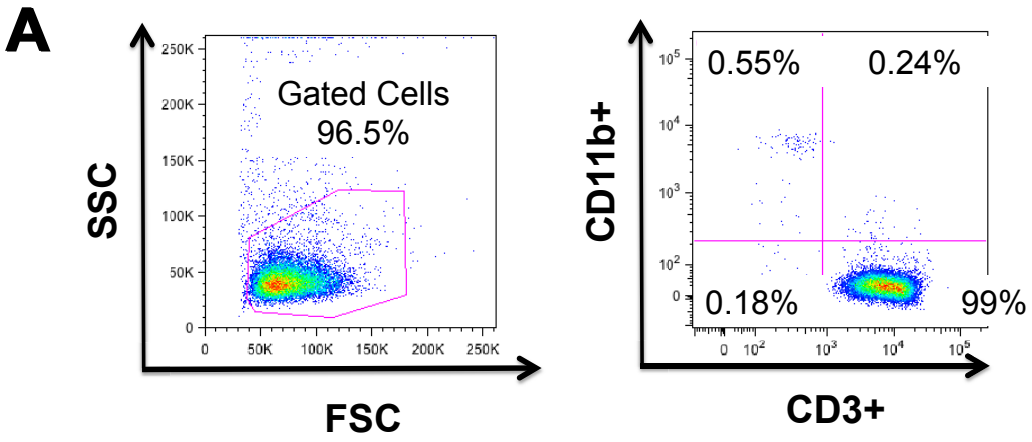
A
SSC
FSC
Gated Cells
96.5%
CD11b+
CD3+
0.55%
0.24%
0.18%
99%

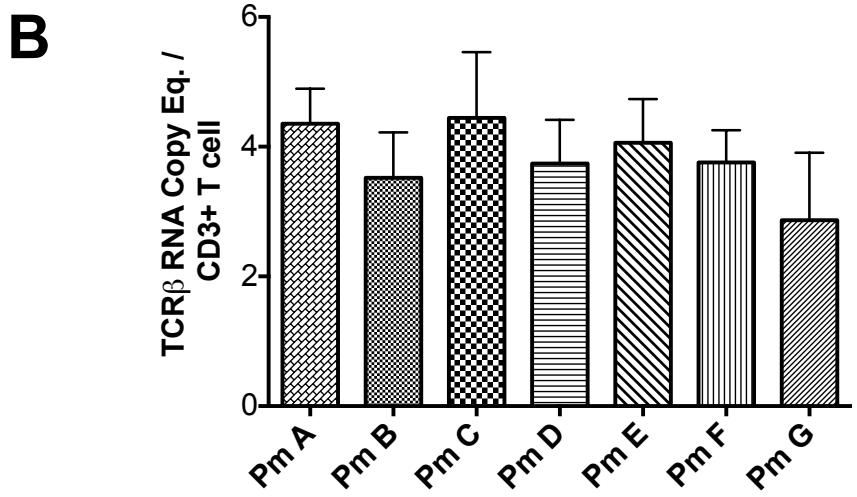
B
TCRβ RNA Copy Eq. / CD3+ T cell
Pm A
Pm B
Pm C
Pm D
Pm E
Pm F
Pm G

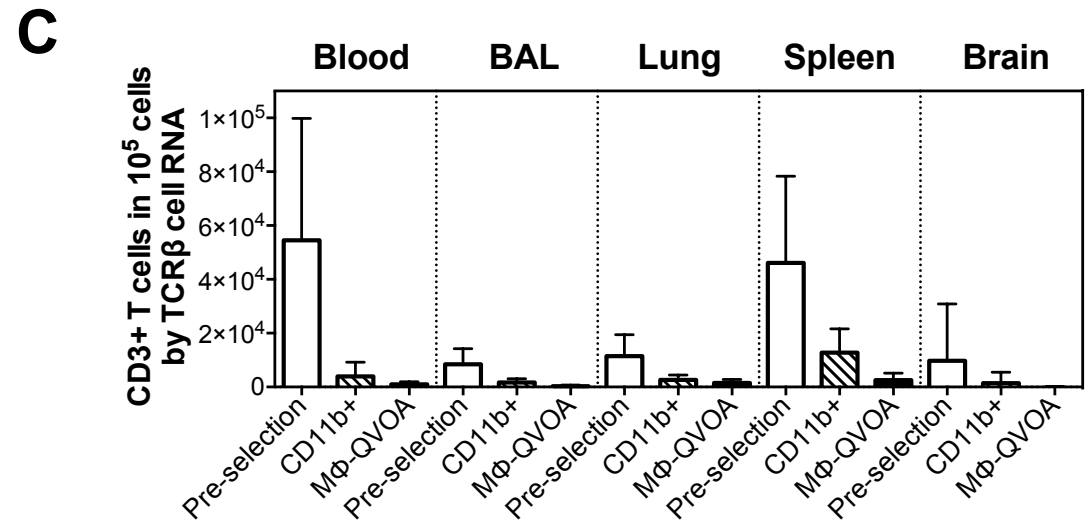
C
Blood
BAL
Lung
Spleen
Brain
CD3+ T cells in 10^5 cells by TCRβ cell RNA
Pre-selection
CD11b+
Mφ-QVOA

Figure 3. Macrophage Quantitative Viral Outgrowth Assay (MΦ-QVOA).

Monocytes from blood and tissue macrophages from BAL, lung, spleen, and brain were collected from SIV infected animals and purified by CD11b bead selection. $CD11b^+$ selected macrophages were plated in serial dilution, in triplicate wells. Cells were cultured with AZT and DRV. Non-adherent cells and anti-retrovirals were removed prior to activation with TNFα and co-culture with CEMx174 cells. (A) Schematic of MΦ-QVOA assay. (B) Live fluorescence microscopy of $CD11b^+$ monocyte-derived-macrophages co-cultured with CEMx174 cells stained with (top row, blue) Nucblue® Live nuclear marker, (middle row, green) pHrodo® green *E.coli* and merged (bottom row). Images were taken on Nikon Eclipse TE200 Microscope 10x magnification.

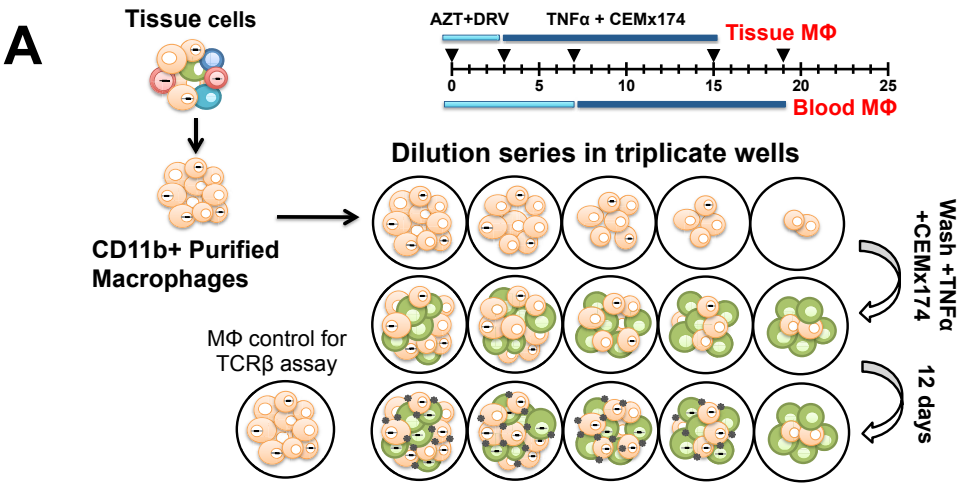
A
Tissue cells
CD11b+ Purified Macrophages
AZT+DRV
TNFα + CEMx174
Tissue MΦ
0
5
10
15
20
25
Blood MΦ
Dilution series in triplicate wells
Wash +TNFα +CEMx174
12 days
MΦ control for TCRβ assay

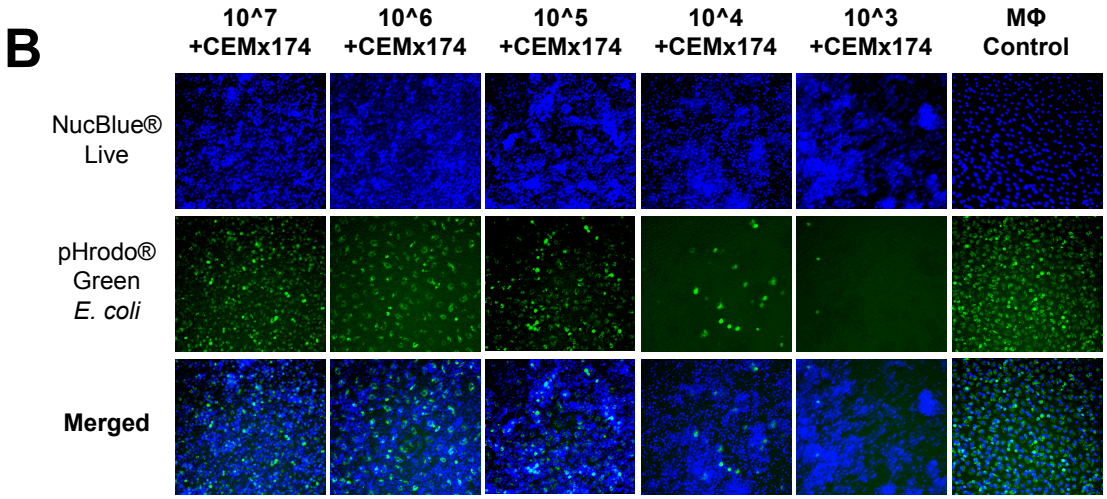
B
10^7 +CEMx174
10^6 +CEMx174
10^5 +CEMx174
10^4 +CEMx174
10^3 +CEMx174
MΦ Control
NucBlue® Live
pHrodo® Green E. coli
Merged

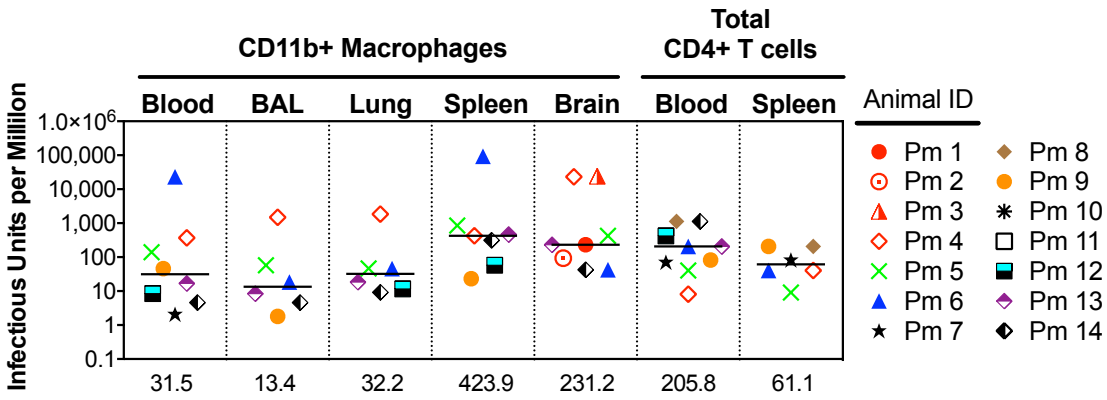

Figure 4. Quantitation of SIV infected monocytes, macrophages, and CD4+ T cells in SIV infected macaques.

Monocytes and macrophages from blood, BAL, lung, spleen, and brain were co-cultured in MΦ-QVOA assay. $CD4^+$ T cells from the blood and spleen were isolated and plated in a limiting dilution similar to MΦ-QVOA assay. Supernatant SIV RNA was measured by qRT-PCR, and the frequency of infectious units per million (IUPM) was calculated using limiting dilution statistics based on the number of positive wells and the input number of cells. The IUPM for macrophages and T cells for each animal assayed is shown with their respective symbols. Horizontal black line represents the median IUPM values (displayed on the x-axis). Red symbols illustrate animals with severe CNS disease.

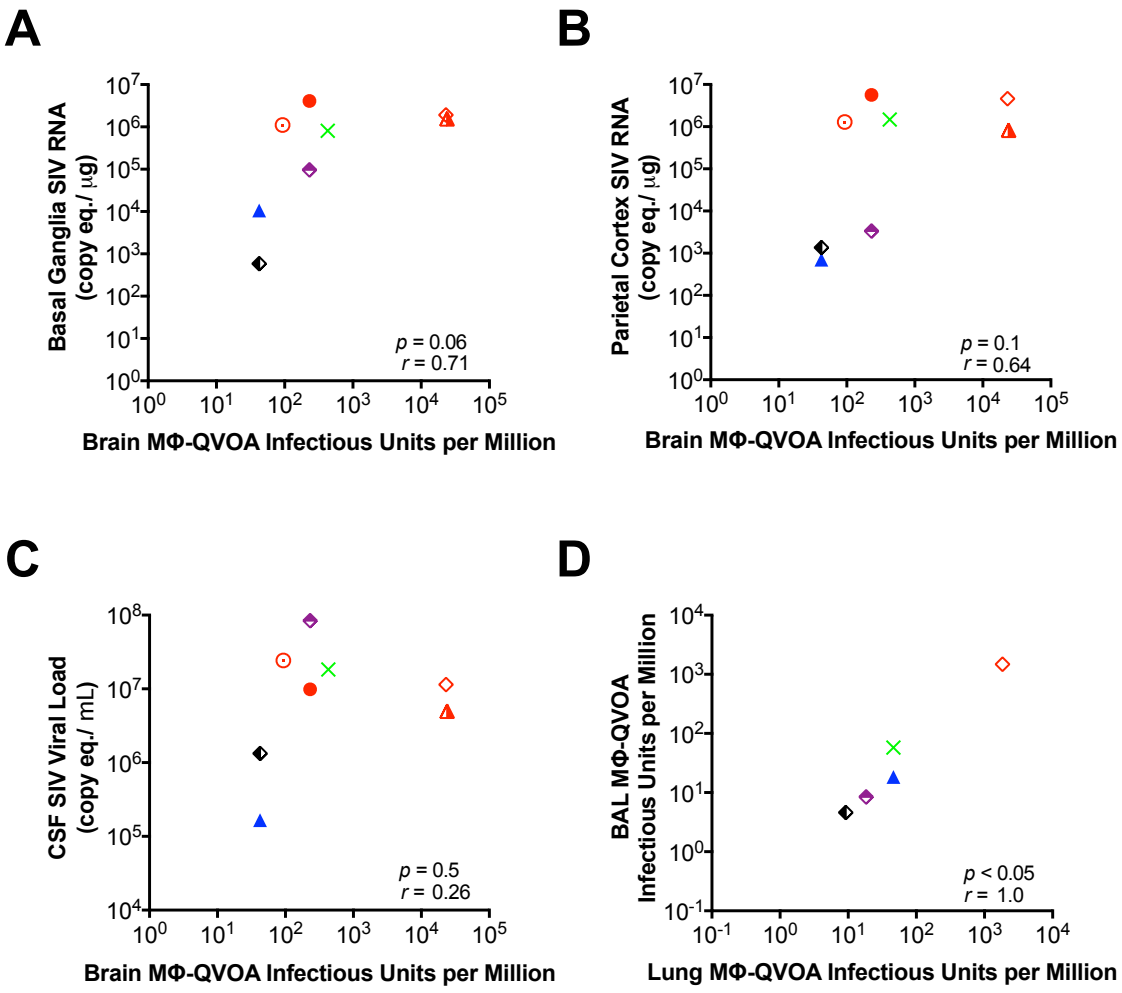

Figure 5. Correlation between the MΦ-QVOA and tissue SIV RNA.

Correlation between the IUPM from brain MΦ-QVOA and basal ganglia tissue SIV RNA (A), parietal cortex tissue SIV RNA (B), and CSF viral load (C). Correlation between the IUPM in lung macrophages was analyzed against (D) BAL macrophage IUPM. Each animal is illustrated with its corresponding symbol, animals with severe CNS disease in red. Significance was determined by Spearman's rank correlation; $p<0.05$ was considered significant.

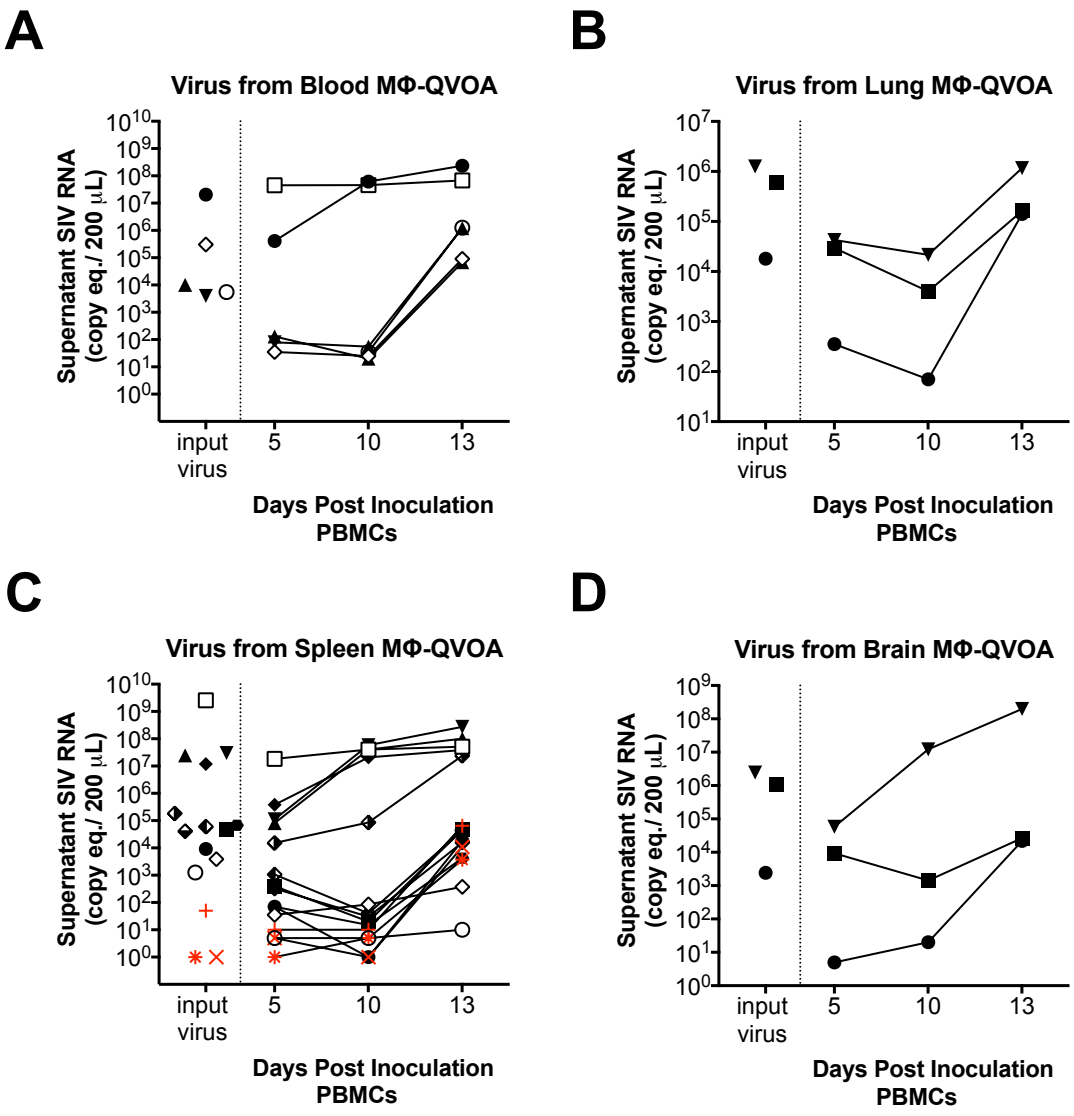

Figure 6. Virus produced in MΦ-QVOA is replication-competent.

Supernatant from Pm4 (filled symbols) and Pm6 (open symbols) from (A) blood MΦ-QVOA, (B) lung MΦ-QVOA, (C) spleen MΦ-QVOA, and (D) brain MΦ-QVOA were collected and used to infect freshly isolated PBMCs by spinoculation. SIV RNA was measured in supernatant by qRT-PCR prior to infection (input virus) and longitudinally for 13 d.p.i. SIV RNA levels presented as copies per 200 μL. Red symbols indicate wells whose input virus was undetectable.

Figure 7. Sequence analyses of virus produced in CD4+ T cell and macrophage QVOAs.

Supernatant from spleen MΦ-QVOA and spleen T cell QVOA from Pm4, Pm5, and Pm6 were collected. Viral RNA was isolated and a two-round nested PCR for SIV *env* was performed. $CD11b^{+}$ macrophage wells without CEMx174 from the MΦ-QVOA were used as controls. The most frequent (red) and the second most frequent (black) sequences are depicted along with the frequency of the viral clone indicated in parentheses. (A) Nucleotide alignment trees for each animal and (B) phylogenetic tree of all clones are shown. (C) Nucleotide sequence alignments are compared with the consensus sequence, with percentages signifying the frequency of the prevailing clones. The scale bar represents the distance between the sequences. Analyses performed by Geneious version 8.0

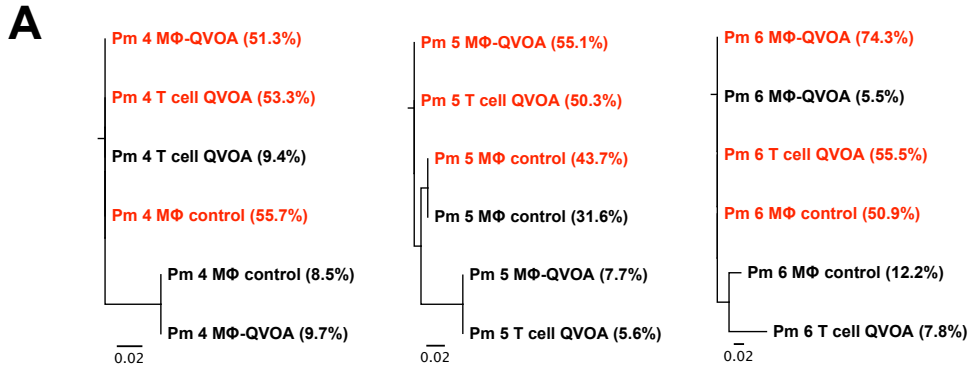
A
Pm 4 MΦ-QVOA (51.3%)
Pm 4 T cell QVOA (53.3%)
Pm 4 T cell QVOA (9.4%)
Pm 4 MΦ control (55.7%)
Pm 4 MΦ control (8.5%)
Pm 4 MΦ-QVOA (9.7%)
0.02
Pm 5 MΦ-QVOA (55.1%)
Pm 5 T cell QVOA (50.3%)
Pm 5 MΦ control (43.7%)
Pm 5 MΦ control (31.6%)
Pm 5 MΦ-QVOA (7.7%)
Pm 5 T cell QVOA (5.6%)
0.02
Pm 6 MΦ-QVOA (74.3%)
Pm 6 MΦ-QVOA (5.5%)
Pm 6 T cell QVOA (55.5%)
Pm 6 MΦ control (50.9%)
Pm 6 MΦ control (12.2%)
Pm 6 T cell QVOA (7.8%)
0.02

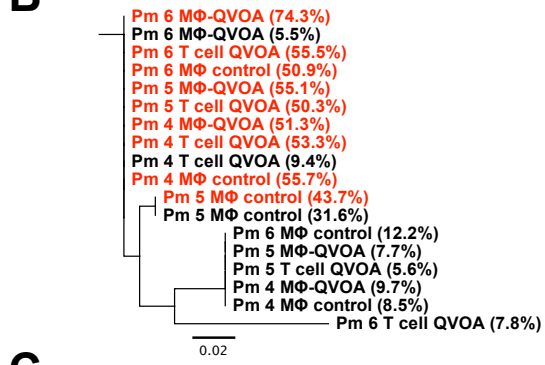
B
Pm 6 MΦ-QVOA (74.3%)
Pm 6 MΦ-QVOA (5.5%)
Pm 6 T cell QVOA (55.5%)
Pm 6 MΦ control (50.9%)
Pm 5 MΦ-QVOA (55.1%)
Pm 5 T cell QVOA (50.3%)
Pm 4 MΦ-QVOA (51.3%)
Pm 4 T cell QVOA (53.3%)
Pm 4 T cell QVOA (9.4%)
Pm 4 MΦ control (55.7%)
Pm 5 MΦ control (43.7%)
Pm 5 MΦ control (31.6%)
Pm 6 MΦ control (12.2%)
Pm 5 MΦ-QVOA (7.7%)
Pm 5 T cell QVOA (5.6%)
Pm 4 MΦ-QVOA (9.7%)
Pm 4 MΦ control (8.5%)
Pm 6 T cell QVOA (7.8%)
0.02

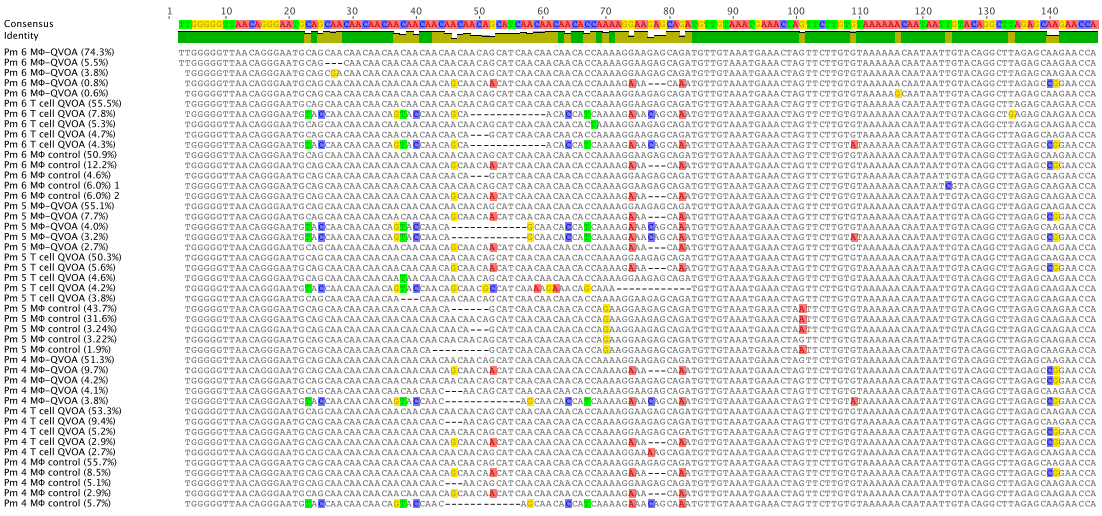
C
Consensus
Identity
Pm 6 MΦ-QVOA (74.3%)
Pm 6 MΦ-QVOA (5.5%)
Pm 6 MΦ-QVOA (3.8%)
Pm 6 MΦ-QVOA (0.8%)
Pm 6 MΦ-QVOA (0.6%)
Pm 6 T cell QVOA (55.5%)
Pm 6 T cell QVOA (7.8%)
Pm 6 T cell QVOA (5.3%)
Pm 6 T cell QVOA (4.7%)
Pm 6 T cell QVOA (4.3%)
Pm 6 MΦ control (50.9%)
Pm 6 MΦ control (12.2%)
Pm 6 MΦ control (4.6%)
Pm 6 MΦ control (6.0%) 1
Pm 6 MΦ control (6.0%) 2
Pm 5 MΦ-QVOA (55.1%)
Pm 5 MΦ-QVOA (7.7%)
Pm 5 MΦ-QVOA (4.0%)
Pm 5 MΦ-QVOA (3.2%)
Pm 5 MΦ-QVOA (2.7%)
Pm 5 T cell QVOA (50.3%)
Pm 5 T cell QVOA (5.6%)
Pm 5 T cell QVOA (4.6%)
Pm 5 T cell QVOA (4.2%)
Pm 5 T cell QVOA (3.8%)
Pm 5 MΦ control (43.7%)
Pm 5 MΦ control (31.6%)
Pm 5 MΦ control (3.24%)
Pm 5 MΦ control (3.22%)
Pm 5 MΦ control (1.9%)
Pm 4 MΦ-QVOA (51.3%)
Pm 4 MΦ-QVOA (9.7%)
Pm 4 MΦ-QVOA (4.2%)
Pm 4 MΦ-QVOA (4.1%)
Pm 4 MΦ-QVOA (3.8%)
Pm 4 T cell QVOA (53.3%)
Pm 4 T cell QVOA (9.4%)
Pm 4 T cell QVOA (5.2%)
Pm 4 T cell QVOA (2.9%)
Pm 4 T cell QVOA (2.7%)
Pm 4 MΦ control (55.7%)
Pm 4 MΦ control (8.5%)
Pm 4 MΦ control (5.1%)
Pm 4 MΦ control (2.9%)
Pm 4 MΦ control (5.7%)

III. Latently Infected Brain Macrophages in SIV-Infected Macaques treated with diverse antiretroviral regimens

The following section of the dissertation is in preparation for publishing and the text is quoted verbatim from the following:

Latently Infected Brain Macrophages in SIV-Infected Macaques treated with diverse antiretroviral regimens. Claudia R. Avalos, Suzanne E. Queen, Ming Li, Sarah L. Price, Erin N. Shirk, Elizabeth L. Engle, Celina M. Abreu, Ellen R. Forsyth, Brandon T. Bullock, Feilim. M. Gabhann, Steven W. Wietgrefe, Ashley T. Haase, Joseph L. Mankowski, Janice E. Clements, Lucio Gama. *Manuscript in preparation.*

The scientific and technical contributions of the other authors to this work can be found in the acknowledgments section at the end of Chapter III.

Latently Infected Brain Macrophages in SIV-Infected Macaques treated with diverse antiretroviral regimens

Claudia R. Avalos[1], Suzanne E. Queen[1], Ming Li[1], Sarah L. Price[1], Erin N. Shirk[1], Elizabeth L. Engle[1], Celina M. Abreu[1], Ellen R. Forsyth[1], Brandon T. Bullock[1], Feilim M. Gabhann[5], Steven W. Wietgrefe[4], Ashley T. Haase[4], Joseph L. Mankowski[1, 2, 3], Janice E. Clements[1, 2, 3, #], Lucio Gama[1, #]

[1] Department of Molecular and Comparative Pathobiology, Johns Hopkins School of Medicine, Baltimore, Maryland, United States of America.

[2] Department of Pathology, Johns Hopkins School of Medicine, Baltimore, Maryland, United States of America.

[3] Department of Neurology, Johns Hopkins School of Medicine, Baltimore, Maryland, United States of America.

[4] Department of Microbiology and Immunology, University of Minnesota Medical School, Minneapolis, Minnesota, United States of America.

[5] Department of Biomedical Engineering and Institute for Computational Medicine, Johns Hopkins University, Baltimore, Maryland, United States of America.

Running Title: *In vivo* SIV latency in brain macrophages

Word Counts: Abstract (243), Importance (145), Text (5,515)

[#]Corresponding authors, E-mail: jclements@jhmi.edu (JEC)

ABSTRACT

An HIV cure requires a better understanding of the cellular and anatomical sites harboring virus that contributes to rebound upon treatment interruption. Despite antiretroviral therapy (ART), HIV-associated neurocognitive disorders (HAND) are still prevalent. Biomarkers for macrophage activation and neuronal damage in CSF of HIV-infected individuals demonstrate continued effects of HIV in the brain and suggest that the CNS may serve as a viral reservoir. To evaluate whether infected cells persist in brain despite ART, SIV-infected pigtailed macaques were suppressed with multiple ART regimens. Plasma and CSF viral loads, and levels of markers of macrophage activation and neuronal damage in CSF were analyzed longitudinally. To assess whether virus persisted in brain macrophages in these macaques we utilized the macrophage quantitative viral outgrowth assay (MΦ-QVOA) as well as *in situ* hybridization (ISH) to measure the frequency and pattern of viral RNA in brain. Despite different ART regimens and length of time of ART suppression, all animals had consistently elevated markers of neuronal damage and detectable levels of productively infected macrophages. ISH in brain showed SIV RNA positive cells. We also showed that virus produced in the MΦ-QVOA was replication competent, demonstrating that latently infected brain macrophages are capable of re-establishing productive infection upon treatment interruption. This study provides the first confirmation of replication-competent SIV in brain macrophages of ART-suppressed macaques and suggests that the highly debated question of viral latency in macrophages, at least in brain, has been addressed in SIV-infected macaques treated with ART.

IMPORTANCE

Resting $CD4^+$ T cells are currently the only cells that fit the definition of a latent reservoir. However, recent evidence suggests that HIV/SIV-infected macrophages persist despite ART. Markers of macrophage activation and neuronal damage are observed in the CSF of HIV-infected individuals and SIV-infected macaques on successful ART regimens, suggesting that the CNS has continued virus infection and latent infection. A controversy exists as to whether brain macrophages represent a latent source of replication-competent virus capable of re-establishing infection upon treatment interruption. In this study we demonstrate the presence of the latent macrophage reservoir in the brains of SIV-infected ART-treated macaques and quantitate the reservoir using our established outgrowth assay to quantitate macrophages harboring replication-competent SIV genomes. Our results support the existence of other latent reservoirs in addition to resting $CD4^+$ T cells and underscore the importance of macrophages when developing strategies to eradicate HIV.

INTRODUCTION

Although the frequency of HIV-associated neurocognitive disorders (HAND) has decreased with the onset of antiretroviral therapy, milder forms of neurologic impairment are still observed in HIV-infected individuals virally suppressed on ART (1-3). HAND is thought to be a result of chronic CNS inflammation in the brain (1, 3-5). It is unclear whether inflammation is caused by incomplete penetrance of ART into the CNS and persistent virus replication or whether brain macrophages harbor latent virus that reactivates causing sporadic inflammatory responses (6). Indeed, some HIV-infected individuals on ART have no detectable virus in the plasma but have measurable levels of HIV RNA in the CSF (7, 8). There is a continuing debate on the sources of virus in the CSF and the cause of the chronic inflammation in brain that leads to HAND.

Viral replication and activation of brain macrophages during infection contribute to the severity of CNS pathology in HIV-infected patients and SIV models of HAND (9-12). Brain-resident macrophages, which are the main targets of productive HIV infection in brain, include perivascular macrophages and microglia, and viral RNA can be detected in these cells by *in situ* hybridization (ISH) in HIV-infected patients (13, 14). Similarly, SIV RNA and DNA in SIV-infected macrophages can be detected throughout infection (15-20). Moreover, SIV DNA remains in the brain of infected pigtailed macaques despite antiretroviral therapy (21). It is still unclear whether brain-resident macrophages are latently infected and contain replication-competent virus.

Currently, the best-characterized latent reservoir is resting $CD4^+$ T cells (rCD4) (22, 23). Further research is needed to demonstrate that macrophages also fit the definition of a latent reservoir. Current strategies towards HIV eradication are aimed at

reactivating, immunologically eliminating, or excising integrated virus, thus reducing or eliminating the functional latent virus reservoirs (24, 25). However, these strategies, such as T cell activating cytokines (26), histone deacetylase inhibitors (27), phorbol esters that stimulate protein kinase C activity (28, 29) and RNA guided excision of integrated HIV (30), have been developed solely to target rCD4. Little is known about the effect of these approaches in latently infected macrophages, or whether macrophages will require a different strategy for elimination.

Measuring the reduction of the latent reservoirs is key in determining the efficacy of any strategy to eradicate HIV. For lymphocytes, the frequency of latently infected rCD4 in HIV-infected ART-treated individuals is best measured by the quantitative viral outgrowth assay (QVOA) (31, 32). Our laboratory previously showed that a similar QVOA used to quantify latently infected rCD4 in SIV-infected ART-treated macaques yielded frequencies similar to those observed in HIV-infected patients (33). However, macrophages had never been examined in a similar manner. Therefore, we developed an analogous assay to measure the frequency of productively infected macrophages in parallel to rCD4 using the macrophage quantitative viral outgrowth assay (MΦ-QVOA) (34). We demonstrated that monocytes from the blood and macrophages from bronchoalveolar lavage fluid, lungs, spleen, and brain of chronic SIV-infected pigtailed macaques harbor replication-competent virus and showed that $CD4^+$ T cells did not contribute to the values from MΦ-QVOA. In this study we examine whether brain macrophages isolated from SIV-infected ART-treated macaques represent a productively infected latent reservoir, and therefore another barrier to HIV eradication.

MATERIALS AND METHODS

Animal Studies

Sixteen juvenile pigtailed macaques (*Macaca nemestrina*) were inoculated intravenously with the SIV/DeltaB670 swarm and the molecular clone SIV/17E-Fr as previously described (12, 35, 36). Macaques were treated 12 days post-inoculation (d.p.i.) with antiretroviral treatment (33). Three regimens of antiretroviral drugs were chosen; macaques in each regimen were separated into corresponding cohorts (Table 1). Cohort A was treated with 30 mg/kg for the first two weeks then 10 mg/kg of 9-R-(2-phosphonomethoxypropyl) adenine (PMPA; Gilead Foster City CA) once daily intramuscularly (i.m.) as previously described (33), 480 mg/kg darunavir (DRV; Janssen, Titusville NJ) orally twice daily, 10 mg/kg of the integrase inhibitor L000870812 (INTI; Merck, Kenilworth NJ) orally twice daily, and 24 mg/kg ritonavir (RTV; AbbVie, North Chicago IL) orally twice daily. Cohorts B1 and B2 were treated with 30 mg/kg for the first two weeks then 10 mg/kg PMPA i.m. once daily, 270 mg/kg atazanavir (ATV; Bristol-Myers Squibb, New York NY) orally twice daily, 10 mg/kg of INTI orally twice daily, and 24 mg/kg RTV orally twice daily. Finally cohort C was treated with 480 mg/kg DRV orally twice daily, 10 mg/kg of INTI orally twice daily, 24 mg/kg RTV orally twice daily, and 25/50 mg/kg abacavir (ABC; ViiV, United Kingdom) orally twice daily. PmC2, C3 and C5 were supplemented with 200 mg/kg maraviroc (MVC; ViiV) orally twice daily.

In addition to antiretroviral drugs, cohort A was treated with latency-reversing agents (LRA). Pigtails PmA1 was kept as control while PmA2 and PmA3 were treated with the PKC activator ingenol B (Amazonia Fitoterapicos, Brazil) from 530-574 d.p.i.,

and then from 592-603 d.p.i. together with the histone-deaceytase inhibitor vorinostat (SAHA; Merck) (Figure 1). In cohort B1, Pm B11 was released from antiretroviral drugs 2 days prior necropsy, Pm B12 was released 9 days prior to necropsy, Pm B13 was released 3 days prior to necropsy, and Pm B14 was released 4 days prior to necropsy (Figure 1).

Blood and cerebrospinal fluid (CSF) samples were collected longitudinally. Before euthanasia, macaques were perfused with sterile saline to remove blood and circulating virus from tissues, as described elsewhere (33). Viral loads in plasma and CSF, $CD4^+$ T cell counts in blood, and tissue RNA and DNA levels in parietal cortex and basal ganglia were determined for all macaques in the study (Table 1). These studies were performed in accordance with federal guidelines and institutional policies.

Brain Macrophage Quantitative Viral Outgrowth Assay (MΦ-QVOA)

Brain parenchymal macrophages were isolated and cultured for MΦ-QVOA as previously described (37). Briefly, myeloid cells were purified based on expression of CD11b with a FITC conjugated anti-CD11b antibody (Beckman Coulter, Brea CA) followed by the EasySep FITC Positive Selection Kit (Stemcell Technologies). Purified macrophages were cultured in triplicate in a ten-fold limiting dilution in the presence of 10 μM zidovudine (Sigma), 25 nM darunavir (Janssen) and 5 nM raltegravir (Merck) for three days for cell attachment in poly-L-lysine coated plates (Sigma). For cohort C, cells were washed twice with HBSS (Life Technologies) to remove non-adherent $CD3^+$ lymphocytes. For the seeding of macrophages from cohorts A and B, an extra step to remove non-adherent $CD3^+$ lymphocytes was performed by briefly incubating the cells

with 0.05% trypsin (Life Technologies). In all cohorts, frequency of $CD3^+$ T cells in the MΦ-QVOA wells, quantitated by levels of TCRβ RNA, was lower than 3.8 % (Figure 3B). Brain macrophages were cultured in DMEM (Life Technologies) supplemented with 5% heat-inactivated bovine serum FBS (Atlanta Biologicals), 5% IS Giant Cell Tumor Conditioned Media (Irvine Scientific, Santa Ana CA), 100 U/mL penicillin- streptomycin (Life Technologies), 70 μg/mL gentamycin (Life Technologies), 2 mM L-glutamine (Life Technologies), 3 mM sodium pyruvate (Sigma), and 10 mM HEPES buffer (Life Technologies). Media containing 10 ng/mL of recombinant human Tumor Necrosis Factor alpha (TNFα; ProSpec, East Brunswick NJ) was used to reactivate latently infected macrophages. In addition to TNFα, $1x10^5$ CEMx174 cells/well were added to each dilution. Supernatants were collected and media were replenished with TNFα after 5 days in co-culture. Supernatants and cell lysates were collected following 10 days of co-culture with CEMx174 cells. The presence of replication-competent virus was determined by isolating RNA from supernatant and measuring SIV RNA by qRT-PCR or by measuring SIV p27 in the supernatant. The frequency of cells harboring replication-competent virus was determined using the IUPMStats v1.0 infection frequency calculator (38) and expressed as infectious units per million (IUPM).

Quantitation of $CD3^+$ T cells in MΦ-QVOA wells by the assessment of TCRβ RNA

TCRβ RNA was quantitated by qRT-PCR using QuantiTect Kit (Qiagen, Valencia CA), as previously described (34). 18s ribosomal RNA was multiplexed with the TCRβ RNA to control for cell counts. Duplicate control wells of macrophages

without CEMx174 cells were analyzed by qRT-PCR for TCRβ RNA and the number of $CD3^+$ T cells was calculated (Table 2).

RNA and DNA Isolation from Cells and Tissues

RNA and DNA from cell cultures were isolated with Allprep DNA/RNA Mini Kit (Qiagen, Valencia CA) according to manufacturer's protocol with modifications. An on-column DNase digestion was performed on the RNA isolation column using the RNase-free DNase kit (Qiagen) with the addition of four units of TURBO DNase (Life Technologies) to the enzyme mix.

SIV RNA from plasma, CSF, plasma, and culture supernatants was isolated using the QIAamp MinElute Virus Spin kit (Qiagen) for 200 µL or the QIAamp MinElute Virus Vacuum kit (Qiagen) for 1 mL of sample, according to manufacturer's protocol with modifications. An on-column DNase digestion was performed using the RNase-free DNase kit (Qiagen), with the addition of three units of RQ1 DNase (Promega, Madison WI) to the enzyme mix.

RNA from frozen tissues was isolated with RNase STAT-60 (Tel Test Inc., Friendswood TX). Tissues were homogenized with the FastPrep®-24 instrument (MP Biomedicals, Santa Ana CA) in lysing matrix D tubes (MP Biomedicals). After the addition of chloroform, samples were centrifuged and the aqueous phase was transferred to another tube for RNA precipitation with isopropanol. RNA was purified with the RNeasy Mini Kit (Qiagen), with an on-column DNase digestion using the RNase-free DNase kit (Qiagen), and the addition of three units of RQ1 DNase (Promega) to the enzyme mix.

DNA from frozen tissues was isolated with the DNeasy Blood and Tissue Kit (Qiagen) according to the manufacturer's protocol with modifications. Tissues were homogenized with the FastPrep®-24 instrument (MP Biomedicals) in lysing matrix A tubes (MP Biomedicals). Samples were incubated with 100 mg/mL RNAse A prior to DNeasy isolation.

Quantitation of SIV RNA and DNA

SIV RNA was measured by qRT-PCR using the QuantiTect Virus Kit (Qiagen) and primers for SIV *gag* as previously described (39-41). Three reactions were performed for each sample. To control for DNA contamination, one reaction was analyzed without reverse transcriptase.

SIV DNA was measured by qRT-PCR using the MP Kit (Qiagen) and primers for SIV *gag* as previously described. Two reactions were performed for each sample and multiplexed with primers for the quantitation of IFNβ. The number of cells per reaction was calculated by IFNβ DNA (two copies per cell) and used to normalize cellular SIV DNA and RNA from the same isolate. Samples were analyzed using the Rotogene thermocycler (Qiagen).

Quantitation of soluble proteins by ELISA

Levels of CCL2 (R&D Systems, Minneapolis MN), neopterin (IBL International, Germany), neurofilament light chain, NF-L (IBL), and IL-6 (R&D Systems) were measured longitudinally in the CSF according to manufacturer protocols. SIV p27

antigen (Zeptometrix, Buffalo NY) was measured from supernatants of MΦ-QVOA according to manufacturer protocol.

In situ hybridization (ISH)

Eight-micrometer-thick sections from fresh frozen brain (occipital cortex) were OCT-embedded and cryosectioned, postfixed in 4% paraformaldehyde, and dehydrated through graded ethanols. Tissue sections were rehydrated through graded ethanols, treated with HCl, triethanolamine, digitonin, and 4 μ g/mL Proteinase K After acetylation with acetic anhydride and dehydration, samples were hybridized at 45°C overnight with a 35S-labeled riboprobe and 0.5 mM aurintricarboxylic acid in hybridization mix. The riboprobe was synthesized from eight approximately 1 kb templates using PCR primer sets with SP6 promoters, amplified from B670 cDNA. After extensive washes and ribonuclease treatment, tissue sections were dehydrated, coated in Kodak NTB emulsion, exposed at 4°C for 7–14 days, and developed and fixed per manufacturer's instructions. They were stained with hematoxylin, dehydrated, and mounted with Permount. Photographic images were taken with a digital camera, and the section areas were obtained by scanning slides with an Aperio CS2 scanner (Leica) (42).

Cleaved Caspase-3 Immunohistochemistry

Cleaved caspase-3 was analyzed as previously described (43) using the Leica Bond RX automated immunostainer (Leica Microsystems, Germany). Cleaved caspase-3 antibody (0.252 μg/mL, Cell Signaling, Danvers MA) was used and immunohistochemistry performed using the Leica Bond Polymer Refine Detection Kit

according to manufacturer's protocol. The Leica Bond Polymer Refine Red Detection Kit was used for double staining with cleaved caspase-3 (0.126 μg/mL, Cell Signaling) and CD68 antibodies according to manufacturer's protocol.

In vitro infection of peripheral blood mononuclear cells (PBMC)

PBMCs from uninfected pigtailed macaques were isolated by Percoll density gradient and plated in 48 well plates in RPMI media supplemented with 2 μg/mL recombinant human IL-2 (Life Technologies) and 2 μg/mL PHA-M (Life Technologies) overnight as previously described (34). PBMCs were spinoculated for 2 hours with 100 μL supernatants of SIV RNA positive wells from brain MΦ-QVOAs. PBMCs were infected for 5 hours at 37°C and excess virus was removed after five washes with sterile saline. Media were replaced and supplemented with 2 μg/mL IL-2 (Life Technologies). Supernatants were collected at days 5, 10, and 13 post-spinoculation.

Statistics

Infected cell frequencies in limiting dilution assays were calculated using the IUPMStats v1.0 infection frequency calculator (http://silicianolab.johnshopkins.edu) (38). Statistics were performed using Prism Software (GraphPad Software, La Jolla CA). The Mann-Whitney analysis of variance test was performed to determine the significant changes of infectious units per million (IUPM) in the brain of SIV-infected ART-treated macaques compared to SIV-infected untreated animals ($p<0.05$). Linear regression was used to determine correlations between brain IUPM values with corresponding animal characteristics ($p<0.05$).

RESULTS

Variations of viral decay and set point in SIV-infected macaques treated with different ART regimens.

We have previously demonstrated that daily administration of PMPA, ATV, SQV, and INTI suppresses plasma and CSF viremia in pigtailed macaques inoculated with SIV/DeltaB670 and SIV/17E-Fr (33). We observed biphasic viral decay in both plasma and CSF similar to the decay of HIV in ART-treated individuals. The frequency of latently SIV-infected rCD4 in blood was very similar to the frequency observed in HIV-1-infected patients on long-term ART (ranging from 0.03 to 3 latently infected cells/per million rCD4) (23, 33, 44). To compare the efficacy of different ART regimens in suppressing viral replication in the CNS, drug combinations were designed based on the CNS penetration-effectiveness (CPE) developed by Dr. Scott Letendre (45). In group A (Figure 1A-B, Table 1), to maintain the same CPE rank of 6 used in our previous studies, the protease inhibitors (PI) ATV and SQV were substituted by DRV plus the PI booster RTV (21, 33). In this group, all treated macaques maintained suppression in plasma and CSF for more than 500 days, indicating that successful SIV control could be achieved with different PIs as part of the regimen. Two of these macaques (Table 1) were also treated with LRAs to test the "shock and kill" strategy for HIV eradication while the third animal (PmA1) served as control (manuscript under review, AIDS). Interestingly, after the second round of LRA, one of the LRA-treated macaques (PmA3) showed viral rebound in plasma and CSF without ART interruption (Figure 1A-B). No viral reactivation was observed in the second LRA-treated macaque (PmA2) or the control

animal PmA1, indicating that these two macaques emulate the virological control of HIV-infected patients in long-term ART.

In a second group (Table 1 and Figure 1C-F), seven macaques were treated with a less CNS-penetrant regimen (CPE rank of 5) where the combination DRV/RTV from group A was replaced by ATV/RTV. ART failed to successfully suppress viremia in three out of seven animals with lack of viral control being observed in both plasma and CSF (Figure 1E-F). For clarity we divided this group in two subgroups: macaques with suppression or efficient control of viremia were grouped as group B1 (Figure 1C-D) while macaques in which ART suppression did not lead to fewer than 30 SIV RNA copies/ml of plasma were placed in group B2 (Figure 1E-F). After 100 days of viral control, ART was interrupted in group B1 animals and macaques were euthanized 24 hours after detection of viral RNA in plasma (> 100 copies/mL) by qRT-PCR (Figure 1C-D).

A third group of animals (group C; Figure 1 G-H) was treated with DRV/RTV, INTI, and the non-nucleoside reverse transcriptase inhibitor ABC, which has a higher CPE than PMPA (3 versus 1). Although the regimen is ranked highly penetrant (CPE rank of 8), SIV RNA in plasma and CSF continued to be detected for more than 100 days post-treatment (Figure 1 G-H). Plasma viremia did not decrease even with the addition of MVC to the antiretroviral regimen in macaques PmC2, C3, and C5 (Table 1). Interestingly, viral RNA levels in all Group C animals were set 3 to 4 logs lower than those observed in SIV-infected untreated macaques (12), suggesting that antiretroviral resistance is not the main reason for the viral replication kinetics in these animals.

Results from these studies offer an opportunity to evaluate the impact of individual ART regimens in control of SIV replication *in vivo*.

CNS inflammation persists despite antiretroviral treatment

To evaluate whether ART-associated viral control in the CNS, measured by CSF viral load, is also followed by a decrease in inflammation, CSF samples were collected longitudinally and assessed for levels of CCL2 (or monocyte chemoattractant protein-1 [MCP- 1]), IL-6, neopterin, and neurofilament light chain (NF-L)(46). Elevated levels of CCL2 and IL-6 in the CSF have been associated with the development of HAND in humans and SIV-infected macaques (47-49). Neopterin is produced by activated myeloid cells, which closely correlates to brain inflammation in a variety of disorders, including HIV and multiple sclerosis (8, 50), and NF-L is a component of neuronal cytoskeleton released to the CSF during neurodegeneration and neuroaxonal damage (46).

Levels of activation markers in the CSF were consistently elevated during acute infection and decreased during ART, despite the regimen. However, after 100 days of suppression, CCL2 (Figure 2A-B) and IL-6 (Figure 2C-D) levels returned to pre-infection values in all cohorts while higher levels of neopterin (Figure 2G-H) and NF-L (Figure 2E-F) were observed in some but not all groups during ART treatment. Neopterin in the CSF appear to be related to plasma or CSF viremia, as levels in virally suppressed animals (groups A and B1) were similar to those before infection. Further, ART-treated animals with limited viral suppression presented significantly higher levels of neopterin in CSF, including the macaques in group B2, which were treated with the same regimen as B1. Conversely, groups B1 and B2 showed lower levels of NF-L in CSF when

compared to the other two regimens, indicating that other events besides viral replication are implicated in neuronal damage.

Quantitation of productively infected microglia in ART-treated macaques

Activation markers in the CSF have been largely associated with macrophages in the CNS (46). The two predominant populations of macrophages in brain are microglia and perivascular macrophages. Although the ratio between these two subsets varies during HIV/SIV infection and other CNS inflammatory changes, the majority of cells are resident microglia (51). Both types of cells are innate immune cell and produce type 1 interferon stimulating genes and cytokines in response to infection (52). In addition, macrophages are the major source of virus replication and virus production in brain. To determine the number of productively infected myeloid cells in the CNS, brain macrophages from the four cohorts of SIV-infected ART treated animals were isolated and the frequency of cells that harbor replication-competent virus was determined by the macrophage quantitative viral outgrowth assay (MΦ-QVOA) as previously described (34). The method of selection for brain macrophages, $CD11b^+$ selection, does not differentiate between distinct subtypes of brain macrophages. Since less than 5% of brain myeloid cells are perivascular macrophages (51), we will henceforth use the term microglia as a representative of all brain macrophages in the assay.

Microglial cells that harbor productively infected SIV virus were found in 13 out of 16 macaques (81%) with numbers varying from 0.07 to 4.62 IUPM (Figure 3A and Table 2). Levels of infected microglia isolated from SIV infected ART-treated macaques were significantly lower than those from SIV-infected untreated animals from a previous

study (34) (IUPM median of 0.3 vs. 231, $p<0.0005$), even for animals that failed to fully suppress viral replication in plasma (Figure 3C). There was no significant difference in the number of infected microglia between the cohorts, regardless of duration of ART treatment and level of plasma viremia, suggesting that SIV reservoirs in brain are maintained independently from viral replication in the periphery. In addition, microglia IUPM values also correlated poorly with levels of blood $CD4^+$ T cells (R= -0.3122, p= 0.2375) and monocytes (R= -0.3181, p= 0.2284) quantitated at necropsy.

Importantly, there was a significant correlation between terminal CSF viral load and number of productively infected microglia measured by MΦ-QVOA (R= 0.5289, p=0.037), underscoring the pivotal role of microglia as the major target cells for viral replication in brain. These data also corroborate previous findings suggesting that microglia function as latent reservoirs for SIV, since a negligible number of $CD4^+$ T cells are detected after microglia isolation (Table 2). Indeed, based on the frequency of $CD4^+$ T cells in the blood and the estimate that one in a million $CD4^+$ T cells is infected in SIV-infected ART treated macaques (33), we calculated that fewer than one potentially infected $CD4^+$ T cell was present in the macrophage cultures (Table 2).

Brain macrophages harbor SIV latent genomes that can be reactivated

The mechanisms that establish or maintain a latent state by HIV or SIV in macrophages have not been fully elucidated. Nonetheless, our results confirm that microglia harbor replication-competent, transcriptionally silenced viral genomes *in vivo* that can be activated *in vitro* in the MΦ-QVOA. Analyses of total SIV RNA isolated from brain (basal ganglia and parietal cortex) show that significant levels of SIV RNA

(>10 copies per μg of tissue) are detectable in only 5 out of 16 of the brain sections (31%) (Table 1), indicating that most microglia used in the MΦ-QVOAs were not transcribing viral RNA prior to *in vitro* cultures. In addition, brain SIV DNA was not observed in 31% of the animals (5 out of 16), despite high plasma viremia (Table 2), supporting the compartmentalization of virus replication during suppressive ART in the periphery and the CNS.

Detection of SIV RNA expressing cells by ISH in brain

ISH in two regions of brain was performed to investigate the frequency and pattern of SIV cell-associated RNA (caRNA) in brain regions in cohorts A and B1. In addition, ISH complements the MΦ-QVOA results as another quantitative technique *in vivo*. In cohort A, macaques were suppressed for over 500 days and remained on ART while treated with LRA, during which macaque PmA3 had reactivation of virus in CSF (Figure 1). In contrast, cohort B1 macaques were suppressed for 100 days, released from ART, and then euthanized 24 hours after detection of viral RNA in plasma (>100 copies /ml) by qRT-PCR. Brain sections (occipital cortex) from macaques PmA1, A2, A3, B13, and B14 were analyzed. RNA positive cells were found in the occipital cortex of macaque PmA3 (Table 3 and Figure 4) at a density of 2,220 SIV^+ cells per gram of tissue whereas PmA1 had a ten fold lower density (202 SIV^+ cells/gram of tissue) in occipital cortex. In both macaques the pattern of *in situ* positive cells was single positive foci per analyzed area, suggesting that expression of SIV RNA in the brain occurred without viral spread to other cells. Macaque PmA2 had no detectable SIV RNA^+ cells in the areas analyzed. In contrast, macaque PmB13 (ART released) presented a higher frequency of

SIV RNA$^+$ cells (10,553 SIV$^+$ cells/gram of tissue) arranged in clusters, suggesting virus spread (Table 3). In addition, macaque PmB13 had detectable viral RNA in CSF (168 SIV RNA copies/mL of CSF). Conversely, macaque PmB14 had undetectable SIV RNA by ISH in brain and undetectable viral RNA in CSF. Interestingly, macaque PmB14 had low but detectable viral RNA in plasma (225 SIV RNA copies/mL,) (Table 1) suggesting that early virus rebound in plasma had not spread to the CNS.

ISH of SIV RNA in brain and the MΦ-QVOA provide very different quantitative approaches to detecting productively infected cells. While ISH analyzes multiple thin sections from brain regions and quantitates cell expression of SIV RNA, the MΦ-QVOA detects replication-competent virus in isolated cells. Our group routinely isolates microglial cells from basal ganglia, leaving other brain regions, such as occipital cortex, for ISH and immunohistochemistry. MΦ-QVOA from SIV-infected macrophages isolated from basal ganglia were positive despite no detectable SIV RNA by HIS was observed in the same section (Table 1), suggesting that there are far more cells in the brain harboring SIV genomes but not expressing viral RNA. Thus, these complementary quantitative techniques strongly support that microglia in the brain of SIV-infected ART treated macaques harbor latent genomes and represent a functional viral reservoir.

Low levels of cleaved caspase-3 reveal microglia are a stable reservoir

To examine whether the microglial cells in the brain undergo apoptosis during ART suppression, immunohistochemistry (IHC) for cleaved caspase-3 (a marker of apoptosis) and CD68 (a marker for macrophages) was performed on brain sections from

ART-suppressed macaques (Figure 4C). Low levels of cleaved caspase-3 expression were found in the both ART-treated and untreated macaques (PmA3, left vs. Pm4, right). Even in the SIV-infected animal with encephalitis (Pm4 from a previous study (34)) there were very low levels of expression of cleaved caspase-3 and no co-localization with CD68. In brain of the ART-treated macaque, cleaved caspase-3 was rarely observed indicating limited apoptotic events in brain macrophages (Figure 4C). The lack of significant apoptosis in brain or in brain myeloid cells of the ART suppressed macaques provided further support for long-term persistence of brain microglia during ART suppression.

SIV virions released by brain macrophages are replication competent

We observed that, in some MΦ-QVOA wells, the levels of SIV RNA or p27 were low, suggesting that the virus was not spreading within the CEMx174 cell line used to amplify the virus released by the activated microglia. To evaluate whether the virions measured in the MΦ-QVOA represented replication competent virus, supernatants collected from microglia MΦ-QVOAs were combined with PMA/IL-2-activated uninfected macaque peripheral blood mononuclear cells (PBMCs) and centrifuged for 2 hours to spinoculate the cells. PBMCs were then incubated for 13 days, supernatants collected at days 5, 10 and 13 p.i, and viral RNA was isolated from the combined time-points. Quantitation of SIV RNA from the MΦ-QVOA supernatants (input virus) and from the infected PBMCs (output virus) is shown in Figure 5. Increase in virus particles was observed in all samples, indicating that the supernatants from the MΦ-QVOA wells contained infectious virus (Figure 5). Moreover, replication-competent SIV was observed

in microglia MΦ-QVOAs isolated from long-term suppressed animals (group A), corroborating our previous findings that brain macrophages harbor latent virus genomes that can contribute to plasma and CSF viremia once ART is withdrawn.

DISCUSSION

One of the major concerns during the initial development of combined ART was whether the compounds would efficiently cross the blood brain barrier and control viral replication in the CNS (53). In the ART era, signs of chronic systemic inflammation are observed in a large percentage of treated patients, even when blood viral load is undetectable and $CD4^+$ T cell counts are restored to pre-infection levels (54, 55), suggesting that viral reservoirs persist in organs and tissues where ART has suboptimal penetrance, such as the brain. Indeed, HAND is still prevalent in ART-treated patients (56). In addition to the evident symptoms associated with neurological dysfunction, such as memory loss and neuropathy, these patients present a 3-fold increased risk of mortality when compared to their HIV-infected non-HAND counterparts (57). A study using tissues from the National NeuroAIDS Tissue Consortium established an association between these morbidities and viral replication in the CNS (58). A broad prevalence of HIV DNA and RNA was reported in 148 brain specimens of cART-treated patients, and higher levels of viral nucleic acids were detected in patients with neuropathological evidence of HIV encephalitis, despite undetectable plasma viral load (58). These findings reaffirm the importance of the brain as a potential viral reservoir during ART.

In contrast to $CD4^+$ T lymphocytes in the periphery, the majority of HIV-infected cells in the CNS are microglia, perivascular macrophages, and astrocytes (59-61). These cells present distinct surface markers and transcriptional networks, which explain why HIV strains identified in the CNS frequently diverge from the ones found concomitantly in the blood of the same patient (62). In addition, at least in $CD4^+$ lymphocytes, HIV latency is a multifactorial process in which distinct mechanisms, at times in cooperation,

drive the virus into transcriptional silence (63). In brain macrophages, however, specific mechanisms for the establishment of viral latency require further examination. For instance, IFNß is able to modulate viral transcription in macrophages - but not in lymphocytes - by increasing the expression of the truncated, dominant-negative form of the transcription factor C/EBP-ß (64, 65), and the repressor CTIP2 is able to inhibit HIV transcription by recruiting chromatin-modifying complexes in microglial cells (66).

Part of these assessments can be done *in vitro* using HIV and human cells. However, *in vivo* experiments using SIV strains combined with a consistent macaque model allow for a more accurate translational evaluation, providing opportunities to characterize viral reservoirs in tissues not easily obtained from HIV-infected patients. Using our consistent and accelerated SIV pigtailed macaque model for HIV/AIDS and HAND, we have previously established a robust SIV model of ART with the combination of four antiretroviral drugs (67, 68). To evaluate the efficacy of other drug combinations in control of viral replication in the periphery and CNS, we tested other CNS-penetrant antiretroviral combinations that closely reflect regimens used by HIV-infected patients.

Despite the suppression of viral replication in the brain in the majority of animals, inflammatory markers that reflect macrophage activation (neopterin), neuronal damage (neurofilament light chain) were detected in the CSF in SIV-infected macaques from all cohorts, including those suppressed for more than 18 months. These results corroborate findings in HIV-infected ART-treated patients (69-71) and suggest continued inflammation in brain, possibly caused by the presence of suppressed or latent virus in the CNS. This hypothesis is supported in this study by the detection of latent, but replication-competent, SIV in brain using an MΦ-QVOA developed in our laboratory

(34). We had previously demonstrated that the MΦ-QVOA could be used to quantify purified populations of macrophages from SIV-infected macaques. In addition, we compared the level of productively infected macrophages to $CD4^+$ T cells measured by QVOA (34). In this study we demonstrate that the MΦ-QVOA is a sensitive and specific assay to measure the number of productively infected cells in brain of SIV-infected macaques suppressed with ART. The MΦ-QVOA detected replication competent virus in microglia isolated from regions of brain with no detectable SIV RNA providing the first demonstration of productively infected latent microglia in brain. In addition, we demonstrated that virus isolated from MΦ-QVOA is infectious in primary macaque PBMCs, which is additional corroboration for a functional latent reservoir in the brain. Further, by sensitive measures of TCRß RNA in the MΦ-QVOA we provide strong evidence that there is no contribution of infected $CD4^+$ T cells to our findings.

Further, SIV RNA^+ macrophages were detected by ISH, not only in the brain of macaques Pm A3 and Pm B13 with detectable SIV RNA in the CSF, but also in the brain of macaque Pm A1, which was fully suppressed on ART. These results strongly suggest that microglia harbor replication competent virus in ART-suppressed macaques in a latent form that is reactivated at low levels during suppression (macaque Pm A1 with 202 SIV^+ cells/gram of tissue), which accounts for the continued expression of neopterin and NF-L. However, when virus is activated by LRAs (macaque Pm A3) or rebound after ART interruption (macaque Pm B13), a higher level of reactivation of the microglial latent reservoir (2,220 and 10,553 cells/gram of tissue, respectively) is observed, with concomitant increase of the macrophage activation marker neopterin.

After 1.7 years of viral suppression in cohort A, macaques PmA1 and PmA2 showed no viral RNA in basal ganglia and parietal cortex whereas PmA3 had viral RNA in occipital cortex (a brain section not used for the MΦ-QVOA). Nevertheless, all three macaques in cohort A had replication competent virus produced in the isolated microglia. The ISH provided different result than the MΦ-QVOA probably due to the different brain regions used for the two assays, occipital cortex used for the *in situ* hybridization had detectable viral RNA and was *in situ* positive. Furthermore, SIV-infected macaques suppressed for six months with little or no detectable virus in the CSF and low levels of SIV RNA in brain also had latently infected microglia that produced virus in the MΦ-QVOA.

The demonstration that there is latent replication-competent virus in macaque brain provides a mechanism for the ongoing macrophage activation. Recent studies have suggested that, while virus does not spread during ART suppression, there is ongoing stochastic activation of virus genomes in latently infected cells (72, 73). Reactivation of virus without spread in the macrophage is likely to induce innate immune responses and cellular activation. In addition, the extremely low level of apoptosis detected in the brain of the suppressed macaques further suggests that the latent microglia reservoir is stable and does not undergo significant loss due to cell death. Thus, our demonstration of productively infected latent microglia in the brain provides a mechanism for the ongoing inflammation of HIV in a fully suppressed individual.

The presence of a long-term functional reservoir of SIV in brain that parallels the biologic and pathologic features of HIV-infected individuals with HAND presents a formidable barrier to strategies to decrease or eliminate the HIV reservoir. First, the brain

is protected by the blood brain barrier, therefore special eradication approaches are required for successful CNS penetrance. Also, strategies that include activation of virus in brain may cause inflammation and neuronal toxicity due to an exacerbated macrophage activation and production of cytokines, which are present during latent HIV infection. However, if the brain is excluded from eradication strategies, there is the potential for incomplete elimination of a functional latent reservoir that can be reactivated when ART is stopped, resulting in the spread of reactivated CNS virus to peripheral blood and tissues. Our studies suggest that the brain harbors a functional latent SIV reservoir and that the CNS must be considered for the complete elimination of latent HIV in AIDS cure strategies.

FUNDING INFORMATION

This study was supported by NCRR and the Office of Research Infrastructure Programs (ORIP) of the NIH (grant P40 OD013117) and NIH grants P01 MH070306, NS077869, NS076357, U19-0AI076113, and R56 AI118753. The funders had no role in the study design, data collection and interpretation, or the decision to submit the work for publication.

ACKNOWLEDGEMENTS

We thank the Johns Hopkins School of Medicine Retrovirus Laboratory for technical assistance and guidance. We declare no conflict of interest.

Author contributions:

C.R.A., J.E.C. and L.G. conceived the study and prepared the manuscript. C.R.A. performed the MΦ-QVOA and TCRβ RNA analyses. S.E.Q. performed the ELISA experiments; L.G. analyzed the data. C.R.A. and M.L. isolated RNA and DNA, and performed qRT-PCR. S.L.P. performed PBMC spinoculation; C.R.A. analyzed the data. E.L.E. prepared immunohistochemistry slides; J.E.C. and J.L.M. analyzed them. E.N.S. and S.E.Q. prepared animal characteristics tables. E.N.S., E.R.F., B.T.B. and S.E.Q. isolated tissue cells. C.M.A. and E.R.F assisted C.R.A. where needed. F.M.G. assembled decay characteristics. S.W.W. and A.T.H. prepared *in situ* hybridization slides; J.E.C., L.G. and J.L.M. analyzed them. C.R.A., J.L.M., L.G. and J.E.C. edited the manuscript.

REFERENCES

1. **Heaton RK, Franklin DR, Ellis RJ, McCutchan JA, Letendre SL, Leblanc S, Corkran SH, Duarte NA, Clifford DB, Woods SP, Collier AC, Marra CM, Morgello S, Mindt MR, Taylor MJ, Marcotte TD, Atkinson JH, Wolfson T, Gelman BB, McArthur JC, Simpson DM, Abramson I, Gamst A, Fennema-Notestine C, Jernigan TL, Wong J, Grant I, Group C, Group H.** 2011. HIV-associated neurocognitive disorders before and during the era of combination antiretroviral therapy: differences in rates, nature, and predictors. J Neurovirol **17:**3-16.
2. **Robertson KR, Smurzynski M, Parsons TD, Wu K, Bosch RJ, Wu J, McArthur JC, Collier AC, Evans SR, Ellis RJ.** 2007. The prevalence and incidence of neurocognitive impairment in the HAART era. AIDS **21:**1915-1921.
3. **Heaton RK, Clifford DB, Franklin DR, Woods SP.** 2010. HIV-associated neurocognitive disorders persist in the era of potent antiretroviral therapy CHARTER Study. Neurology doi:10.1212/WNL.0b013e318200d727.
4. **Rao VR, Ruiz AP, Prasad VR.** 2014. Viral and cellular factors underlying neuropathogenesis in HIV associated neurocognitive disorders (HAND). AIDS research and therapy **11:**13.
5. **Rappaport J, Volsky DJ.** 2015. Role of the macrophage in HIV-associated neurocognitive disorders and other comorbidities in patients on effective antiretroviral treatment. J Neurovirol **21:**235-241.
6. **Zayyad Z, Spudich S.** 2015. Neuropathogenesis of HIV: from initial neuroinvasion to HIV-associated neurocognitive disorder (HAND). Curr HIV/AIDS Rep **12:**16-24.
7. **Canestri A, Lescure F-X, Jaureguiberry S, Moulignier A, Amiel C, Marcelin A, Peytavin G, Tubiana R, Pialoux G, Katlama C.** 2010. Discordance between cerebral spinal fluid and plasma HIV replication in patients with neurological symptoms who are receiving suppressive antiretroviral therapy. Clinical Infectious Diseases **50:**773-778.
8. **Eden A, Fuchs D, Hagberg L, Nilsson S, Spudich S, Svennerholm B, Price RW, Gisslen M.** 2010. HIV-1 viral escape in cerebrospinal fluid of subjects on suppressive antiretroviral treatment. J Infect Dis **202:**1819-1825.
9. **Williams K, Westmoreland S, Greco J, Ratai E, Lentz M, Kim WK, Fuller RA, Kim JP, Autissier P, Sehgal PK, Schinazi RF, Bischofberger N, Piatak M, Lifson JD, Masliah E, Gonzalez RG.** 2005. Magnetic resonance spectroscopy reveals that activated monocytes contribute to neuronal injury in SIV neuroAIDS. J Clin Invest **115:**2534-2545.
10. **Navia BA, Jordan BD, Price RW.** 1986. The AIDS dementia complex: I. Clinical features. Ann Neurol **19:**517-524.
11. **Zink MC, Clements JE.** 2002. A novel simian immunodeficiency virus model that provides insight into mechanisms of human immunodeficiency virus central nervous system disease. J Neurovirol **8 Suppl 2:**42-48.
12. **Zink MC, Suryanarayana K, Mankowski JL, Shen A, Piatak M, Jr., Spelman JP, Carter DL, Adams RJ, Lifson JD, Clements JE.** 1999. High viral

load in the cerebrospinal fluid and brain correlates with severity of simian immunodeficiency virus encephalitis. J Virol **73:**10480-10488.
13. **Schnell G, Joseph S, Spudich S, Price RW.** 2011. HIV-1 replication in the central nervous system occurs in two distinct cell types. PLoS … doi:10.1371/journal.ppat.1002286.
14. **Joseph SB, Arrildt KT, Sturdevant CB.** 2015. HIV-1 target cells in the CNS. Journal of … doi:10.1007/s13365-014-0287-x.
15. **Williams KC, Corey S, Westmoreland SV, Pauley D, Knight H, deBakker C, Alvarez X, Lackner AA.** 2001. Perivascular macrophages are the primary cell type productively infected by simian immunodeficiency virus in the brains of macaques: implications for the neuropathogenesis of AIDS. J Exp Med **193:**905-915.
16. **Sinclair E, Gray F, Ciardi A, Scaravilli F.** 1994. Immunohistochemical changes and PCR detection of HIV provirus DNA in brains of asymptomatic HIV-positive patients. Journal of neuropathology and experimental neurology **53:**43-50.
17. **Clements JE, Babas T, Mankowski JL, Suryanarayana K, Piatak M, Jr., Tarwater PM, Lifson JD, Zink MC.** 2002. The central nervous system as a reservoir for simian immunodeficiency virus (SIV): steady-state levels of SIV DNA in brain from acute through asymptomatic infection. J Infect Dis **186:**905-913.
18. **Clements JE, Mankowski JL, Gama L, Zink MC.** 2008. The accelerated simian immunodeficiency virus macaque model of human immunodeficiency virus-associated neurological disease: from mechanism to treatment. J Neurovirol **14:**309-317.
19. **Koenig S, Gendelman HE, Orenstein JM, Dal Canto MC, Pezeshkpour GH, Yungbluth M, Janotta F, Aksamit A, Martin MA, Fauci AS.** 1986. Detection of AIDS virus in macrophages in brain tissue from AIDS patients with encephalopathy. Science **233:**1089-1093.
20. **Shaw GM, Harper ME, Hahn BH, Epstein LG, Gajdusek DC, Price RW, Navia BA, Petito CK, O'Hara CJ, Groopman JE, et al.** 1985. HTLV-III infection in brains of children and adults with AIDS encephalopathy. Science **227:**177-182.
21. **Zink MC, Brice AK, Kelly KM, Queen SE, Gama L, Li M, Adams RJ, Bartizal C, Varrone J, Rabi SA, Graham DR, Tarwater PM, Mankowski JL, Clements JE.** 2010. Simian immunodeficiency virus-infected macaques treated with highly active antiretroviral therapy have reduced central nervous system viral replication and inflammation but persistence of viral DNA. J Infect Dis **202:**161-170.
22. **Finzi D, Blankson J, Siliciano JD, Margolick JB, Chadwick K, Pierson T, Smith K, Lisziewicz J, Lori F, Flexner C, Quinn TC, Chaisson RE, Rosenberg E, Walker B, Gange S, Gallant J, Siliciano RF.** 1999. Latent infection of CD4+ T cells provides a mechanism for lifelong persistence of HIV-1, even in patients on effective combination therapy. Nat Med **5:**512-517.
23. **Finzi D, Hermankova M, Pierson T, Carruth LM, Buck C, Chaisson RE, Quinn TC, Chadwick K, Margolick J, Brookmeyer R, Gallant J, Markowitz**

M, Ho DD, Richman DD, Siliciano RF. 1997. Identification of a reservoir for HIV-1 in patients on highly active antiretroviral therapy. Science **278:**1295-1300.
24. **Richman DD, Margolis DM, Delaney M, Greene WC, Hazuda D, Pomerantz RJ.** 2009. The challenge of finding a cure for HIV infection. Science **323:**1304-1307.
25. **Lewin S, Evans V, Elliott J, Spire B, Chomont N.** 2011. Finding a cure for HIV: will it ever be achievable? Journal of the International AIDS Society **14:**4.
26. **Chun T-W, Engel D, Mizell SB, Ehler LA, Fauci AS.** 1998. Induction of HIV-1 Replication in Latently Infected CD4+ T Cells Using a Combination of Cytokines. The Journal of Experimental Medicine **188:**83-91.
27. **Archin NM, Espeseth A, Parker D, Cheema M, Hazuda D, Margolis DM.** 2009. Expression of Latent HIV Induced by the Potent HDAC Inhibitor Suberoylanilide Hydroxamic Acid. AIDS Research and Human Retroviruses **25:**207-212.
28. **Kulkosky J.** 2001. Prostratin: activation of latent HIV-1 expression suggests a potential inductive adjuvant therapy for HAART. Blood **98:**3006-3015.
29. **Jiang G, Mendes EA, Kaiser P, Sankaran-Walters S, Tang Y, Weber MG, Melcher GP, Thompson GR, Tanuri A, Pianowski LF, Wong JK, Dandekar S.** 2014. Reactivation of HIV latency by a newly modified Ingenol derivative via protein kinase Cδ-NF-κB signaling. AIDS (London, England) **28:**1555-1566.
30. **Kaminski R, Chen Y, Fischer T, Tedaldi E, Napoli A, Zhang Y, Karn J, Hu W, Khalili K.** 2016. Elimination of HIV-1 Genomes from Human T-lymphoid Cells by CRISPR/Cas9 Gene Editing. Scientific reports **6:**22555.
31. **Laird GM, Eisele EE, Rabi SA, Lai J, Chioma S, Blankson JN, Siliciano JD, Siliciano RF.** 2013. Rapid quantification of the latent reservoir for HIV-1 using a viral outgrowth assay. PLoS Pathog **9:**e1003398.
32. **Eriksson S, Graf EH, Dahl V, Strain MC, Yukl SA, Lysenko ES, Bosch RJ, Lai J, Chioma S, Emad F, Abdel-Mohsen M, Hoh R, Hecht F, Hunt P, Somsouk M, Wong J, Johnston R, Siliciano RF, Richman DD, O'Doherty U, Palmer S, Deeks SG, Siliciano JD.** 2013. Comparative analysis of measures of viral reservoirs in HIV-1 eradication studies. PLoS Pathog **9:**e1003174.
33. **Dinoso JB, Rabi SA, Blankson JN, Gama L, Mankowski JL, Siliciano RF, Zink MC, Clements JE.** 2009. A simian immunodeficiency virus-infected macaque model to study viral reservoirs that persist during highly active antiretroviral therapy. J Virol **83:**9247-9257.
34. **Avalos CR, Price SL, Forsyth ER, Pin JN, Shirk EN, Bullock BT, Queen SE, Li M, Gellerup D, O'Connor SL, Zink CM, Mankowski JL, Gama L, Clements JE.** 2016. Quantitation of Productively Infected Monocytes and Macrophages of SIV-Infected Macaques. Journal of Virology doi:10.1128/JVI.00290-16**:**16.
35. **Babas T, Dewitt JB, Mankowski JL, Tarwater PM, Clements JE, Zink MC.** 2006. Progressive selection for neurovirulent genotypes in the brain of SIV-infected macaques. AIDS **20:**197-205.
36. **Mankowski JL, Flaherty MT, Spelman JP, Hauer DA, Didier PJ, Amedee AM, Murphey-Corb M, Kirstein LM, Munoz A, Clements JE, Zink MC.**

1997. Pathogenesis of simian immunodeficiency virus encephalitis: viral determinants of neurovirulence. J Virol **71:**6055-6060.

37. **Babas T, Munoz D, Mankowski JL, Tarwater PM, Clements JE, Zink MC.** 2003. Role of microglial cells in selective replication of simian immunodeficiency virus genotypes in the brain. J Virol **77:**208-216.
38. **Rosenbloom DIS, Elliott O, Hill AL, Henrich TJ.** 2015. Designing and interpreting limiting dilution assays: general principles and applications to the latent reservoir for HIV-1. bioRxiv.
39. **Shen A, Zink MC, Mankowski JL, Chadwick K, Margolick JB, Carruth LM, Li M, Clements JE, Siliciano RF.** 2003. Resting CD4+ T Lymphocytes but Not Thymocytes Provide a Latent Viral Reservoir in a Simian Immunodeficiency Virus-Macaca nemestrina Model of Human Immunodeficiency Virus Type 1-Infected Patients on Highly Active Antiretroviral Therapy. Journal of Virology **77:**4938-4949.
40. **Gama L, Shirk EN, Russell JN, Carvalho KI, Li M, Queen SE, Kalil J, Zink MC, Clements JE, Kallas EG.** 2012. Expansion of a subset of CD14highCD16negCCR2low/neg monocytes functionally similar to myeloid-derived suppressor cells during SIV and HIV infection. J Leukoc Biol **91:**803-816.
41. **Meulendyke KA, Pletnikov MV, Engle EL, Tarwater PM, Graham DR, Zink MC.** 2012. Early minocycline treatment prevents a decrease in striatal dopamine in an SIV model of HIV-associated neurological disease. J Neuroimmune Pharmacol **7:**454-464.
42. **Miller CJ, Li Q, Abel K, Kim EY, Ma ZM, Wietgrefe S, La Franco-Scheuch L, Compton L, Duan L, Shore MD, Zupancic M, Busch M, Carlis J, Wolinsky S, Haase AT.** 2005. Propagation and dissemination of infection after vaginal transmission of simian immunodeficiency virus. J Virol **79:**9217-9227.
43. **Williams DW, Engle EL, Shirk EN, Queen SE, Gama L, Mankowski JL, Zink MC, Clements JE.** 2016. Splenic Damage during SIV Infection: Role of T-Cell Depletion and Macrophage Polarization and Infection. Am J Pathol doi:10.1016/j.ajpath.2016.03.019.
44. **Siliciano JD, Kajdas J, Finzi D, Quinn TC.** 2003. Long-term follow-up studies confirm the stability of the latent reservoir for HIV-1 in resting CD4+ T cells. Nature medicine doi:10.1038/nm880.
45. **Letendre S, Marquie-Beck J.** 2008. Validation of the CNS Penetration-Effectiveness rank for quantifying antiretroviral penetration into the central nervous system. Archives of … doi:10.1001/archneurol.2007.31.
46. **Beck SE, Queen SE, Witwer KW, Pate KA, Mangus LM, Gama L, Adams RJ, Clements JE, Zink CM, Mankowski JL.** 2015. Paving the path to HIV neurotherapy: predicting SIV CNS disease. European journal of pharmacology **759:**303-312.
47. **Mankowski JL, Queen SE, Clements JE, Zink MC.** 2004. Cerebrospinal fluid markers that predict SIV CNS disease. J Neuroimmunol **157:**66-70.
48. **Zink MC, Coleman GD, Mankowski JL, Adams RJ, Tarwater PM, Fox K, Clements JE.** 2001. Increased macrophage chemoattractant protein-1 in

cerebrospinal fluid precedes and predicts simian immunodeficiency virus encephalitis. The Journal of infectious diseases **184:**1015-1021.
49. **Sevigny JJ, Albert SM, McDermott MP, McArthur JC.** 2004. Evaluation of HIV RNA and markers of immune activation as predictors of HIV-associated dementia. Neurology.
50. **Fuchs D, Spira TJ, Hausen A, Reibnegger G, Werner ER, Felmayer GW, Wachter H.** 1989. Neopterin as a predictive marker for disease progression in human immunodeficiency virus type 1 infection. Clin Chem **35:**1746-1749.
51. **Bennett ML, Bennett FC, Liddelow SA.** 2016. New tools for studying microglia in the mouse and human CNS. Proceedings of the … doi:10.1073/pnas.1525528113.
52. **Alammar L, Gama L, Clements JE.** 2011. Simian immunodeficiency virus infection in the brain and lung leads to differential type I IFN signaling during acute infection. J Immunol **186:**4008-4018.
53. **McArthur JC.** 1997. NeuroAIDS: diagnosis and management. Hosp Pract (1995) **32:**73-74, 77-79, 84 passim.
54. **Appay V, Sauce D.** 2008. Immune activation and inflammation in HIV-1 infection: causes and consequences. The Journal of pathology **214:**231-241.
55. **Kamat A, Misra V, Cassol E, Ancuta P, Yan Z, Li C, Morgello S, Gabuzda D.** A plasma biomarker signature of immune activation in HIV patients on antiretroviral therapy. PLoS ONE **7**.
56. **Simioni S, Cavassini M, Annoni J-M, Rimbault Abraham A, Bourquin I, Schiffer Vr, Calmy A, Chave J-P, Giacobini E, Hirschel B, Du Pasquier R.** Cognitive dysfunction in HIV patients despite long-standing suppression of viremia. AIDS (London, England) **24:**1243-1250.
57. **Vivithanaporn P, Heo G, Gamble J, Krentz H, Hoke A, Gill M, Power C.** Neurologic disease burden in treated HIV/AIDS predicts survival: a population-based study. Neurology **75:**1150-1158.
58. **Gelman B, Lisinicchia J, Morgello ea.** Neurovirological correlation with HIV-associated neurocognitive disorders and encephalitis in a HAART-era cohort. JAIDS doi:10.1097/QAI.0b013e31827f1bdb.
59. **Wiley C, Schrier R, Nelson J, Lampert P, Oldstone M.** 1986. Cellular localization of human immunodeficiency virus infection within the brains of acquired immune deficiency syndrome patients. Proceedings of the National Academy of Sciences of the United States of America **83:**7089-7093.
60. **Spudich S, Gonzalez-Scarano F.** HIV-1-related central nervous system disease: current issues in pathogenesis, diagnosis, and treatment. Cold Spring Harb Perspect Med **2:**a007120.
61. **Shi B, De Girolami U, He J, Wang S, Lorenzo A, Busciglio J, Gabuzda D.** 1996. Apoptosis induced by HIV-1 infection of the central nervous system. J Clin Invest **98:**1979-1990.
62. **Harrington P, Schnell G, Letendre S, Ritola K, Robertson K, Hall C, Burch C, Jabara C, Moore D, Ellis R, Price R, Swanstrom R.** 2009. Cross-sectional characterization of HIV-1 env compartmentalization in cerebrospinal fluid over the full disease course. AIDS (London, England) **23:**907-915.

63. **Donahue D, Wainberg M.** Cellular and molecular mechanisms involved in the establishment of HIV-1 latency. Retrovirology **10:**11.
64. **Henderson AJ, Calame KL.** 1997. CCAAT/enhancer binding protein (C/EBP) sites are required for HIV-1 replication in primary macrophages but not CD4(+) T cells. Proc Natl Acad Sci U S A **94:**8714-8719.
65. **Barber S, Gama L, Dudaronek J, Voelker T, Tarwater P, Clements J.** 2006. Mechanism for the establishment of transcriptional HIV latency in the brain in a simian immunodeficiency virus-macaque model. The Journal of infectious diseases **193:**963-970.
66. **Marban Cl, Suzanne S, Dequiedt F, de Walque Sp, Redel L, Van Lint C, Aunis D, Rohr O.** 2007. Recruitment of chromatin-modifying enzymes by CTIP2 promotes HIV-1 transcriptional silencing. The EMBO journal **26:**412-423.
67. **Dinoso J, Rabi S, Blankson J, Gama L, Mankowski J, Siliciano R, Zink M, Clements J.** 2009. A simian immunodeficiency virus-infected macaque model to study viral reservoirs that persist during highly active antiretroviral therapy. Journal of Virology **83:**9247-9257.
68. **Zink M, Brice A, Kelly K, Queen S, Gama L, Li M, Adams R, Bartizal C, Varrone J, Rabi S, Graham D, Tarwater P, Mankowski J, Clements J.** Simian immunodeficiency virus-infected macaques treated with highly active antiretroviral therapy have reduced central nervous system viral replication and inflammation but persistence of viral DNA. The Journal of infectious diseases **202:**161-170.
69. **Garvey LJ, Pavese N, Politis M, Ramlackhansingh A, Brooks DJ, Taylor-Robinson SD, Winston A.** 2014. Increased microglia activation in neurologically asymptomatic HIV-infected patients receiving effective ART. AIDS (London, England) **28:**67-72.
70. **Edén A, Price RW, Spudich S, Fuchs D, Hagberg L, Gisslén M.** 2007. Immune activation of the central nervous system is still present after >4 years of effective highly active antiretroviral therapy. The Journal of infectious diseases **196:**1779-1783.
71. **Kamat A, Lyons JL, Misra V, Uno H, Morgello S, Singer EJ, Gabuzda D.** 2012. Monocyte activation markers in cerebrospinal fluid associated with impaired neurocognitive testing in advanced HIV infection. Journal of acquired immune deficiency syndromes (1999) **60:**234-243.
72. **Martinez-Picado J, Deeks SG.** 2016. Persistent HIV-1 replication during antiretroviral therapy. Current opinion in HIV and AIDS **11:**417-423.
73. **Joos B, Fischer M, Kuster H, Pillai SK, Wong JK, Böni J, Hirschel B, Weber R, Trkola A, Günthard HF, Study S.** 2008. HIV rebounds from latently infected cells, rather than from continuing low-level replication. Proceedings of the National Academy of Sciences of the United States of America **105:**16725-16730.

	Animal Identifier	ART (days)	Cell Counts (cells/ uL blood)		Viral Load (SIV RNA Eq./mL)		RNA (SIV RNA Eq./ µg RNA)		DNA (SIV DNA Eq./ 10^6 cells)		ART Regimen[c]
			$CD4^+$ T cell	Monocyte	Plasma	CSF	Basal Ganglia	Parietal Cortex	Basal Ganglia	Parietal Cortex	
Cohort A	Pm A1	615	474	1092	<10[d]	<10[d]	<10[d]	<10[d]	<10[d]	<10[d]	PMPA DRV INTI RTV
	Pm A2[b]	616	1074	485	<10[d]	<10[d]	<10[d]	<10[d]	<10[d]	<10[d]	
	Pm A3[b]	605	320	1346	1,800	18,000	<10[d]	<10[d]	<10[d]	64	
Cohort B1	Pm B11[a]	364	228	618	182,070	364	<10[d]	<10[d]	<10[d]	<10[d]	PMPA ATV INTI RTV
	Pm B12[a]	370	235	465	2,343	57	<10[d]	<10[d]	<10[d]	<10[d]	
	Pm B13[a]	283	596	314	216	168	165	<10[d]	11	16	
	Pm B14[a]	224	653	547	225	<10[d]	<10[d]	<10[d]	<10[d]	14	
Cohort B2	Pm B21	222	391	455	425,000	8,910	<10[d]	<10[d]	46	342	PMPA ATV INTI RTV
	Pm B22	214	388	429	12,400	3,305	<10[d]	<10[d]	<10[d]	17	
	Pm B23	215	624	870	90,200	14,375	826	5,468	155	243	
Cohort C	Pm C1	149	613	800	8,292	43	<10[d]	<10[d]	<10[d]	<10[d]	DRV INTI RTV ABC
	Pm C2[e]	150	575	580	1,457	5,592	288	88	30	16	
	Pm C3[e]	156	919	510	4,756	<10[d]	<10[d]	<10[d]	<10[d]	41	
	Pm C4	151	509	310	36,808	37,837	152	<10[d]	16	42	
	Pm C5[e]	158	267	240	<10[d]	<10[d]	<10[d]	<10[d]	39	14	
	Pm C6	157	109	290	164,416	144,469	<10[d]	1,209	58	10	

[a]The animal was released from anti-retroviral treatment prior to sacrifice.
[b]The animal was treated with SAHA and Ingenol B.
[c]Anti-retroviral regimens were started at day 12 pi.
[d]Below the limit of detection.
[e]Anti-retroviral regimen was supplemented with maraviroc.
Pm, pigtailed macaque. ART, anti-retroviral treatment. PMPA, 9-R-(2-phosphonomethoxypropyl) adenine. DRV, darunavir.
INTI, integrase inhibitor L-000870812. RTV, ritonavir. ABC, abacavir.

Table 1. Antiretroviral regimens and animal characteristics.

	Animal ID	TCRβ in MΦ-QVOA control (RNA Copies/ 10^5 cells)	% $CD3^+$ T cells in MΦ-QVOA by TCRβ RNA	% $CD4^+$ T Cells in Blood $CD3^+$ Lymphocytes	% $CD4^+$ T cells in MΦ-QVOA	Infected $CD4^+$ T cells in MΦ-QVOA	Brain MΦ-QVOA IUPM
Cohort A	Pm A1	3,871	0.97	50.9	0.50	0.005	0.43
	Pm A2	0	0	60.2	0	0	0.0918
	Pm A3	20,428	5.11	35.1	1.80	0.018	0.0917
Cohort B1	Pm B11	38,017	9.50	39.9	3.79	0.038	4.62
	Pm B12	0	0	31	0	0	<0.21[a]
	Pm B13	0	0	45.9	0	0	2.4
	Pm B14	0	0	49.2	0	0	<0.021[a]
Cohort B2	Pm B21	0	0	39.7	0	0	0.074
	Pm B22	19,209	4.80	39.7	1.91	0.019	0.16
	Pm B23	0	0	59.3	0	0	0.093
Cohort C	Pm C1	0	0	50	0	0	<0.04[a]
	Pm C2	0	0	53	0	0	0.21
	Pm C3	925	0.23	47.6	0.11	0.001	1.52
	Pm C4	3,182	0.80	58.4	0.46	0.005	0.955
	Pm C5	5,763	1.44	46.5	0.67	0.007	0.14
	Pm C6	5,223	1.31	40.4	0.53	0.005	0.375

[a]Below the limit of detection. Pm, pigtailed macaque. ART, anti-retroviral treatment

Table 2. Estimate of the number of SIV+ $CD4^+$ T cells in MΦ-QVOA wells based on levels of TCRβ RNA and frequency of lymphocytes in blood.

	Animal ID	Area Analyzed (μm^2)	Positive foci per analyzed field	Density of SIV+ cells per gram of tissue
Cohort A	Pm A1	$1.41x10^8$	0,1,0,0,0,0,0	202
	Pm A2	$2.54x10^8$	0,0,0,0,0,0,0	<102[a]
	Pm A3	$1.16x10^8$	1,1,1,1,1,3,1	2,220
Cohort B1	Pm B13	$1.41x10^8$	24,5,23,19,28	10,553
	Pm B14	$1.41x10^8$	0,0,0,0,0,0,0	<128[a]

[a]Below the limit of detection. Pm, pigtailed macaque.

Table 3. Brain SIV *in situ* hybridization.

Figure 1. Viral load measurements of four cohorts of SIV-infected ART treated macaques.

Four cohorts of SIV-infected pigtailed macaques were treated with different ART regimens, marked in green. Macaques in cohort A (graphs A and B) were also treated with LRAs (orange and purple lines). Macaques in cohort B1 (graphs C and D) were released from ART (light blue lines). Macaques in cohorts B2 (graphs E and F) and C (graphs G and H) did not suppress viral replication during ART. Median values for each group of animals are depicted in red for plasma and dark blue for CSF.

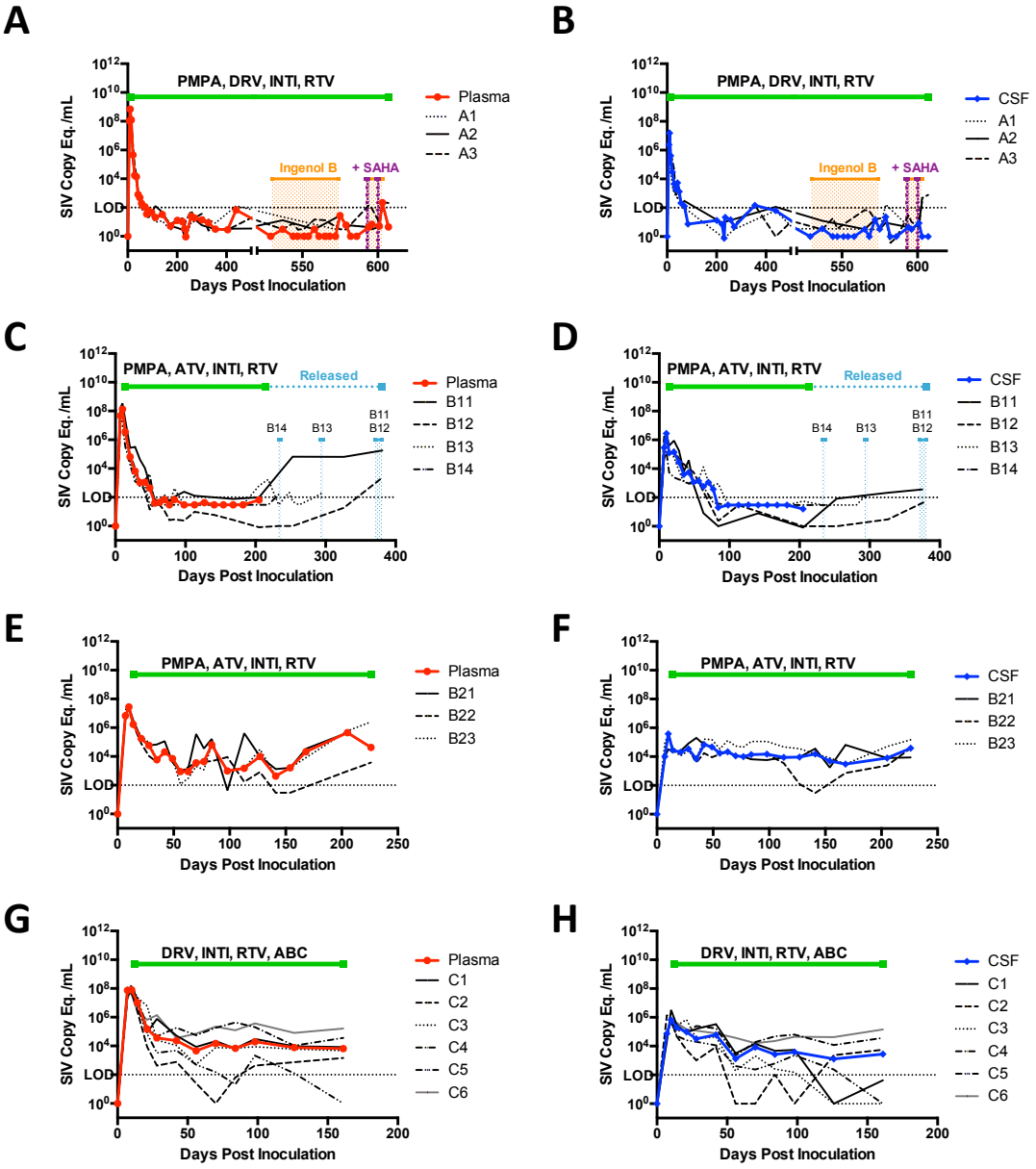
A
PMPA, DRV, INTI, RTV
Ingenol B
+ SAHA
Plasma
A1
A2
A3
SIV Copy Eq./mL
LOD
Days Post Inoculation
B
PMPA, DRV, INTI, RTV
Ingenol B
+ SAHA
CSF
A1
A2
A3
SIV Copy Eq./mL
LOD
Days Post Inoculation
C
PMPA, ATV, INTI, RTV
Released
B14
B13
B11
B12
Plasma
B11
B12
B13
B14
SIV Copy Eq./mL
LOD
Days Post Inoculation
D
PMPA, ATV, INTI, RTV
Released
B14
B13
B11
B12
CSF
B11
B12
B13
B14
SIV Copy Eq./mL
LOD
Days Post Inoculation
E
PMPA, ATV, INTI, RTV
Plasma
B21
B22
B23
SIV Copy Eq./mL
LOD
Days Post Inoculation
F
PMPA, ATV, INTI, RTV
CSF
B21
B22
B23
SIV Copy Eq./mL
LOD
Days Post Inoculation
G
DRV, INTI, RTV, ABC
Plasma
C1
C2
C3
C4
C5
C6
SIV Copy Eq./mL
LOD
Days Post Inoculation
H
DRV, INTI, RTV, ABC
CSF
C1
C2
C3
C4
C5
C6
SIV Copy Eq./mL
LOD
Days Post Inoculation

Figure 2. Longitudinal measurement of markers of macrophage activation and neuronal damage in CSF.

CSF was analyzed longitudinally for each cohort. Relative concentrations of CCL2 (A-B), IL-6 (C-D), NF-L (E-F), and neopterin (G-H) are shown. Graphs A, C, D, and E represent the median concentration and standard deviation in each group. Scatter plots show individual values for each macaque at 100 days post ART. Horizontal black lines denote the median concentration per cohort.

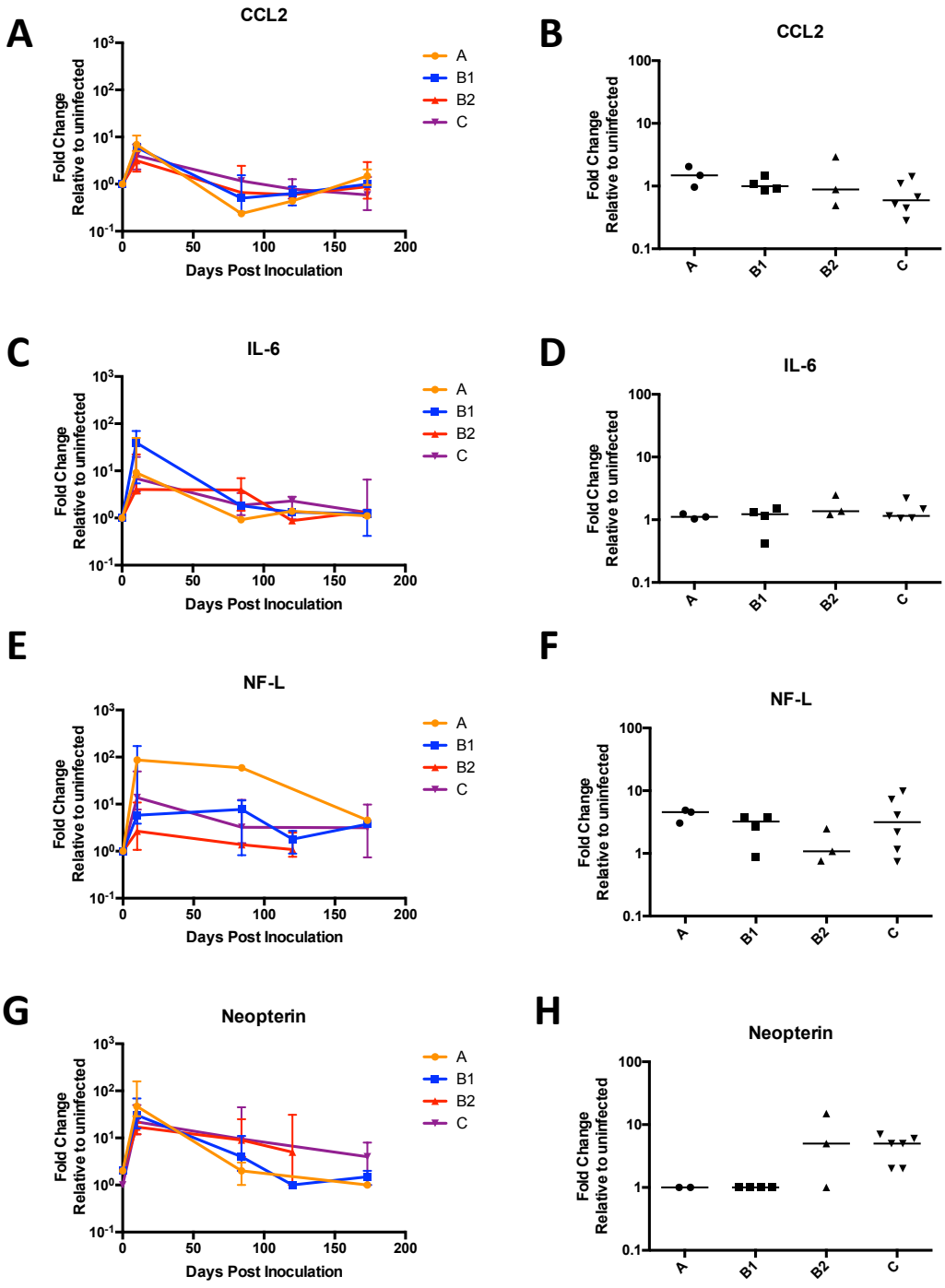
A
CCL2
Fold Change Relative to uninfected
Days Post Inoculation
A
B1
B2
C
B
CCL2
C
IL-6
D
IL-6
E
NF-L
F
NF-L
G
Neopterin
H
Neopterin

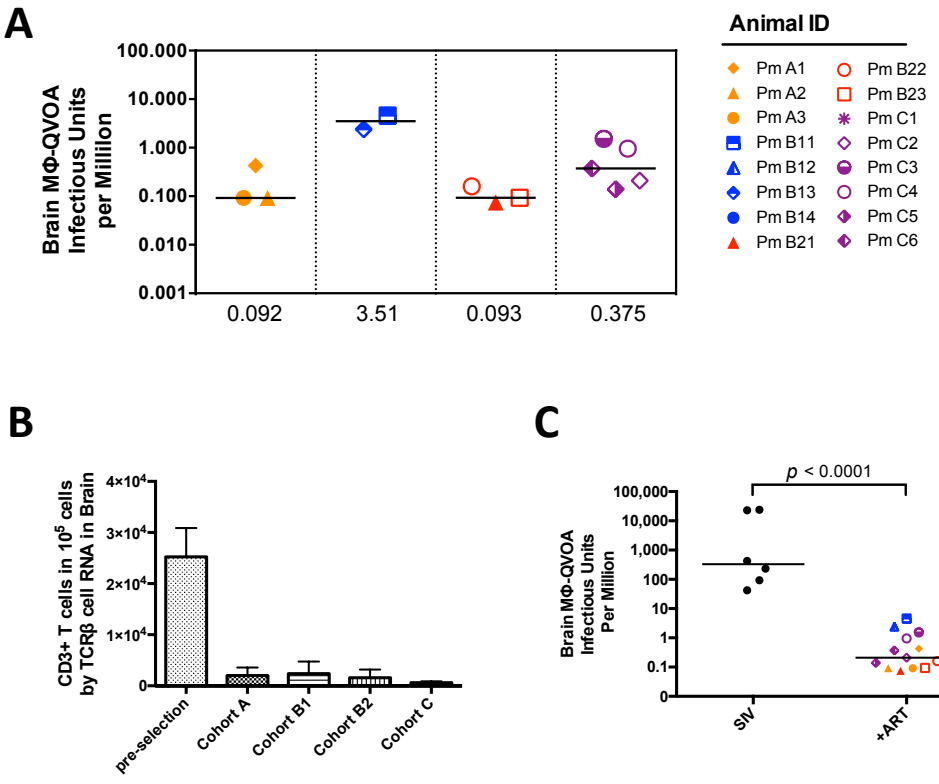

Figure 3. Quantitation of latently infected microglia in ART treated macaques by MΦ-QVOA.

(A) Quantitation of infected brain macrophages from four cohorts of ART-treated macaques. Number of functionally SIV-infected macrophages for each animal is shown with their respective symbols. Horizontal black line represents the median IUPM values (displayed on the x-axis). (B) TCRβ RNA levels in MΦ-QVOA cell lysates were measured by qRT-PCR and the number of $CD3^+$ T cells per 10^5 cells was calculated prior to $CD11b^+$ isolation or plating (pre-selection) and in macrophage control wells of the four cohorts. Data represented as mean with standard error. (C) Numbers of functionally SIV-infected brain macrophages treated with or without ART are compared. Horizontal black line represents the median IUPM values. Significance was determined by Mann-Whitney non-parametric t-test; $p<0.05$ was considered significant.

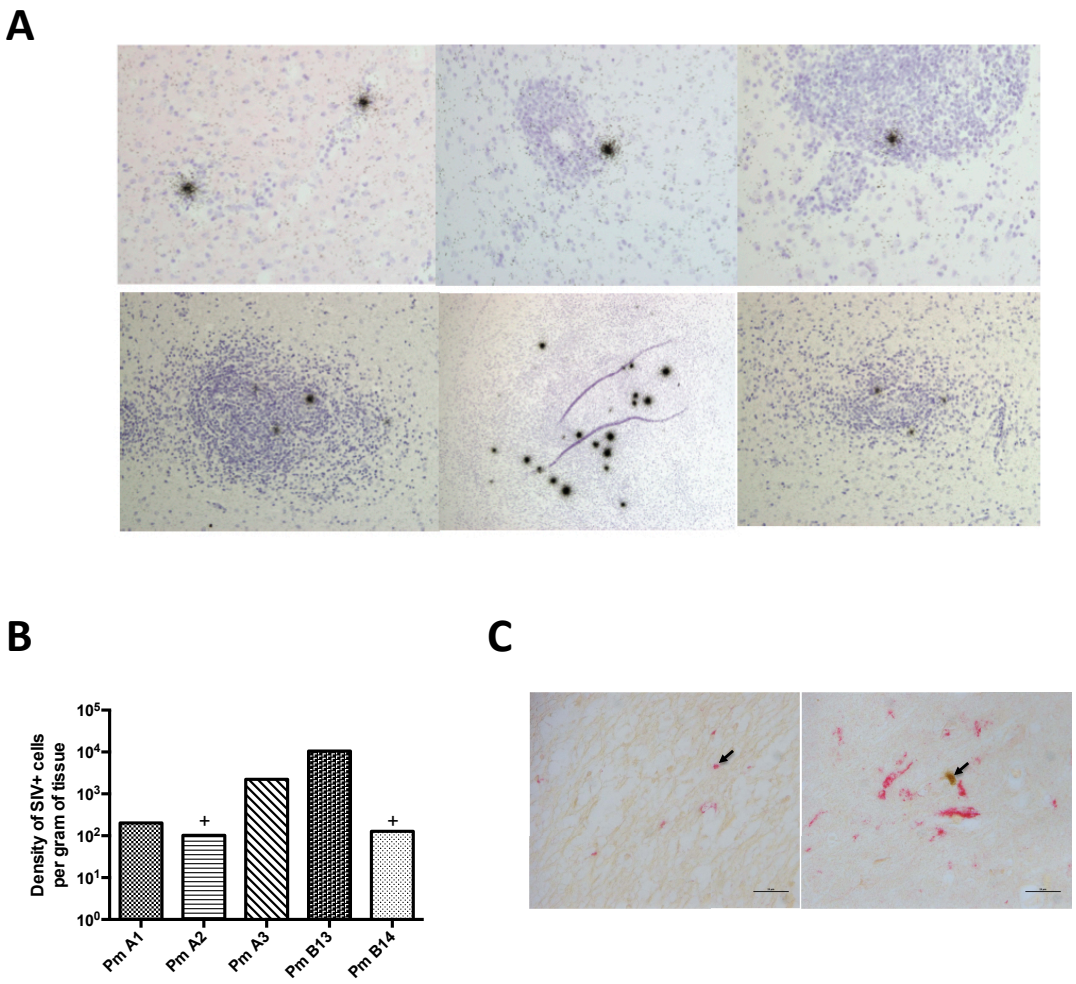

Figure 4. ISH and IHC analysis from brain sections.

(A) Representative *in situ* hybridization from occipital cortex brain sections for SIV RNA of PmA3 (top row) and PmB13 (bottom row). (B) Quantitation of SIV^{+} cells per gram of brain tissue by ISH for indicated animals. Symbol (+) represents values below the limit of detection. (C) IHC for cleaved caspase-3 (brown) and CD68 (pink) in basal ganglia of PmA3 (left) compared to a SIV-infected macaque untreated with ART with encephalitis from a previous study, Pm4 (right).

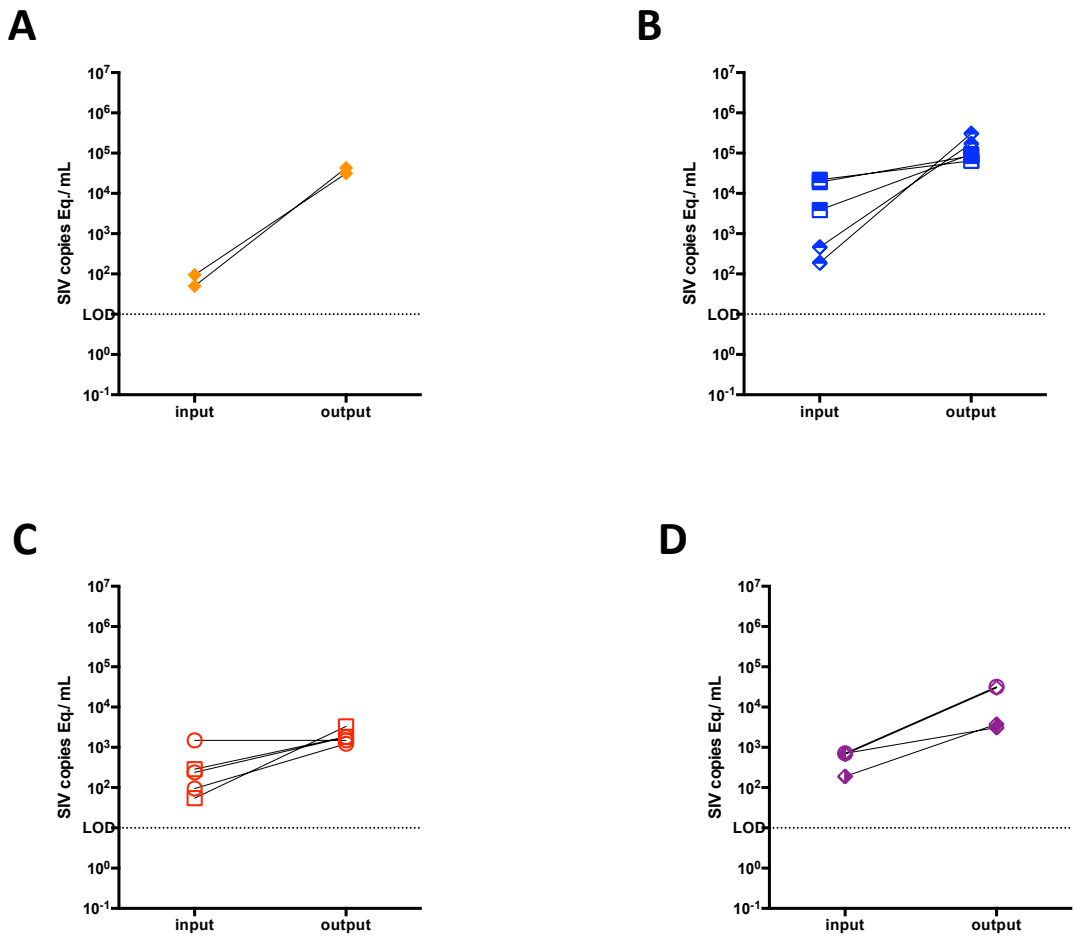

Figure 5. SIV virus produced by microglia in MΦ-QVOAs is infectious.

Supernatant from SIV infected microglia MΦ-QVOA wells were collected and used to infect freshly isolated PBMCs by spinoculation. (A-C) SIV RNA was measured in supernatant by qRT-PCR prior to infection (input virus) and from combined collections of 5, 10, 13 d.p.i. PBMCs (output virus). Individual wells used from each cohort are individually labeled per corresponding pigtailed macaque. SIV RNA levels presented as copies per 1 mL of supernatant.

IV. Summary of Findings and Future Directions

Summary of Findings

Pigtailed macaques were infected with SIV/DeltaB670, a viral swarm and the macrophage-trophic clone, SIV/17E-Fr. Monocytes from blood and macrophages from bronchoalveolar lavage fluid, lung, spleen, and brain from fourteen SIV-infected macaques were isolated and the frequency of infected macrophages was quantitated using a macrophage quantitative viral outgrowth assay (MΦ-QVOA). $CD4^+$ T cells from the blood and spleen were isolated and quantitated in parallel using the gold standard, $CD4^+$ T cell quantitative viral outgrowth assay (QVOA). To ensure that only virus produced by macrophages were quantified in the MΦ-QVOA, myeloid cells were selected based on expression of CD11b and plated in serial dilution in the presence of antiretroviral drugs. Macrophages naturally adhere to the tissue culture plates while $CD4^+$ T cells (the other SIV infected cell) are non-adherent cells and were removed prior quantification of infected macrophages. $CD11b^+$ isolation was successful in discriminating myeloid cells with little to no $CD3^+$ T cells remaining in the macrophage culture. However, to ensure that there were very few $CD4^+$ T cells we quantified the number of $CD3^+$ T cells remaining in the MΦ-QVOA. A TCRβ assay was developed which detected the number of TCRβ RNA copies, expressed only in $CD3^+$ T cells, and calculated the number of $CD3^+$ T cells in each macrophage isolate. Less than 1 infected $CD4^+$ T cell remained in any of the MΦ-QVOA, thus the virus produced in the assays originated from infected macrophages not $CD4^+$ T cells. The frequency of infected macrophages in brain and spleen of SIV-infected macaques mirrored that of $CD4^+$ T cells in the blood (424 and 231 vs. 206). The number of infected macrophages in the lung, BAL and blood were more analogous to spleen $CD4^+$ T cell infection (31, 13, 32 vs. 61 respectively). Five of the

animals in the study developed CNS pathology, which was scored as mild or severe encephalitis. Interestingly, the frequency of infected macrophages in the brain correlated with tissue RNA in parietal cortex and basal ganglia, supporting the hypothesis that infection of macrophages are the main contributors to CNS infection.

Following the completion of this study, we hypothesized that infected macrophages in brain had the potential to become latent in SIV-infected ART-treated pigtailed macaques. Sixteen animals were treated with three ART regimens organized in four cohorts. The ART regimens were chosen based on their CNS penetrance score (CPE). Cohort A was treated with a highly penetrant regimen (score of 6) and maintained suppression for 500 days after which they were treated with latency reversing agents (LRAs). The second ART regimen was less penetrant (score of 5), the animals were divided into two cohorts based on viral suppression. Animals that maintained suppression were released from ART treatment a few days prior sacrifice. The fourth group of ART treated macaques did not achieve suppression despite the highly penetrant regimen (score of 8), and virus was detected throughout the study, albeit 3 to 4 logs lower than that observed in untreated macaques. Despite the differences in ART regimens and duration of suppression, latently infected brain macrophages were observed by ISH and MΦ-QVOA. As previously discussed, TCRβ assay demonstrated that less than 1 infected $CD4^+$ T cells remained in the MΦ-QVOA, thus lymphocytes did not contribute to the virus produced in the assay. ART treatment was sufficient to significantly decrease the frequency of infection of brain macrophages compared to the SIV-infected untreated macaque study. Finally, we demonstrated that replication-competent virus was produced in the MΦ-QVOAs; by using the MΦ-QVOA supernatant to infect PBMCs. Altogether

we demonstrated that brain macrophages are latently infected in ART-treated macaques and represent a functional viral reservoir capable of re-seeding the periphery upon treatment interruption.

Optimization of MΦ-QVOA

Devising a macrophage quantitative viral outgrowth assay to measure the number of infected macrophages in SIV-infected pigtailed macaques required surpassing multiple obstacles. Prior to developing the MΦ-QVOA we needed to isolate a pure population of macrophages or deplete all $CD3^+$ T cells in the assay. First, we attempted to remove all $CD4^+$ and $CD8^+$ T cells based on expression of CD3 using two strategies: 1) CD3 antibody-mediated complement killing, and 2) CD3 depletion by magnetic bead isolation. The first strategy failed to eliminate the lymphocytes in the cultures (data not shown). For the second strategy, we needed to develop our own custom magnetic bead isolation kit for CD3 lymphocytes in non-human primate cell preparations. To do so, blood PBMCs were isolated and labeled based on expression of CD3 with a PE conjugated anti-CD3 antibody (clone SP34, BD Biosciences) that cross-reacted with our pigtailed macaque samples. Following cell labeling, the EasySep PE Positive Selection Kit (Stemcell Technologies) provided us a magnetic bead isolation system that specifically bound all PE conjugated cells. Although the CD3 positive selection kit produced 99% pure $CD3^+$ lymphocytes in the positive isolation fraction, the depleted fraction contained 7% $CD3^+$ T cells and only 20% macrophages (Figure S1). Therefore, we concluded that isolating a pure population of macrophages, rather than depleting $CD3^+$ cells, would be a better approach.

CD14 and CD11b, two markers consistent among macrophage populations were tested. Spleen macrophages from three pigtailed macaques were isolated based on expression of CD14 with the non-human primate CD14 microbead kit (Miltenyi) or based on expression of CD11b with the non-human primate CD11b microbead kit (Miltenyi). Both isolation strategies produced an average of 47% and 67% macrophages respectively in the positive fraction with less than 12% and 7% $CD3^+$ T cells remaining respectively (Figure S1). However, we suspected that the tissue digestion techniques used on spleen preparations disrupted the CD14 surface marker expression because an average of 32% macrophages were recovered in the negative fraction of the CD14 kit, whereas only 2% were recovered in the negative fraction of the CD11b kit (Figure S1). We concluded that the CD11b surface marker was a better surface marker for the purification of tissue macrophages and blood monocytes.

During ART treatment, the frequency of latently infected cells significantly decreases to 1 or less than 1 infected cell in a million. Therefore, it became increasingly important to not only isolate a pure population of macrophages, but also optimize the yield of the isolation technique such that we could assay more than a million cells in triplicate. We observed that purification using the CD11b non-human primate microbead kit (Miltenyi) yielded variable results. We suspected that using a column-based system resulted in loss of myeloid cells during the purification procedure due to macrophages' strong adhesion to the columns. Therefore, we decided to move on to a column-free isolation technique using a FITC conjugated anti-CD11b antibody (clone Bear1, Beckman Coulter) followed by the EasySep FITC Positive Selection Kit (Stemcell

Technologies). The EasySep FITC kit improved our recovery of $CD11b^+$ macrophages while maintaining a 90% or greater purity (data not shown).

Finally, optimizing the MΦ-QVOA required testing several macrophage activation agents. In a small study of five SIV-infected pigtailed macaques, brain macrophages were isolated and plated alone, with CEMx174 cells, CEMx174 cells with LPS, and CEMx174 cells with PHA. Preliminary data from this study showed that macrophages co-cultured with CEMx174 consistently produced SIV+ assays. PHA and LPS had little to no effect in activating brain macrophages to produce virus (data not shown). Next, we tested the effect of TNFα in activating brain macrophages from two SIV-infected pigtailed macaques. In both cultures, TNFα increased the number of SIV positive dilutions, thus we concluded that TNFα and CEMx174 co-culture optimized the limit of detection of the MΦ-QVOA.

In other small studies, we tried to re-activate latently infected cells with IL4, LPS, IL10, IL1β, prostaglandin E2 (TLR4 agonist), PAM3CSK4 (TLR2/1 agonist), PMA, and Ingenol B. However, all of our attempts have been unsuccessful and only TNFα in combination with prostaglandin E2 and PAM3CSK4 have shown slightly improved re-activation in comparison to TNFα alone (data not shown). Furthermore, we observed that macrophage escape from latency is highly variable; for example, brain macrophages sometimes produce virus early during the MΦ-QVOA assay but later become silenced. Additionally, the majority of the MΦ-QVOA cultures are SIV DNA positive but not all reactivate to produce SIV RNA despite prolonged TNFα activation or TNFα in combination with prostaglandin E2 and PAM3CSK4 (data not shown).

Further research is needed to understand the behavior of latently infected macrophages and the best strategies of re-activation of latently infected macrophages *in vitro* and *in vivo*. Understanding the cells that comprise latent reservoirs and their frequency of infection compared to $CD4^+$ T cells, the recognized long lived viral reservoir in HIV and SIV infection, will provide better strategies for eradicating HIV infection.

Future Directions

The research included in this dissertation demonstrated that macrophages are infected in the SIV-infected tissues and that virus persists despite ART treatment in the brain. However, latency has never been demonstrated in tissue macrophages. We hypothesize that SIV-infected tissue macrophages also persist in tissues of ART-treated macaques. Thus we performed the MΦ-QVOA in blood monocytes and tissue macrophages from BAL, lungs and spleen of the sixteen SIV-infected ART-treated macaques previously discussed in section III. Monocytes and macrophages were magnetically isolated based on their expression of CD11b and plated in serial dilution. TCRβ RNA was quantified (Figure S2) and less than 5% $CD3^+$ T cells remained in the spleen, which had the highest number of $CD3^+$ T cells. The number of $CD3^+$ T cells remaining did not contribute to the virus observed in the MΦ-QVOA. Next, infection in monocytes and macrophages from tissues, and resting $CD4^+$ T cells was quantified (Figure S3). The size of the reservoir was consistent between BAL, lung and spleen macrophages and $CD4^+$ T cells in the blood (1.2, 1.5, 1.4 vs. 1.3 infected cells per million respectively), with spleen macrophages having the widest range of infected cells. The

size of the viral reservoir in spleen resting $CD4^+$ T cells was the largest of the tissues studied (6.9 IUPM), also varying widely. Finally, similar to our study of brain macrophages, ART treatment allowed the establishment of a latent reservoir in all the tissues (Figure S4), which was significantly lower than in SIV-infected untreated macaques.

Future directions of this research include characterizing the sequences of the virus produced in the MΦ-QVOA and comparing them to the virus obtained from resting $CD4^+$ T cells. Additionally, we will investigate whether the virus produced in all tissue MΦ-QVOAs is functional, and examine whether it is capable of re-seeding the periphery. Finally, we will measure the half-life of latently infected cells (macrophages and lymphocytes) using mathematical models and study the effect of "shock and kill" latency reactivating agents in reducing the size of the latent reservoirs as a viable cure strategy.

Implications for HIV research

We showed that the frequency of latently infected macrophages is rare but could lead to re-infection upon treatment interruption despite eradication of HIV infection in $CD4^+$ T cells. More than ten million purified macrophages are needed to measure the size of the latent myeloid reservoir. Translating the results in this study to human experiments will require performing multiple biopsies of infected tissues for detection of latently infected macrophages. Spleen extractions during surgical procedures in HIV^+ patients could be used to study latently infected macrophages and re-capitulate the pigtailed macaque results.

Several questions remain about macrophage infection in HIV. Further research is needed to identify which sub-sets of macrophages are latently infected in tissues and whether macrophage activation/polarization agents have any effect in promoting latency. Moreover, studying the transcriptome and metabolic state of latently infected macrophages may allow for better targets of latency reversal. Additionally, it is unclear whether latently infected macrophages continue to present HIV peptides, or whether cytokine activation because of other infections contributes to bystander HIV infection. Finally, more work is needed to determine whether a sterilizing cure that aims to eliminate all latently infected macrophages and lymphocytes will ever be possible. A functional cure may be more achievable by permanently silencing all latently infected macrophages and $CD4^+$ T cells rather than re-activating them.

We hope that the work presented in this dissertation will change how macrophages are perceived in the field of HIV persistence. We have demonstrated that macrophages are clearly not a silent player in HIV infection and must be taken into account when devising HIV cure strategies.

Figure S1. Efficiency of magnetic bead isolation strategies used to purify tissue macrophages.

Flow cytometry analysis for CD11b (macrophages) and CD3 (lymphocytes) was performed prior to the isolation strategy and in the two resulting fractions. (A) Both $CD4^+$ and $CD8^+$ lymphocytes in blood PBMCs were isolated based on expression of CD3 with a PE conjugated anti-CD3 antibody followed by the EasySep PE Positive Selection Kit (Stemcell Technologies). (B) Spleen macrophages were isolated based on expression of CD14 with a non-human primate CD14 microbead kit (Miltenyi). (C) Spleen macrophages were isolated based on expression of CD11b with a non-human primate CD11b microbead kit (Miltenyi).

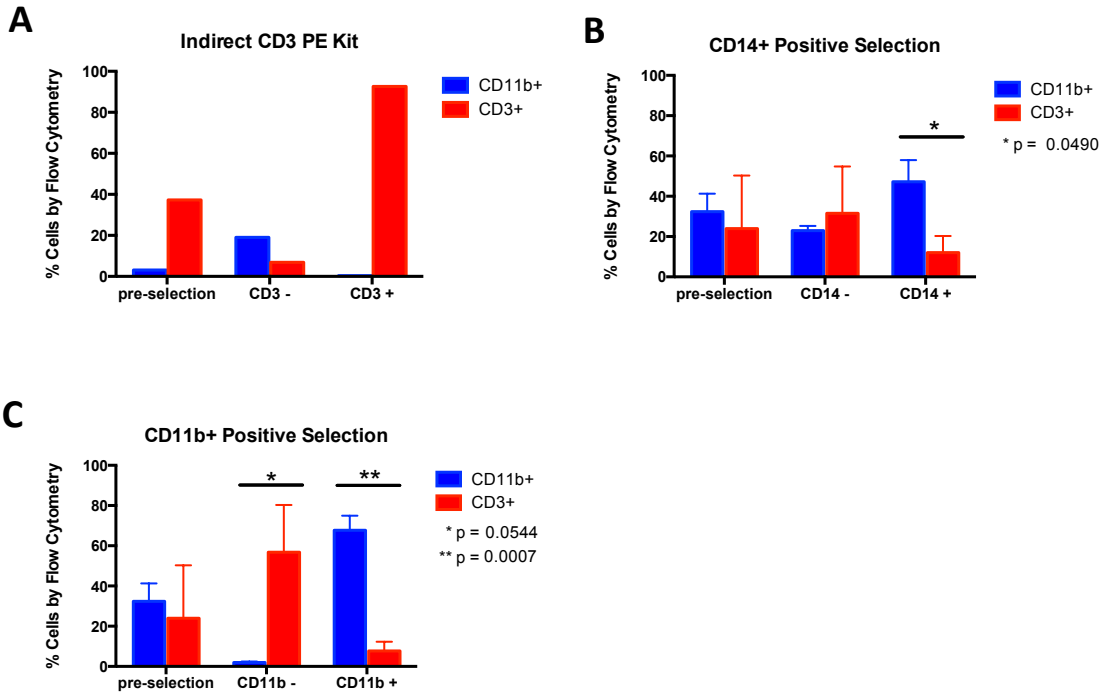
A
Indirect CD3 PE Kit
% Cells by Flow Cytometry
100
80
60
40
20
0
pre-selection
CD3 -
CD3 +
CD11b+
CD3+
B
CD14+ Positive Selection
% Cells by Flow Cytometry
pre-selection
CD14 -
CD14 +
*
CD11b+
CD3+
* p = 0.0490
C
CD11b+ Positive Selection
% Cells by Flow Cytometry
pre-selection
CD11b -
CD11b +
*
**
CD11b+
CD3+
* p = 0.0544
** p = 0.0007

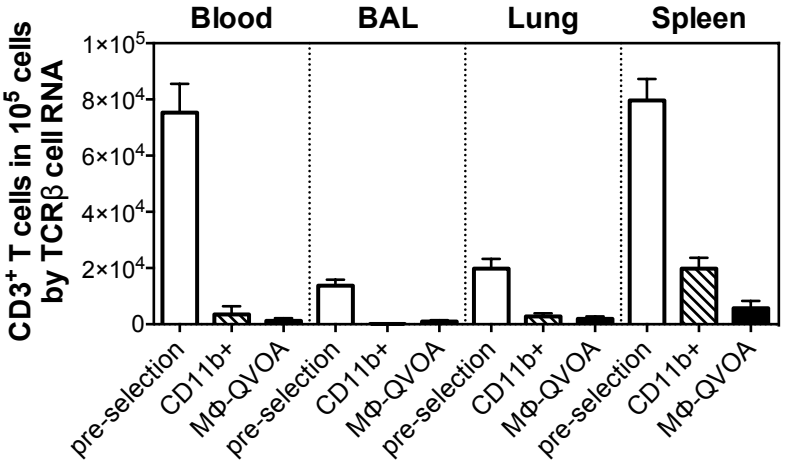

Figure S2. Quantitation of $CD3^+$ T cells in MΦ-QVOA by TCRβ RNA assay

TCRβ RNA in MΦ-QVOA cell lysates was measured by qRT-PCR and the number of $CD3^+$ T cells per 10^5 cells was calculated prior to $CD11b^+$ isolation (or plating) and in the macrophage control wells of the five cohorts. Data represented as mean with standard error.

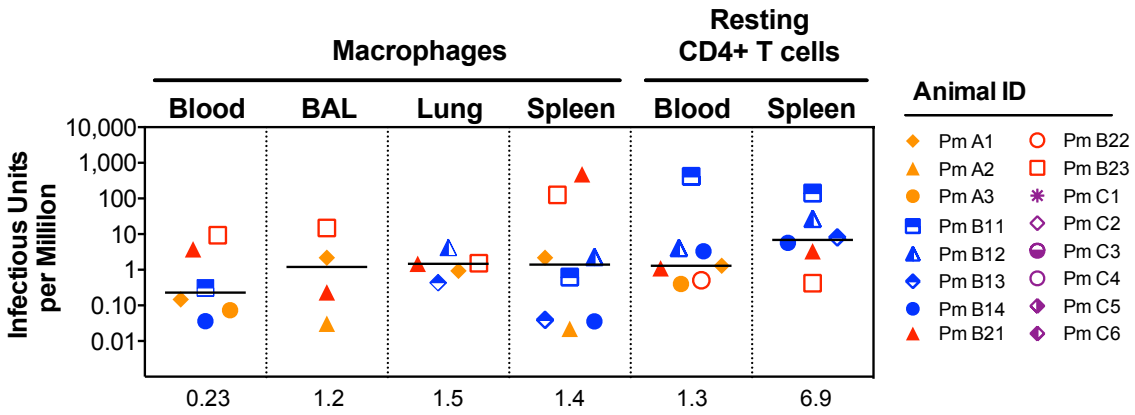

Figure S3. Quantitation of latently infected cells in tissues of SIV-infected ART-treated macaques.

Quantitation of infected macrophages and $CD4^+$ T cells in blood, bronchoalveolar lavage fluid, lung, and spleen from the four cohorts of ART-treated macaques. The IUPM for the animals assayed is shown with their respective symbols. Horizontal black line represents the median IUPM values (displayed on the x-axis).

Figure S4. ART treatment is sufficient in decreasing the size of the reservoir

IUPM values from brain macrophages of SIV infected pigtailed macaques treated with or without antiretrovirals are compared in blood monocytes (A), spleen macrophages (B), lung macrophages (C), BAL macrophages (D), and resting $CD4^+$ T cells in blood (E) and spleen (F). Horizontal black line represents the median IUPM values. Significance was determined by Mann-Whitney non-parametric t-test; $p<0.05$ was considered significant.

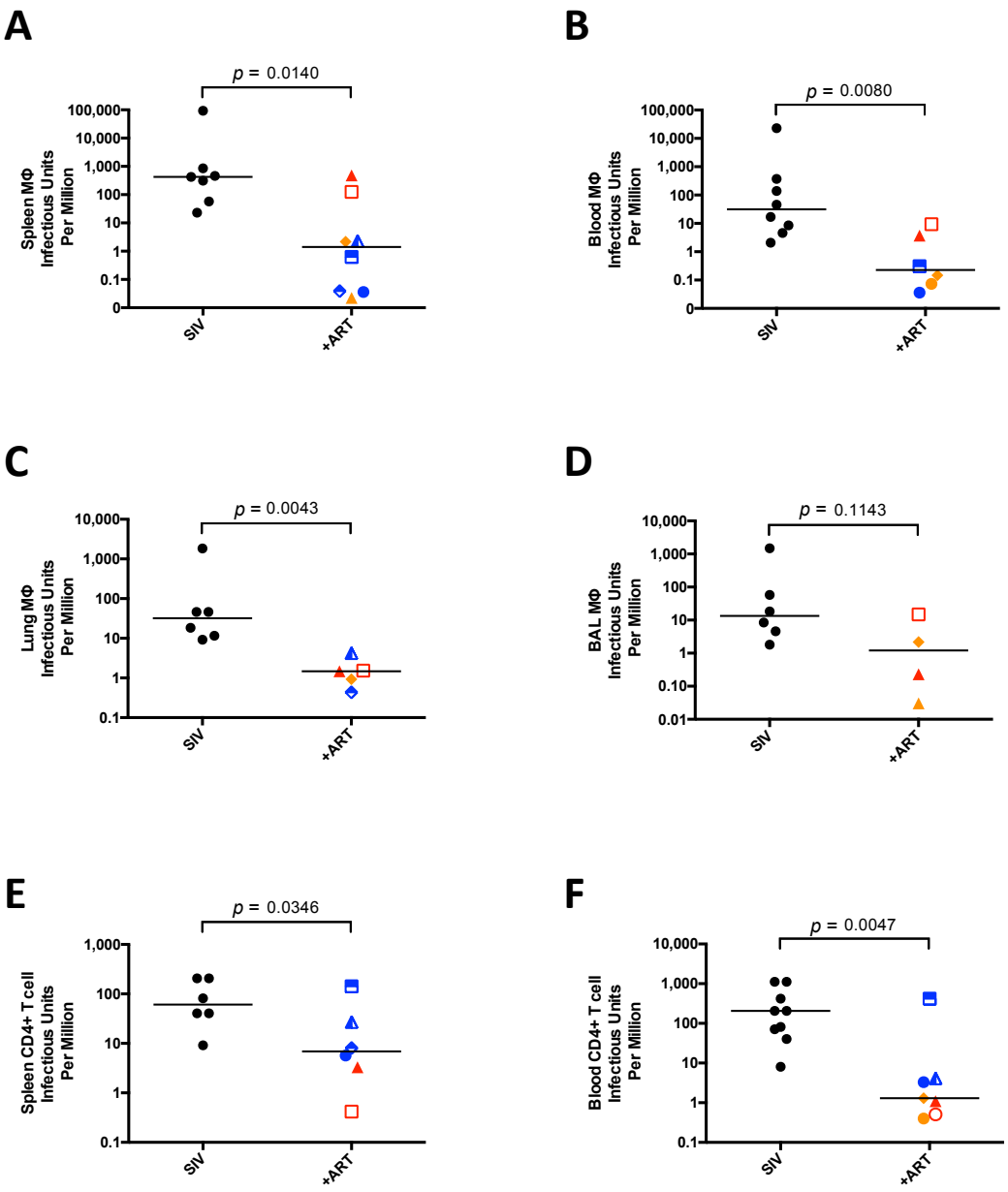
A
p = 0.0140
Spleen MΦ Infectious Units Per Million
100,000
10,000
1,000
100
10
1
0.1
0
SIV
+ART
B
p = 0.0080
Blood MΦ Infectious Units Per Million
100,000
10,000
1,000
100
10
1
0.1
0
SIV
+ART
C
p = 0.0043
Lung MΦ Infectious Units Per Million
10,000
1,000
100
10
1
0.1
SIV
+ART
D
p = 0.1143
BAL MΦ Infectious Units Per Million
10,000
1,000
100
10
1
0.10
0.01
SIV
+ART
E
p = 0.0346
Spleen CD4+ T cell Infectious Units Per Million
1,000
100
10
1
0.1
SIV
+ART
F
p = 0.0047
Blood CD4+ T cell Infectious Units Per Million
10,000
1,000
100
10
1
0.1
SIV
+ART

Curriculum Vitae

CURRICULUM VITAE

The Johns Hopkins University School of Medicine

Claudia Avalos **July 12th 2016**

EDUCATIONAL HISTORY

Ph.D., Johns Hopkins University School of Medicine, 2016
Cellular and Molecular Medicine
Mentor: Janice E. Clements, Ph.D.

B.S., Florida State University, 2010
Biochemistry

B.S., Florida State University, 2010
Biomathematics

PROFESSIONAL EXPERIENCE

Research Rotation, Lab of Landon King, M.D., 2010-2012
Johns Hopkins School of Medicine
Department of Pulmonary and Critical Care Medicine

Research Rotation, Lab of Harry Dietz, M.D., 2011
Johns Hopkins School of Medicine
Department of Molecular Biology and Genetics

Research Rotation, Lab of David Kass, M.D., 2010
Johns Hopkins School of Medicine
Department of Cardiology

Laboratory Research Assistant, Lab of Timothy Cross, Ph.D., 2009-2010
Florida State University Department of Chemistry and Biochemistry

Laboratory Research Assistant, Lab of Gregory Dudley, Ph.D., 2008-2009
Florida State University Department of Chemistry and Biochemistry

Laboratory Research Assistant, Lab of Gavin Naylor, Ph.D., 2009
Florida State University Department of Biological Sciences

Laboratory Research Assistant, Lab of Nick Cogan, Ph.D., 2007-2008
Florida State University Department of Mathematics

INTERNSHIPS

2013- 2015, Generation Tomorrow: Project Re_ Agency Internship
HIV and Hepatitis C Testing and Counseling
Center for AIDS Research
Johns Hopkins University

2009, LeaderShape Institute
Florida State University

2008, Minority Students in Health Careers Motivation Program
University of Miami School of Medicine

ACADEMIC HONORS AND AWARDS

2015, Best Three Minute Thesis Talk
Cellular and Molecular Medicine Retreat
Johns Hopkins School of Medicine

2013, Pollard Scholars Teaching Assistantship
Cellular and Molecular Medicine
Johns Hopkins School of Medicine

2013, Thirty under 30 Alumni Award
Florida State University

2010, Honors Medallion
Florida State University

2009, Undergraduate Research and Creative Activity Award
Florida State University

2006- 2010, Florida Bright Futures Medallion Scholarship
Florida State University

2006-2010, Dean's and President List
Florida State University

PUBLICATIONS

Latently Infected Brain Macrophages in SIV-Infected Macaques treated with diverse antiretroviral regimens. **C.R. Avalos**, S.E. Queen, M. Li, S.L. Price, E.N. Shirk, E.L. Engle, C.M. Abreu, E.R. Forsyth, B.T. Bullock, F.M. Gabhann, S.W. Wietgrefe, A.T. Haase, F.M. Gabhann, J.L. Mankowski, J.E. Clements, L. Gama. *In preparation.*

Quantitation of Productively Infected Myeloid Cells in Blood and Tissues of SIV Infected Macaques. **C.R. Avalos**, S.L. Price, E.R. Forsyth, J.N. Pin, E.N. Shirk, B.T. Bullock, S.E. Queen, M. Li, D. Gellerup, S.L. O'Connor, M.C. Zink, J.L. Mankowski, L. Gama, J.E. Clements. *Journal of Virology*, Vol. 90, No. 12 (2016), pp. 5643-5656. PMCID: PMC4886778

Macrophage A2A Adenosinergic Receptor Modulates Oxygen-Induced Augmentation of Murine Lung Injury. N.R. Aggarwal, F.R. D'Alessio, Y. Eto, E. Chau, **C.R. Avalos**, A.T. Waickman, B.T. Garibaldi, J.R. Mock, D.C. Files, V.K. Sidhaye, V.Y. Polotsky, J. Powell, M. Horton, L.S. King. *American Journal of Respiratory Cell and Molecular Biology*, Vol. 48, No.5 (2013), pp. 635-646. PMCID: PMC3707379

Resolution of Experimental Lung Injury by Monocyte-Derived Inducible Nitric Oxide Synthase. F.R. D'Alessio, K. Tsushima, N R. Aggarwal, J.R. Mock, Y. Eto, B.T. Garibaldi, D.C. Files, **C.R. Avalos**, J.V. Rodriguez, A.T. Waickman, S.P. Reddy, D.B. Pearse, V.K. Sidhaye, P.M. Hassoun, M.T. Crow, L.S. King. *The Journal of Immunology*, Vol. 189, No. 5 (2012), pp. 2234-2245. PMCID: PMC3424351

CONFERENCE ABSTRACTS

Novel Macrophage Latency Assay to Quantitate Myeloid Viral Reservoirs**. C.R. Avalos**, S.E. Queen, B.T. Bullock, M. Li, E.N. Shirk, L. Gama, J.E. Clements. *6th International Workshop on HIV Persistence during Therapy (2013).* Poster presentation.

Characterization of monocytes and microglia of SIV infected pigtailed macaques. **C.R. Avalos**, S.E. Queen, B.T. Bullock, M. Li, E.N. Shirk, L. Gama, J.E. Clements. *12th International Symposium on NeuroVirology (2013).* Poster and oral presentation.

Characterization of macrophage phenotypes and their susceptibility to SIV infection. **C.R. Avalos**, E.N. Shirk, L. Gama, J.E. Clements. *Keystone Symposium, Myeloid Cells: Regulation and Inflammation (2013).* Poster presentation.

Anionic Rearrangement of Benzyloxypyridines. **C.R. Avalos,** J. Yang, G.B. Dudley. *Florida Annual Meeting and Exposition (2009).* Poster presentation.

Enantioselective Rearrangement of Benzyloxypyridines. **C.R. Avalos**, J. Yang, G.B. Dudley. *Undergraduate Research and Creative Activity Award (2009).* Oral presentation.

SERVICE AND LEADERSHIP

2015- present, Project Re_ HIV and Hepatitis C Testing and Counseling
Community Based Health Agency, Baltimore MD

2013- 2015, **Vice President of Programs**
Association for Women in Science, Baltimore

2012- 2014, **President**
Biomedical Scholars Association
Johns Hopkins University

2013-2014, Nurse Assistant, Neonatal Intensive care Unit
Mercy Medical Center, Baltimore MD

2012-2013, Junior Biomedical Scholar Mentor
Biomedical Scholars Association
Johns Hopkins University

2011, Bienestar Outreach Program
Johns Hopkins University

2009-2010, Respite Volunteer
Big Bend Hospice

2008-2009, Chemistry Outreach Program
Florida State University

SKILLS

2014- Present, Certified HCV Basic Educator
Hepatitis C Support Project, Baltimore MD

2013- Present, Certified HIV Counseling Skills Level 1
Maryland Department of Health and Mental Hygiene
Prevention and Health Promotion Administration, Baltimore MD

2013- Present**,** Certified Research Laboratory Phlebotomist
All about the Blood Phlebotomy*,* Baltimore MD

2011- Present, Purple Belt Level 5 Kyu in Shotokan Karate
Baltimore Karate Club, Baltimore MD

Language Proficiency
Native, Spanish
Fluent, English and French
Basic, Japanese and Bulgarian